Chapter 14
Spin Dynamics Tutorial: Numerical Simulations

Kiel Hock, François Méot, and Vasiliy Morozov

The next two Sections provide the material of a miniworkshop which extended over the two weeks of the Summer 2021 USPAS Spin Class, and was integral part of the teachings.

The work proposed to the attendees essentially consisted in the numerical simulation of polarized beam manipulations in the AGS injector—"AGS Booster"—starting from basic principles (computation of resonance strengths, resonance crossing, effect of synchrotron radiation, etc.), and extending to the application of polarization preservation techniques (harmonic orbit correction or excitation, ac dipole, snakes, spin matching, etc.). As a matter of fact, for simplicity the same lattice, the AGS Booster, with magnetic rigidity adapted in consequence,

K. Hock · F. Méot (✉)
Brookhaven National Laboratory, Upton, NY, USA
e-mail: khock@bnl.gov; fmeot@bnl.gov

V. Morozov
Oak Ridge National Laboratory, Oak Ridge, TN, USA
e-mail: morozovvs@ornl.gov

F. Méot et al. (eds.), *Polarized Beam Dynamics and Instrumentation in Particle Accelerators*, Particle Acceleration and Detection,
https://doi.org/10.1007/978-3-031-16715-7_14

was used for simulations concerning indifferently hadron polarization, or electron polarization and the effect of synchrotron radiation.

The miniworkshop covers many of the theoretical aspects addressed during the lectures, and the main goal in performing these numerical simulations is to compare their outcomes and theoretical expectations.

Section 14.1 gives the assignments. A first part addresses hadron (precisely, helion, Table 14.1) beams (Sects. 14.1.1.1–14.1.1.17 and Tables 14.2, 14.3), a second part deals with electrons and synchrotron radiation (Sects. 14.1.2.1–14.1.2.5).

Section 14.2 gives detailed solutions of these numerical simulation exercises.

Finally, everything starts from a single input data file, "superA.inc", short enough to be given in its entirety in Table 14.4 and subsidiary Tables 14.5 and 14.6, the latter two being a series of 6 cells constitutive of the AGS Booster ring. Nothing else is needed but the code executable, "zgoubi", downloadble from sourceforge [1]. The execution for instance of the said input data file is a mere

```
zgoubi -in superA.inc
```

All gnuplot [2] and zpop[1] graphs in the present assignments and in their solutions (Sect. 14.2) derive from ancillary files produced (readable during and upon completion of simulation) by this simple execution instruction. The input data file taken from these Tables 14.4, 14.5 and 14.6 is developed further when needed, namely very little, as required in one or the other of these various problems.

However, simulation input and output data files of many of the exercises have been saved in Zgoubi development repository, where they can be downloaded from:
https://sourceforge.net/p/zgoubi/code/HEAD/tree/trunk/exemples/uspasSpinClass_2021/

Besides, users may want to consider the use of python interfaces to zgoubi, subject to continuing development and available on web, pyZgoubi [4] and zgoubidoo [5], or the *ad hoc* HPC environment interface in Sirepo [6] where as well AGS Booster input data files may be found.

14.1 Numerical Simulations: Problems

The numerical simulations proposed in this Section address many of the theoretical aspects of polarized hadron beam acceleration and of electron polarization, introduced in the lectures. They use stepwise ray-tracing techniques (i.e., a step-by-step integration of the equations of particle and spin motion), the reason for this is that the method allows detailed inspection of motion across optical elements, whether using analytical magnetic/electric field models or field maps, and it allows accurate Monte Carlo simulations such as stochastic emission of photons (synchrotron radiation) and its effects on particle and spin dynamics.

[1] Zgoubi's plotting and data treatment companion [3].

Table 14.1 Parameters of helion, $^3He^{2+}$, the particle considered in the exercises. Proton data are given for comparison. Note: atomic mass unit: 931.4940954 MeV/c^2; $\mu_N = e\hbar/2m$

	Units	Proton	$^3He^{2+}$
Mass, m	MeV/c^2	938.27208	2808.39158
	amu	1.00727646	3.0149322
Charge	$\|e\|$	+1	+2
Number of nucleons		1	3
Number of protons, Z		1	2
Spin angular momentum, I	$\hbar$	1/2	1/2
Magnetic moment, μ	μ_N	2.7928474	−2.1276253
Gyromagnetic ratio $g = \frac{\mu}{\mu_N} \times 2\frac{m}{Ze\hbar I}\mu_N$	μ/μ_N	2	−6.368306745
Anomalous magnetic moment $G = \frac{g-2}{2}$		1.7928474	−4.18415382
Imperfection resonance interval $\|mc^2/G\|$	MeV	523.3	671.2

Three different classes of problems regarding the manipulation of polarized beams in circular accelerators are addressed:

- excitation of depolarizing resonances, and their effect on bunch polarization,
- preservation of polarization of hadron beams during acceleration,
- maximization of polarization and polarization life-time, in an electron storage ring.

Both series of simulation problems will use the same lattice, namely the AGS Booster ring. This means in particular, the same optical sequence input data files, *mutatis mutandis*.

Hadron Polarization Simulations

Beam-beam collisions involving polarized helion ($^3He^{2+}$) are part of the physics programs at the EIC. Polarized helion beams are produced using an EBIS source. Prior to injection in the EIC HSR (Hadron Storage Ring, an evolution of RHIC collider rings), helion beams are accelerated in the AGS Booster and in the AGS (Fig. 14.1).

At low rigidity, the cold snakes in the AGS cause harmful optical distortions, including linear coupling. A path to overcome this issue is by injecting ^{3}He beams at a high enough energy that these distortions become negligible. On the other hand, under the effect of two partial snakes, the stable spin direction $\mathbf{n}_0$ in the AGS is at an angle to the guiding field, with a least magnitude every $|G\gamma| = 3n + 1.5$ (Fig. 14.2). As a result, it is foreseen to extract ^{3}He beams from the Booster at $|G\gamma| = 10.5$. These will be the conditions considered in these exercises, regarding hadron polarization.

Electron Polarization Simulations

High polarization of the electron beam at the collision points is required by the EIC physics program. Relativistic electrons emit photons, and a small fraction of these radiated photons contribute to spin flip, which builds up beam polarization

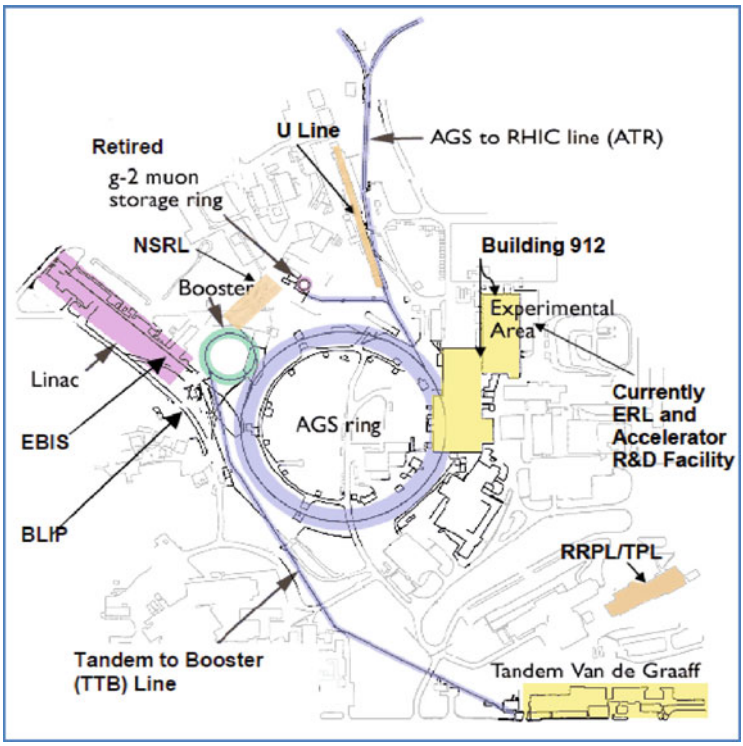

Fig. 14.1 RHIC injector cascade, the future EIC hadron injector system, in 2021 (RHIC itself is not shown): H^- 200 MeV linac, EBIS ion sources, AGS booster (which also accelerates ions for the NSRL, NASA Space Research Lab), the AGS, and the AGS to RHIC (AtR) injection line

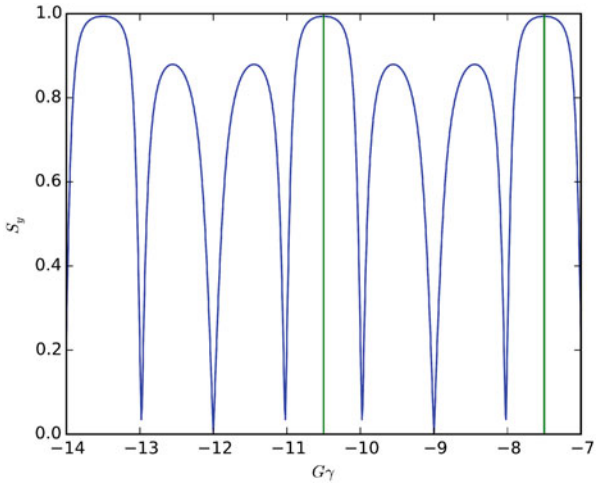

Fig. 14.2 Vertical component of AGS $\mathbf{n}_0$ spin eigenvector, in the presence of two partial snakes. The angle to the vertical guide field is minimal every three units, $G\gamma = -7.5,\ -10.5,\ -13.5$, etc

through the Sokolov-Ternov effect. In the vast majority of cases, photon emission is associated with noisy orbital motion causing extra spin diffusion, i.e. depolarization.

In the present simulations regarding high energy electrons in a storage ring, rather than using the EIC electron storage ring (ESR) lattice, the very ring considered for hadrons, the AGS Booster, is used. There are various reasons for that: the Booster is a short ring (200 m), whereas the ESR is 3.8 km, this results in quicker tracking; it allows, quite efficiently, for dealing with a single lattice for studies of both, hadron and electron spin dynamics; the AGS Booster lattice is much simpler than the ESR one, input data files are easier to handle; moving from hadron to electron simulations (or vice versa) reduces to essentially a matter of changing the reference rigidity and the nature of the particle.

The goals in the electron polarization simulations are to:

- establish stable particle motion in the AGS Booster lattice for an electron beam energy of 10 GeV, checking the damping parameters;
- calculate the invariant spin field $\mathbf{n}_0$;
- understand depolarization through the deviation of $\mathbf{n}_0$ from the vertical in arc dipoles, and
- practice a spin matching mechanism, which maximizes electron polarization.

Practical Aspects Regarding These Numerical Simulations
When developing simulation input data files, or when using existing ones, in order for what's computed, and the physics behind it, to be clear to the user, it can not be avoided to refer to the Users' Guide [1]. Having it at hand, ready to use, and consulting it whenever something happens which looks weird, or looks like going awry, is recommended.

A good thing to do when questions arise—and many will, is to navigate in the INDEX section of the Users' Guide. Note the two main parts in the Users' Guide: PART A which comments on the physics content and capabilities of the various optical elements and commands, and PART B which details the formatting of the data in an input data file. Two bold numbers generally appear in the guide INDEX, for any item; the first points to Part A, and the second to Part B. Additional considerations that may usefully be given some attention, are documented in the Appendix.

The computation of spin and orbital motion in this code uses stepwise ray-tracing techniques. This means that it solves the Lorentz and T-BMT differential equations proper, with no approximations on particle or spin dynamics, step-by-step. This allows accurate field modeling (and that does not preclude approximate field models if desired anyway) and detailed insight regarding their effect on spin motion.

In any event, one should not lose sight of the goal of the present simulation exercises, which is not especially to learn about a computer code. It is rather to play with, and learn about, spin dynamics in electric and magnetic fields, snakes, rotators, synchrotron radiation and spin diffusion, as a complement to the various theoretical chapters.

14.1.1 Polarized Helion in AGS Booster

14.1.1.1 AGS Booster Parameters

The ring lattice used for these exercises is a simplified version of the AGS Booster, composed of 6 superA super cells. Lattice parameters are given in Table 14.2, the table needs to be completed as part of the exercises.

The superA sequence (Table 14.4) is taken from the MAD8 [7] model used for Booster operation. The resulting optical functions of superA are displayed in Fig. 14.3.

Question 14.1.1.1-1: Complete Table 14.2 with the missing numerical values. These parameters will be used throughout the simulations, in particular in setting proper data values in the simulation input data files.

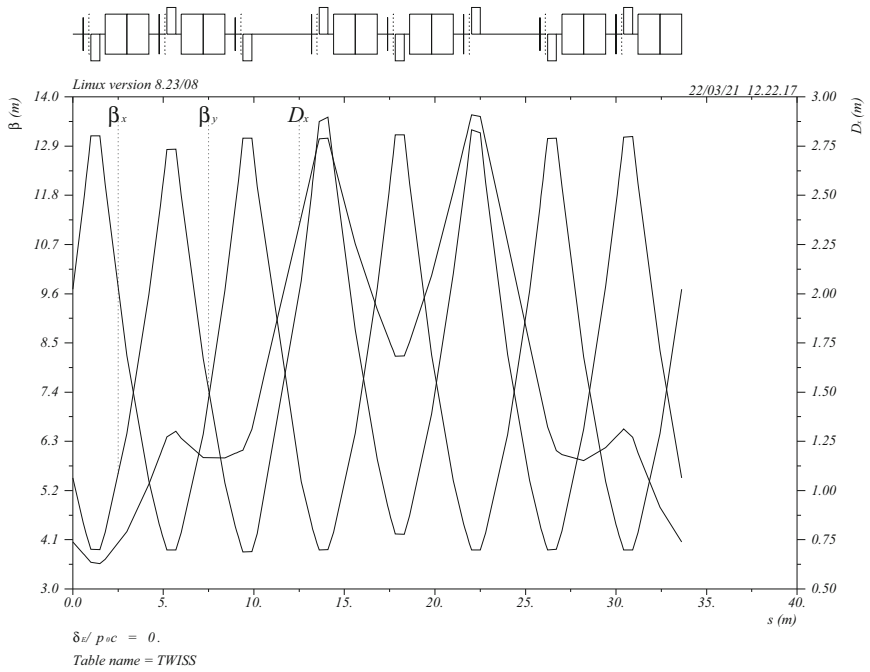

Fig. 14.3 Booster superA cell optical functions, as per MAD8 [7] model used for Booster operation. A simplified Booster lattice, comprised of 6 such super cells (parameters given in Table 14.2), is used in the present simulations

Table 14.2 Booster parameters. The table is to be completed in answer to Question 14.1.1.1-1, accounting for $^3He^{2+}$ parameters given in Table 14.1. The injector DTL (drift tube linac) determines the ion velocity at Booster entrance, namely, $\beta = v/c = 0.0655$ value

Injection β		0.0655
Injection energy	MeV/u	2.0146
Injection $G\gamma$		
Injection $B\rho$	T m	
Extraction energy	GeV/u	
Extraction $G\gamma$		-10.5
Extraction $B\rho$	T m	
Lattice		
Orbit length	m	201.78
Tunes, ν_x, ν_y		4.73, 4.82
Chromaticities, ξ_x, ξ_y		-4.8, -5.2
Momentum compaction α		0.043998
Transition γ		
RF system		
Revolution frequency, f_{rev}	MHz	to
RF harmonic, h		4
Peak voltage	MV	0.4
Frequency, f_{rf}	MHz	to
Spin		
$dG\gamma/d\theta$		

Table 14.3 Beam parameters

Normalized emittances, ε_x, ε_y	($\pi\,\mu$m)	2.5
Longitudinal emittance	eV s	0.5
Momentum spread		$\pm 3\,10^{-4}$

14.1.1.2 Cell and Lattice Optics

It is necessary to first check lattice parameters, *viz* simulation input data files, prior to engaging in fancy spin tracking simulations.

The Zgoubi input data file superA.inc (Table 14.4) has been translated from the MAD model (Sect. 14.1.1.1); this and other Zgoubi input data files used in subsequent exercises can be found in [8].

Question 14.1.1.2-1: Run that file, namely (with [pathTo]/ being the address of the folder that contains the Zgoubi executable on your computer):

```
[pathTo]/zgoubi -in superA.inc
```

This produces the transport matrix of super cell A, and its periodic beam matrix and tunes (logged in zgoubi.res).

Explain the role of the FIT procedure.

Question 14.1.1.2-2: Check the lattice parameters against Table 14.2 data (they are logged at the end of the sequence, bottom of zgoubi.res result listing).

Table 14.4 The superA cell sequence in this superA.inc data file features the markers MARKER[LABEL1=superA_S] and MARKER[LABEL1=superA_E] at its extremities. These labeled MARKERs allow that very section of superA.inc, and that section only, to be INCLUDEd in further job files—INCLUDE has a similar function to CALL in MAD job files. This input file superA.inc itself INCLUDEs the LA1, LA2, LA3, LA6 subsections (Tables 14.5 and 14.6). Comments are provided for guidance, consulting the Users' Guide is unavoidable

```
superA.inc data file
'OBJET'
1000.000000                                                    ! Reference rigidity (kG.cm).
5                ! An option to generate 11 particles (convenient for MATRIX computation),
.01 .001 .01 .001 0. .001                          ! with the sampling specified in this line,
0. 0. 0. 0. 0. 1.                          ! and centered on these values, Y, T, Z, P, s, D.
'FAISCEAU'                                                     ! Local particle coordinates.

'SCALING'                          ! A sort of "power supplies rack", allows tweaking fields
1 5                    ! (a field scaling factor), in 7 different families of magnets, here.
BEND
-1
1.
1
MULTIPOL
-1
1.
1
MULTIPOL  QHA*                          ! These two families, QHA* and QVA* (* is a wild card)
-1                                                                          ! control the tunes.
1.0864492                                                                  !  FIT variable #12.
1
MULTIPOL  QVA*
-1
1.0657342                                                                  !  FIT variable #16.
1
MULTIPOL DVCA*                                  ! Make sure all vertical kickers are zero-ed.
-1
0.
1

'MARKER'  superA_S
'INCLUDE'
1
LA1.inc[LA1S:LA1E]
'INCLUDE'
1
LA2.inc[LA2S:LA2E]
'INCLUDE'
1
LA3.inc[LA3S:LA3E]
'INCLUDE'
1
LA2.inc[LA2S:LA2E]
'INCLUDE'
1
LA1.inc[LA1S:LA1E]
'INCLUDE'
1
LA6.inc[LA6S:LA6E]
'INCLUDE'
1
LA1.inc[LA1S:LA1E]
'INCLUDE'
1
LA2.inc[LA2S:LA2E]

'MARKER'  superA_E

'FIT'                  ! Find the 4D closed orbit (nil, in the present case of perfect cell)
6   nofinal                                    ! and set the (fractional) cell tune values.
1 30 0 [-1,1]
1 31 0 [-10,10]
1 32 0 [-1,1]
1 33 0 [-10,10]
3 12 0 1.
3 16 0 1.
6  1e-15                                                ! 6 constraints (and penalty = 1e-15):
3.1 1 2 #End 0. 1. 0                                                  ! Y_0= Y(end of sequence),
3.1 1 3 #End 0. 1. 0                                                  ! T_0= T(end of sequence),
3.1 1 4 #End 0. 1. 0                                                  ! Z_0= Z(end of sequence),
3.1 1 5 #End 0. 1. 0                                                  ! P_0= P(end of sequence).
0.1 7 7 #End 0.788333333333 1. 0                                             ! 6-cell Qy=4.73/6.
0.1 8 8 #End 0.803333333333 1. 0                                             ! 6-cell Qy=4.82/6.
'FAISCEAU'                                                    ! Local particle coordinates.
'MATRIX'
1  11
'END'
```

Table 14.5 LA1.inc and LA2.inc optical sequences. These are two of the 4 different files (LA1.inc, LA2.inc, LA3.inc, LA6.inc) that make up the LA1.inc-LA2.inc-LA3.inc-LA2.inc-LA1.inc-LA6.inc-LA1.inc-LA2.inc superA.inc super cell sequence of Booster. These LA*.inc are subject to INCLUDE in superA.inc data file (Table 14.4)

```
'MARKER'      LA1S
'DRIFT'    DRIF      L057
57.0400
'MULTIPOL' DVCA1     VKIC
0  .kicker
0.1E-03 10.0000 -0.0E+00 0. 0. 0. 0. 0. 0. 0. 0.
.0 .0  1.00 0.00 0.00 0.00 0.00 0. 0. 0. 0.
4  .1455   2.2670  -.6395  1.1558  0. 0.  0.
.0 .0  1.00 0.00 0.00 0.00 0.00 0. 0. 0. 0.
4  .1455   2.2670  -.6395  1.1558  0. 0.  0.
1.570796327 0. 0. 0. 0. 0. 0. 0. 0. 0.
#20|3|20  Kick
1 0. 0. 0.
'DRIFT'    DRIF      L007
6.9600
'MULTIPOL' SVA1      SEXT
0  .Sext
0.1E+02 10.  0.  0.  0.000 0. 0. 0. 0. 0. 0. 0.
0.00 0.00  1.00 0. .0 0. .0 0. .0 0. .0
6  .1122 6.2671 -1.4982 3.5882 -2.1209 1.723
0.00 0.00  1.00 0. .0 0. .0 0. .0 0. .0
6  .1122 6.2671 -1.4982 3.5882 -2.1209 1.723
0. 0. 0. 0. 0. 0. 0. 0. 0. 0.
2.  ! cm  MultSVA1
1 0. 0. 0.
'DRIFT'    DRIF      L014
13.8050
'DRIFT'    MONI      PUEVA1
0.0000
'DRIFT'    DRIF      L011
11.6867
'MULTIPOL' QVA1      QUAD
0  .Quad
0.493916E+02 10.  0. -0.5472896982 0. 0. 0. 0. 0. 0. 0.
0. 0. 6.00  3.00 1.00 0.00 0.00 0.00 0.00 0. 0. 0. 0.
6  .1122 6.2671 -1.4982 3.5882 -2.1209 1.723
0. 0. 6.00  3.00 1.00 0.00 0.00 0.00 0.00 0. 0. 0. 0.
6  .1122 6.2671 -1.4982 3.5882 -2.1209 1.723
0. 0. 0. 0. 0. 0. 0. 0. 0. 0.
2.  ! cm  MultQVA1
1 0. 0. 0.
'DRIFT'    DRIF      L029
29.4917
'BEND'     DHA1T     SBEN
0  .Bend
1.2096161E+02   0.00E+00   7.2121043E-01
0.00  0.00   0.00000000
4 .2401  1.8639  -.5572  .3904 0. 0. 0.
0.00  0.00   0.00000000
4 .2401  1.8639  -.5572  .3904 0. 0. 0.
1.0000E+00 cm  Bend
3 0. 0. 0.
'BEND'     DHA1Z     SBEN
0  .Bend
1.2096161E+02   0.00E+00   7.2121043E-01
0.00  0.00   0.00000000
4 .2401  1.8639  -.5572  .3904 0. 0. 0.
0.00  0.00   0.00000000
4 .2401  1.8639  -.5572  .3904 0. 0. 0.
1.0000E+00 cm  Bend
3 0. 0. 0.
'MARKER'      LA1E
'END'
```

```
'MARKER'      LA2S
'DRIFT'    DRIF      L057
57.0400
'MULTIPOL' DHCA2     HKIC
0  .kicker
0.1E-03 10.0000 -0.0E+00 0. 0. 0. 0. 0. 0. 0. 0.
.0 .0  1. 0. 0. 0. 0. 0. 0. 0. 0.
4  .1455   2.2670  -.6395  1.1558  0. 0.  0.
.0 .0  1. 0. 0. 0. 0. 0. 0. 0. 0.
4  .1455   2.2670  -.6395  1.1558  0. 0.  0.
0.00 0. 0. 0. 0. 0. 0. 0. 0. 0.
#20|3|20  Kick
1 0. 0. 0.
'DRIFT'    DRIF      L007
6.9600
'MULTIPOL' SHA2      SEXT
0  .Sext
0.1E+02 10.  0.  0.  0.000 0. 0. 0. 0. 0. 0. 0.
0.00 0.00  1.00 0. .0 0. .0 0. .0 0. .0
6  .1122 6.2671 -1.4982 3.5882 -2.1209 1.723
0.00 0.00  1.00 0. .0 0. .0 0. .0 0. .0
6  .1122 6.2671 -1.4982 3.5882 -2.1209 1.723
0. 0. 0. 0. 0. 0. 0. 0. 0. 0.
2.  ! cm  MultSHA2
1 0. 0. 0.
'DRIFT'    DRIF      L014
13.8050
'DRIFT'    MONI      PUEHA2
0.0000
'DRIFT'    DRIF      L012
12.1317
'MULTIPOL' QHA2      QUAD
0  .Quad
0.485016E+02 10.  0.  0.5256342158 0. 0. 0. 0. 0. 0. 0.
0. 0. 6.00  3.00 1.00 0.00 0.00 0.00 0.00 0. 0. 0. 0.
6  .1122 6.2671 -1.4982 3.5882 -2.1209 1.723
0. 0. 6.00  3.00 1.00 0.00 0.00 0.00 0.00 0. 0. 0. 0.
6  .1122 6.2671 -1.4982 3.5882 -2.1209 1.723
0. 0. 0. 0. 0. 0. 0. 0. 0. 0.
2.  ! cm  MultQHA2
1 0. 0. 0.
'DRIFT'    DRIF      L031
29.9367
'BEND'     DHA2T     SBEN
0  .Bend
1.2096161E+02   0.00E+00   7.2121043E-01
0.00  0.00   0.00000000
4 .2401  1.8639  -.5572  .3904 0. 0. 0.
0.00  0.00   0.00000000
4 .2401  1.8639  -.5572  .3904 0. 0. 0.
1.0000E+00 cm  Bend
3 0. 0. 0.
'BEND'     DHA2Z     SBEN
0  .Bend
1.2096161E+02   0.00E+00   7.2121043E-01
0.00  0.00   0.00000000
4 .2401  1.8639  -.5572  .3904 0. 0. 0.
0.00  0.00   0.00000000
4 .2401  1.8639  -.5572  .3904 0. 0. 0.
1.0000E+00 cm  Bend
3 0. 0. 0.
'MARKER'      LA2E
'END'
```

Table 14.6 LA3.inc and LA6.inc optical sequences. These are two of the 4 different files (LA1.inc, LA2.inc, LA3.inc, LA6.inc) that make up the LA1.inc-LA2.inc-LA3.inc-LA2.inc-LA1.inc-LA6.inc-LA1.inc-LA2.inc superA.inc super cell sequence of Booster. These LA*.inc are subject to INCLUDE in superA.inc data file (Table 14.4)

```
'MARKER'      LA3S
'DRIFT'    DRIF      L057
57.0400
'MULTIPOL' DVCA3     VKIC
0  .kicker
0.1E-03 10.0000 -0.0E+00 0. 0. 0. 0. 0. 0. 0. 0. 0.
.0 .0  1. 0. 0. 0. 0. 0. 0. 0. 0.
4  .1455   2.2670  -.6395  1.1558  0. 0.  0.
.0 .0  1. 0. 0. 0. 0. 0. 0. 0. 0.
4  .1455   2.2670  -.6395  1.1558  0. 0.  0.
1.570796327 0. 0. 0. 0. 0. 0. 0. 0. 0.
#20|3|20  Kick
1 0. 0. 0.
'DRIFT'    DRIF      L007
6.9600
'MULTIPOL' SVA3      SEXT
0  .Sext
0.1E+02 10.  0.  0.  0.000 0. 0. 0. 0. 0. 0. 0.
0.00 0.00  1.00 0. .0 0. .0 0. .0 0. .0
6  .1122 6.2671 -1.4982 3.5882 -2.1209 1.723
0.00 0.00  1.00 0. .0 0. .0 0. .0 0. .0
6  .1122 6.2671 -1.4982 3.5882 -2.1209 1.723
0. 0. 0. 0. 0. 0. 0. 0. 0. 0.
2.  ! cm  MultSVA3
1 0. 0. 0.
'DRIFT'    DRIF      L014
13.8050
'DRIFT'    MONI      PUEVA3
0.0000
'DRIFT'    DRIF      L011
11.6867
'MULTIPOL' QVA3      QUAD
0  .Quad
0.493916E+02 10.  0. -0.5472896982 0. 0. 0. 0. 0. 0. 0. 0.
0. 0. 6.00  3.00 1.00 0.00 0.00 0.00 0.00 0. 0. 0. 0.
6  .1122 6.2671 -1.4982 3.5882 -2.1209 1.723
0. 0. 6.00  3.00 1.00 0.00 0.00 0.00 0.00 0. 0. 0. 0.
6  .1122 6.2671 -1.4982 3.5882 -2.1209 1.723
0. 0. 0. 0. 0. 0. 0. 0. 0. 0.
2.  ! cm  MultQVA3
1 0. 0. 0.
'DRIFT'    DRIF      L029
29.4917
'DRIFT'    DRIF      LDHH
121.0000
'MARKER'      CAVITY
'DRIFT'    DRIF      LDHH
121.0000
'MARKER'      LA3E
'END'
```

```
'MARKER'      LA6S
'DRIFT'    DRIF      L057
57.0400
'MULTIPOL' DHCA6     HKIC
0  .kicker
0.1E-03 10.0000 -0.0E+00 0. 0. 0. 0. 0. 0. 0. 0. 0.
.0 .0  1. 0. 0. 0. 0. 0. 0. 0. 0.
4  .1455   2.2670  -.6395  1.1558  0. 0.  0.
.0 .0  1. 0. 0. 0. 0. 0. 0. 0. 0.
4  .1455   2.2670  -.6395  1.1558  0. 0.  0.
0.00 0. 0. 0. 0. 0. 0. 0. 0. 0.
#20|3|20  Kick
1 0. 0. 0.
'DRIFT'    DRIF      L007
6.9600
'MULTIPOL' SHA6      SEXT
0  .Sext
0.1E+02 10.  0.  0.  0.000 0. 0. 0. 0. 0. 0. 0.
0.00 0.00  1.00 0. .0 0. .0 0. .0 0. .0
6  .1122 6.2671 -1.4982 3.5882 -2.1209 1.723
0.00 0.00  1.00 0. .0 0. .0 0. .0 0. .0
6  .1122 6.2671 -1.4982 3.5882 -2.1209 1.723
0. 0. 0. 0. 0. 0. 0. 0. 0. 0.
2.  ! cm  MultSHA6
1 0. 0. 0.
'DRIFT'    DRIF      L014
13.8050
'DRIFT'    MONI      PUEHA6
0.0000
'DRIFT'    DRIF      L012
12.1317
'MULTIPOL' QHA6      QUAD
0  .Quad
0.485016E+02 10.  0.  0.5256342158 0. 0. 0. 0. 0. 0. 0.
0. 0. 6.00  3.00 1.00 0.00 0.00 0.00 0.00 0. 0. 0. 0.
6  .1122 6.2671 -1.4982 3.5882 -2.1209 1.723
0. 0. 6.00  3.00 1.00 0.00 0.00 0.00 0.00 0. 0. 0. 0.
6  .1122 6.2671 -1.4982 3.5882 -2.1209 1.723
0. 0. 0. 0. 0. 0. 0. 0. 0. 0.
2.  ! cm  MultQHA6
1 0. 0. 0.
'DRIFT'    DRIF      L031
29.9367
'DRIFT'    DRIF      LDH
242.0000
'MARKER'      LA6E
'END'
```

Question 14.1.1.2-3: Check the periodic optical functions (logged in zgoubi.res) against MAD8 results (logged in MAD8 "*print*" file).

Question 14.1.1.2-4: Run a TWISS command (replace MATRIX command in superA.inc) to produce the optical functions along the super cell (TWISS logs these in the file zgoubi.TWISS.out). Produce a graph of the latter, compare to Fig. 14.3 from MAD8.

14.1.1.3 Spin Optics

Injection energy (see Table 14.2) is considered in this question. Tracking is needed in some of the questions, it is performed using the input data file given in Table 14.7, in which, compared to Table 14.4, OBJET[BORO] and SCALING coefficients have

Table 14.7 Input data file to track 3 helion ions, on-momentum and at $\delta p/p = \pm 10^{-4}$, and their spins, along Booster. This data file also defines the [SCALING_S:SCALING_E] segment, for INCLUDE purpose—for shortness—in subsequent exercises

```
Track 3 particles and their spin vectors, along superA cell.
! Additional non-void lines here require a comment sign '!'

! Periodic dispersion (from prior lattice parameter computation), for chromatic orbit
! calculation: eta_Y=0.7428, eta'_Y=-0.10475

'OBJET'
0.3074552E3           ! Reference rigidity/kG.cm, for 3He++, at injection beta value 0.0655.
2                          ! An option to define initial particle coordinates, one by one.
3 1                        ! 3 particles are defined, launched on their closed orbit:
 0.742818e-2 -0.10475e-1 0. 0. 0. 1.0001 'p'  ! +1e-4 off-momentum (chromatic orbit coord.);
 0. .0 0. 0. 0. 1. 'o'                 ! on-momentum particle (coordinates are zero, D=1);
-0.742818e-2  0.10475e-1 0. 0. 0. 0.9999 'p'  ! -1e-4 off-momentum (chromatic orbit coord.).
1 1 1

'PARTICUL'   ! Defining the particle species is necessary, in order for the program to solve
HELION                                                          ! the T-BMT equation.
'SPNTRK'                              ! Define initial spin vector. Switch on spin tracking.
4
0.866025403784 0. 0.5                                  ! Initial S_X=S_Z=1/sqrt(2), S_Y=0.
0.707106781187 0. 0.707106781187                       ! Initial S_X=S_Z=1/sqrt(2), S_Y=0.
0.5            0. 0.866025403784                       ! Initial S_X=S_Z=1/sqrt(2), S_Y=0.

'MARKER' SCALING_S   ! A segment, down to "'MARKER' SCALING_E", defined for further INCLUDE.
'SCALING'      ! This sets the magnet power supplies, now that the rigidity has been changed
1 5               ! from 1 Tm to 0.3074552 (injection value). This ensures unchanged optics.
BEND
-1
0.3074552
1
MULTIPOL           ! Default value for any ULTIPOL, unless otherwise specified furtehr down.
-1
0.3074552
1
MULTIPOL  QH*                      ! These two families, QH* and QV* (* stands for whatever),
-1                                                                  ! control the tunes.
0.3074552  * 1.0864492                                             !  FIT variable #12
1
MULTIPOL  QV*
-1
0.3074552   * 1.0657342                                           !  FIT variable #16
1
MULTIPOL DVCA*                                  ! Make sure all vertical kickers are zero-ed.
-1
0.
1
'MARKER'  SCALING_E                                  ! End of [SCALING_S:SCALING_E] segment.

'OPTIONS'
1 1
.plt  2

'INCLUDE'
1
6* superA.inc[superA_S:superA_E]     ! INCLUDE superA segment from superA.inc file, 6 times.

'FAISCEAU'                                                      ! Particle coordinates, here!
'SPNPRT'                  ! Print out spin data, at his location along the optical sequence.

'SYSTEM'                                                                    ! System call.
2                                                        ! 2 successive commands, as follows:
gnuplot <./gnuplot_Zplt_sSpin.gnu      ! Produce a graph of spin components versus distance.
okular gnuplot_Zplt_sSpin.eps &                                  ! Display that graph.

'END'
```

been set to injection rigidity, leaving the optics unchanged (cell optical functions as in Fig. 14.3).

Question 14.1.1.3-1: The spin closed orbit in the ideal ring (six superA cells, planar, no defects) is vertical everywhere.

Tracking shows that this is also the case for off-momentum particles. Is it what's expected? Please explain.

Question 14.1.1.3-2: provide the following simulation: track the spin closed orbit over a turn, for an on-momentum particle, and for off-momentum particles at $dp/p = -10^{-4}$ and $dp/p = +10^{-4}$. Provide a graph of the spin components for these 3 particles.

Add the computation of the spin matrix to get the 1-turn spin map and the spin tune.

Explain the value of the 1-turn spin precession angle (as found for instance under SPNPRT in zgoubi.res).

Question 14.1.1.3-3: What are the spin tune values, on-momentum and at $dp/p = \pm 10^{-4}$?

14.1.1.4 Depolarizing Resonances

Question 14.1.1.4-1: Begin filling in Tables 14.8 and 14.9, for the moment with the respective locations ($G\gamma$ values) of

- imperfection resonances,
- systematic intrinsic resonances,

over the energy range of concern (Table 14.2). These data will be used in subsequent questions.

Table 14.8 Imperfection resonance locations ($G\gamma$) and strengths (ϵ_n); table to be completed. Note: give resonance strengths normalized to *rms* closed orbit amplitude

$G\gamma$	$\lvert\epsilon_n\rvert/y_{\text{co, rms}}$		
	Theory	Tracking	
		Stationary	Crossing
-5			
-6			
etc.			

Table 14.9 Systematic intrinsic resonances; table to be completed. Note: give resonance strengths normalized to the square root of the invariant value

$kM \pm \nu_y$	$G\gamma$	$\lvert\epsilon_n\rvert/\sqrt{\varepsilon_y/\pi}$		
		Theory	Tracking	
			Stationary	Crossing
$0 - \nu_y$				
$-12 + \nu_y$				
etc.				

Question 14.1.1.4-2: Illustrate the crossing of intrinsic resonances (the strengths of which are ε_y-dependent) with two graphs of $S_y(G\gamma)$, as follows:

- take a few particles evenly distributed in phase on the same vertical invariant ε_y (OBJET[KOBJ=8] can be used; or initial coordinates may be generated off-line and then OBJET[KOBJ=2] used). The horizontal invariant ε_x can be taken null (explain why);
- accelerate (use CAVITE, placed for simplicity at either end of the optical sequence) from injection $G\gamma$ to some $G\gamma \lesssim -18 + \nu_y$ in two different cases: $\varepsilon_y = 2.5\,\pi\,\mu$m and 10 times less.

Comparing these two graphs, essentially two things are observed: please comment.

Question 14.1.1.4-3: Provide a graph showing the span of the magnetic field strengths experienced in the vertical quadrupoles by the orbiting particles, depending on their initial betatron phase.

14.1.1.5 Imperfection Resonance Strengths

Introduce a particular series of random vertical misalignments of the 48 quadrupoles around Booster. ERRORS could be used for that, to randomly modify MULTIPOL[KPOS=5] alignment data; however, it is suggested instead to use the misalignment series proposed in Table 14.10, for consistency with the detailed solution to this and subsequent questions given in Sect. 14.2 (Sects. 14.2.1.5 and 14.2.1.7).

A python script amongst other means can be written to apply this series to the six, now distinct, superA, superB, superC, . . ., superF super cells. An example script is shown in Table 14.11 that saves a new include file that contains superA through superF as zgoubi_misaligned.INC. These modified super*.inc files will be used in place of the six superA.inc in the previous exercises.

Question 14.1.1.5-1: Calculate the strengths of the imperfection resonances excited from $|G\gamma| = 5$ to $|G\gamma| = 10$, using the theoretical thin lens model (Eq. 2.29).

Hint: produce a zgoubi.TWISS.out file using TWISS command, accounting for the now non-zero vertical closed orbit excursion using FIT (preceding TWISS), to evaluate Eq. 2.29.

Complete the "theory" column of Table 14.8 accordingly.

14.1.1.6 Intrinsic Resonance Strengths

Assume an invariant value equal to the transverse beam emittance (Table 14.3). Use your input file without quadrupole misalignments.

Question 14.1.1.6-1: Calculate the strengths of the intrinsic resonances, using the theoretical thin lens model (Eq. 2.35).

Table 14.10 A possible random vertical misalignments series for the 48 quadrupoles around Booster (this is the data series used in the solutions, Sects. 14.2 and 14.2.1.5). It is now necessary to distinguish the 48 quadrupoles of the six, now distinct, super cells: essentially a matter of renaming each quadrupole, for instance with suffixes A1 to A8 (superA cell), B1 to B8 (superB cell), . . ., F1 to F8 (superF cell)

```
# superA:                    # superD:
 0.6723850    QVA1           -0.0082470    QVD1
 0.7345750    QHA2            0.0172110    QHD2
 0.7262320    QVA3            0.0307940    QVD3
 0.5887510    QHA4            0.0098080    QHD4
 0.4926790    QVA5           -0.0629690    QVD5
 0.4026180    QHA6           -0.2462660    QHD6
 0.3593190    QVA7           -0.5099270    QVD7
 0.3802380    QHA8           -0.7531260    QHD8
# superB:                    # superE:
 0.3218880    QVB1           -0.9371040    QVE1
 0.2246450    QHB2           -1.1170480    QHE2
 0.1578100    QVB3           -1.1903730    QVE3
 0.1243620    QHB4           -1.2219470    QHE4
 0.0929490    QVB5           -1.2518560    QVE5
 0.0385940    QHB6           -1.2414150    QHE6
-0.0469160    QVB7           -1.2676770    QVE7
-0.0152930    QHB8           -1.2564210    QHE8
# superC:                    # superF:
-0.0345980    QVC1           -1.2332150    QVF1
-0.0029100    QHC2           -1.1096020    QHF2
 0.0949500    QVC3           -0.9485780    QVF3
 0.0761360    QHC4           -0.6493420    QHF4
 0.0156440    QVC5           -0.4064320    QVF5
 0.0002140    QHC6           -0.1635210    QHF6
-0.0111360    QVC7            0.0906590    QVF7
-0.0080890    QHC8            0.3853270    QHF8
```

Hint: use the optical file zgoubi.TWISS.out produced in Sect. 14.1.1.2 to evaluate Eq. 2.35.

Complete the "theory" column of Table 14.9 accordingly.

14.1.1.7 Spin Motion Through Imperfection Resonances

It is suggested here to use the input file with misaligned quadrupoles of Sect. 14.1.1.5 (this is the case for the solutions provided in Sects. 14.2 and 14.2.1.7).

Question 14.1.1.7-1: Stationary case (fixed energy).

Complete Table 14.8, "stationary" column, by tracking at various distances near resonance, using Eq. 2.49.

Question 14.1.1.7-2: Accelerating through the resonance.

CAVITE[IOPT=3] may be used for acceleration.

Complete Table 14.8, "crossing" column, by tracking through every integer resonance from $G\gamma = -5$ to $G\gamma = -10$.

14.1.1.8 Spin Motion Through Intrinsic Resonances

Question 14.1.1.8-1: Stationary case (fixed energy).

Consider one of the strong resonances found in 14.1.1.5.

Table 14.11 Example python code to modify given .inc files to allow quadrupole misalignments using KPOS=5 and allow these alignments to be based off an external file. The code: reads in existing include files and quadrupole alignment data, parses through them and finds quadrupoles, modifies the quadrupole KPOS line to use KPOS=5 with alignment data from external file, compiles all modified include files, saves a new include file for the entire Booster lattice, zgoubi_misaligned.INC. Commented lines allow modifying vertical corrector strengths in order to use the harmonic correction method

```
### Python code to parse existing .inc files and change quadrupole alignment to KPOS=5
#   Alignments for quadrupoles provided by external file (alignment.txt)
#   alignment.text should contain alignment data with a single column, '\n' separated
#   To be run in folder with LA1.inc, LA2.inc, LA3.inc, LA6.inc, and alignment.txt

import numpy as np

### Read in lattice files
A1=open('LA1.inc').read()
A2=open('LA2.inc').read()
A3=open('LA3.inc').read()
A6=open('LA6.inc').read().replace("'END'","")   #Remove 'END' from cell

### Load in alignment data
Dz=np.loadtxt('alignment.txt')

### Process cell files to insert KPOS5 syntax to Quadrupoles
def insert_KPOS5(line,index):
    temp=line.split('\n')          #Split file on new line
    for i in range(0,len(temp)):   #Loop through file
        if 'QUAD' in temp[i]:      #Mark line if keyword QUAD is used
            idx=i
    temp2=[]
    for i in range(0,len(temp)):
        if i==idx+9:               #From QUAD keyword, 9th line after calling keyword is KPOS parameters
            temp2.append("""5 0 0 %.8f 0 0 0 """%(Dz[index]))
        else:                      #Input line as is if it is not QUAD KPOS line
            temp2.append(temp[i])
    LINE="\n".join(temp2)          #Recombine lines into one string
    return LINE

### Set harmonic corrector current based off the harmonic and corrector number
def harm_corr(harmonic_number, corrector_number, phase_shift,currents):
    [corrcalsO,corrcalcO]=currents
    corrector_strength=0.
    for i in harmonic_number:
        phase=2*i*corrector_number*np.pi*8.40729167/201.8+phase_shift
        corrector_strength+=(np.multiply(corrcalsO[i],0.975*1e3*np.sin(phase))+np.multiply(corrcalcO[i],0.975*1e3*np.cos(phase)))
    return corrector_strength

### Modify vertical corrector strengths for harmonic orbit correction
def set_VCorr(line,index,currents):
    temp=line.split('\n')
    for i in range(0,len(temp)):
        if 'VKIC' in temp[i]:
            idx=i
    BCorr=harm_corr(harm_no, index,0,currents)
    temp2=[]
    for i in range(0,len(temp)):
        if i==idx+2:
            temp2.append("""0.100000E-03 10.0000 %.8f 0.0 0.0 0.0 0.0 0.0 0.0 0.0 0.0 0.0 0.0"""%(BCorr))
        else:
            temp2.append(temp[i])
    LINE="\n".join(temp2)
    return LINE

### Function to build each Booster superperiod.
def build_super(sindex,line,currents):
    KEY=line.replace('super','')   #Get the super period letter from name
    #Set temporary cell with inserting KPOS5
    tA1=insert_KPOS5(A1,sindex*8+0)
#    tA1=set_VCorr(tA1,sindex*8/2+0,currents)   #Modify vertical corrector strengths to desired harmonic correction
    #Replace all names to have correct superperiod letter and cell number
    L1=tA1.replace("DVCA1",'DVC%s1'%KEY).replace("SVA1",'SV%s1'%KEY).replace("QVA1",'QV%s1'%KEY).replace("DHA1",'DH%s1'%KEY)
    #Repeat for each cell
    tA2=insert_KPOS5(A2,sindex*8+1);
    L2=tA2.replace("DHCA2",'DHC%s2'%KEY).replace("SHA2",'SH%s2'%KEY).replace("QHA2",'QH%s2'%KEY).replace("DHA2",'DH%s2'%KEY)
    tA3=insert_KPOS5(A3,sindex*8+2); #    tA3=set_VCorr(tA3,sindex*8/2+1,currents)
    L3=tA3.replace("DVCA3",'DVC%s3'%KEY).replace("SVA3",'SV%s3'%KEY).replace("QVA3",'QV%s3'%KEY)
    tA4=insert_KPOS5(A2,sindex*8+3);
    L4=tA4.replace("DHCA2",'DHC%s4'%KEY).replace("SHA2",'SH%s4'%KEY).replace("QHA2",'QH%s4'%KEY).replace("DHA2",'DH%s4'%KEY)
    tA5=insert_KPOS5(A1,sindex*8+4); #    tA5=set_VCorr(tA5,sindex*8/2+1,currents)
    L5=tA5.replace("DVCA1",'DVC%s5'%KEY).replace("SVA1",'SV%s5'%KEY).replace("QVA1",'QV%s5'%KEY).replace("DHA1",'DH%s5'%KEY)
    tA6=insert_KPOS5(A6,sindex*8+5);
    L6=tA6.replace("DHCA6",'DHC%s6'%KEY).replace("SHA6",'SH%s6'%KEY).replace("QHA6",'QH%s6'%KEY)
    tA7=insert_KPOS5(A1,sindex*8+6); #    tA7=set_VCorr(tA7,sindex*8/2+1,currents)
    L7=tA7.replace("DVCA1",'DVC%s7'%KEY).replace("SVA1",'SV%s7'%KEY).replace("QVA1",'QV%s7'%KEY).replace("DHA1",'DH%s7'%KEY)
    tA8=insert_KPOS5(A2,sindex*8+7);
    L8=tA8.replace("DHCA2",'DHC%s8'%KEY).replace("SHA2",'SH%s8'%KEY).replace("QHA2",'QH%s8'%KEY).replace("DHA2",'DH%s8'%KEY)
```

(continued)

Table 14.11 (continued)

```
    #Add strings together line to build new include files
    RETURN="""
%s\n%s\n%s\n%s\n%s\n%s\n%s\n%s"""%(L1,L2,L3,L4,L5,L6,L7,L8)
    return RETURN

### Function to execute zgoubi based off desired snake rotation angle, phi
def Generate_INC():
    #Build the superperiods
    Asuper=build_super(0,"Asuper",'')
    Bsuper=build_super(1,"Bsuper",'')
    Csuper=build_super(2,"Csuper",'')
    Dsuper=build_super(3,"Dsuper",'')
    Esuper=build_super(4,"Esuper",'')
    Fsuper=build_super(5,"Fsuper",'')
    DAT_file='''MARKER'      START  \n%s\n%s\n%s\n%s\n%s\n%s\n'MARKER'      END"%(Asuper,Bsuper,Csuper,Dsuper,Esuper,Fsuper))
    DATA=open('zgoubi_misaligned.INC','w')
    DATA.write('%s'%DAT_file)
    DATA.close()
#Build and save new include file using KPOS=5 in quadrupoles
Generate_INC()
```

For various distances to the resonance (say, $\Delta_n = N \times |\epsilon_n|$, N is a small integer), produce a graph of the motion of the spin components $S_{x,s,y}$(turn), over a few hundred turns—assume vertical initial spin vector orientation for simplicity.

Produce a Fourier spectrum of the horizontal components (Fourier amplitude versus frac(ν_{sp})); explain the frequency components observed in the spectrum.

Produce tables, or graphs, which compare theory with the following results:

(i) average values of the vertical component S_y; of the horizontal components S_x, S_s.
(ii) dependence of spin component precession frequencies upon distance to the resonance.

Question 14.1.1.8-2: Complete Table 14.9, "stationary" column, by tracking at various distances near the resonance, using Eq. 2.49.

Question 14.1.1.8-3: Accelerating through the resonance.

CAVITE[IOPT=3] may be used for acceleration.

Consider the strong resonance of Question 14.1.1.8-1.

Deduce the resonance strength from the Froissart-Stora formula; check against the theoretical value obtained in Question 14.1.1.6-1 and against the numerical value(s) in Question 14.1.1.8-2.

Question 14.1.1.8-4: Complete Table 14.9, "crossing" column, by tracking through every systematic intrinsic resonance.

14.1.1.9 Spin Motion Through a Weak Resonance

Consider a weak intrinsic resonance (take for instance a random one, or otherwise a systematic with a small enough invariant value), such that $P_f \approx 0.99\, P_i$.

Question 14.1.1.9-1: Compute the turn-by-turn spin motion S_y(turn) across that resonance, produce S_y(turn) graph.

Match that spin motion S_y(turn) with the Fresnel integral model. From this match, obtain the resonant $G\gamma$ value, vertical tune, and resonance strength.

14.1.1.10 Beam Depolarization Using a Solenoid

Depolarization of the beam while it is still in the accelerator may be a method for calibrations. A longitudinal field can be introduced locally in the lattice for that. Depolarization is obtained by crossing an integer resonance. This is the object of the present simulation.

Question 14.1.1.10-1: Introduce a $L = 1$ meter solenoid, field B_s (SOLENOID may be used for that, or a 1-D axial field map using BREVOL), in a straight section in the defect free Booster lattice.

Determine B_s from theory for proper value of the strength $|\epsilon_n|$ of an appropriate integer resonance. Plot $P_f(B_s L)$.

Accelerate (using CAVITE[IOPT=3]) a particle with vertical initial spin through that resonance, check that spin motion ends up in the vicinity of the median plane, asymptotically.

Repeat the simulation using SPINR, a pure spin rotation, in lieu of SOLENOID.

Question 14.1.1.10-2: Check depolarization of a beam with Gaussian coordinate distributions in transverse coordinates and momentum spread, with the following parameters:

$$\varepsilon_x = \varepsilon_y = 1\,\pi\,\mu m, \qquad \sigma_{\frac{\delta p}{p}} = 10^{-3}$$

14.1.1.11 Introduce a Partial Snake

A partial Siberian snake makes imperfection resonances strong, so causing complete adiabatic spin flip at every imperfection resonance crossing (Chap. 1). The forbidden spin tune band it induces near integer $G\gamma$ allows for placing the fractional part of the vertical betatron tune inside this gap, so forbidding crossing of intrinsic resonances $\nu_{\mathrm{sp}} = n \pm \nu_y$.

The goal in this exercise is to assess the efficiency of a partial snake in overcoming integer resonances, and the necessary partial snake strength for preservation of polarization during acceleration.

Question 14.1.1.11-1: Create a vertical closed orbit around Booster lattice. This can use ERRORS to generate random vertical misalignment of lattice quadrupoles (this is the case for the solutions provided in Sects. 14.2 and 14.2.1.11; another possibility would be to re-use the input file with misaligned quadrupoles of Sect. 14.1.1.5). Only one ring optics, meaning a single set of quadrupole misalignments is considered in the exercise, as it mostly aims at addressing principles (it is not intended to perform statistics on misalignment samples).

Calculate the strengths of the spin resonances so excited.

Accelerate a particle on the vertical closed orbit, over $G\gamma : -6.5 \rightarrow -10.5$, provide a graph of $\mathrm{S_y}$(turn).

Check the location and spacing of the resonances, confirm theoretical expectations.

Question 14.1.1.11-2: Install in a drift a longitudinal-axis partial snake (use SPINR for pure spin rotation, avoiding any orbit and optics perturbation).

Inhibit ERRORS (ERRORS[ONF=0]) and set the snake angle to $\phi_{\text{snake}} = 2\pi|Jn|$, with $|Jn|$ being the strength of the strongest resonance.

Set the lattice rigidity on $G\gamma_n = 7$ resonance. Find the spin closed orbit for an on-momentum particle. Plot the spin orbit components around the ring, $S_{x,y,s}(s)$. Explain what is observed.

Question 14.1.1.11-3: Still in the case of a perfect ring, planar closed orbit, compute the $G\gamma$ dependence of the spin closed orbit vector, observed at the snake. Produce a graph of the spin orbit components $S_{\text{x,s,y}}(G\gamma)$.

Produce a graph of the spin tune dependence on $G\gamma$, $\nu_{\text{sp}}(G\gamma)$.

Question 14.1.1.11-4: Add quadrupole misalignments now (ERRORS[ONF=1]). Thus, spin-wise, both effects now apply, a vertical closed orbit distortion and local spin rotation by a snake (SPINR[$\phi_{\text{snake}} = 1.224°$]).

Accelerate a particle on the vertical closed orbit, over $G\gamma : -6.5 \rightarrow -10.5$, provide a graph of S_y(turn). Explain what is observed.

Question 14.1.1.11-5: Increase the spin precession in the snake in steps, observe how it affects spin rotation, confirm theoretical expectations.

Justify a minimal spin precession by the snake for spin flip upon resonance crossing.

14.1.1.12 Introduce Full Snakes

Imperfection resonance strengths increase in proportion to γ, thus full Siberian snakes are used at high energy, in order to overcome integer resonances (Chap 1). A full Snake maintains the stable spin precession direction unperturbed as long as the spin rotation it causes (its strength) is much larger than the spin rotation due to the resonance driving fields (Chap. 1).

Based on the previous exercises, set lattice and beam input data in the following way:

- Set the vertical beam emittance to large enough a value to cause polarization losses at one or more intrinsic resonances.
- Introduce a random closed orbit distortion sufficiently large that some imperfection resonances create polarization loss during acceleration.
- Set the snake to "full" mode, $\phi_{\text{snake}} = 180°$, longitudinal-axis rotation.
- $G\gamma : -6.5 \rightarrow -13.5$ acceleration range will be considered, so to include three systematic intrinsic resonances (as comes out of the studies in Sect. 14.1.1.4).

Question 14.1.1.12-1: Compute spin closed orbit and spin tune. Compute spin orientation at opposite azimuth ($\Delta\theta = 180°$) to the snake.

Repeat for $dp/p = 10^{-4}$ beam momentum offset.

Which parameters depend on the energy and which do not? Check against expectation from theory.

Question 14.1.1.12-2: Accelerate over $G\gamma : -6.5 \rightarrow -13.5$. Is there any polarization loss?
Question 14.1.1.12-3: Now use a horizontal emittance as large as the vertical one. Accelerate over $G\gamma : -6.5 \rightarrow -13.5$. Is there any polarization loss?
Question 14.1.1.12-4: Add a second snake, at proper location and with proper axis orientation to obtain a spin tune of 0.5 independent of beam energy.

Compute the spin closed orbit around the ring. How is it different from the single snake case?

Compute the spin closed orbit and spin tune for $dp/p = 10^{-4}$ beam momentum offset. Compare with on-momentum parameters, check against expectation from theory.

Accelerate a beam over $G\gamma : -6.5 \rightarrow -13.5$. Is there any polarization loss?

14.1.1.13 High Order Snake Resonances

Set the vertical beam emittance to a value which is large enough to create polarization losses at one or more intrinsic resonances. Introduce a random closed orbit distortion sufficiently large that some imperfection resonances create polarization loss during acceleration. Use the lattice with two snakes. Select the snake axes such that a condition for 2nd order snake resonance with the vertical betatron tune is satisfied.
Question 14.1.1.13-1: Accelerate over $G\gamma : -6.5 \rightarrow -13.5$, produce a graph of $\langle S_y(\text{turn}) \rangle$.

Remove the closed orbit distortion, repeat the acceleration cycle, produce a graph of $\langle S_y(\text{turn}) \rangle$.

Compare the results, explain the difference in the polarization loss between the cases with and without the closed orbit distortion.
Question 14.1.1.13-1: Select the snake axes orientation such that a condition for 3rd order snake resonance with vertical betatron tune is satisfied.

Accelerate over $G\gamma : -6.5 \rightarrow -13.5$, produce a graph of $\langle S_y(\text{turn}) \rangle$. Is there polarization loss? Explain the difference in the polarization loss between 2nd and 3rd order resonances.

14.1.1.14 Harmonic Orbit Correction

Using the quadrupole alignment data, perform a harmonic scan for both a strong and a weak imperfection resonance found in Question 14.1.1.5-1. Each corrector magnet is 10 cm long, has an excitation of 9.75 G/A, and a maximum corrector current of 25 A. Power the corrector magnets according to:

$$B_{j,h} = a_h \sin(h\theta_j) + b_h \cos(h\theta_j) \tag{14.1}$$

where j is the corrector number, θ_j is the location in the ring, a_h and b_h are the amplitudes for harmonic h. Provide the resulting P_f data and fit it with a Gaussian to find $I_{c,0}$ and $I_{s,0}$, and the associated σ_s and σ_c values.
At each of the resonances, is it more reasonable to correct the harmonics or exacerbate them?
How accurate must the harmonic corrector currents of the two families be to have a $< 1\%$ polarization loss at each of the resonances?
Track particles through the two imperfection resonances with your desired corrector current. What is the polarization loss through the two resonances?

14.1.1.15 Preserve Polarization Using Tune-Jump

When particles encounter a resonance, if the crossing speed is fast enough, the spin will not be disturbed by the resonance and the polarization will be preserved. The acceleration speed is limited by the RF system and magnet ramping rate, so fast crossing speed needs to come from another method.

The tune jump technique uses dedicated quadrupoles to cause a swift tune change $\frac{d\nu_y}{d\theta}$, so increasing the resonance crossing speed according to

$$\alpha = \frac{dG\gamma}{d\theta} \pm \frac{d\nu_y}{d\theta}, \tag{14.2}$$

The $|G\gamma| = 0 + \nu_y$ resonance is considered in this exercise, to simulate the fast tune jump method as sketched in Fig. 14.4. Booster simulation input data files of Sect. 14.1.1.2 (Tables 14.4, 14.5, 14.6, and 14.7) will be used in the following questions, possibly modified as needed.
Question 14.1.1.15-1: No tune-jump setting of the quadrupoles in this first question, perfect Booster ring optics is considered.

Take an RF cavity voltage of 100 kV (30° synchronous phase) so an appreciable depolarization can be observed. What is the expected value of $\frac{dG\gamma}{d\theta}$ with this RF setting?

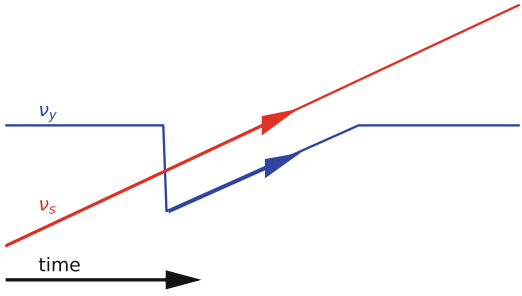

Fig. 14.4 Cartoon showing the fast tune jump method where ν_y sweeps across ν_s quickly, increasing the crossing speed (Eq. 14.2) so minimizing polarization loss as follows from Eq. 2.44

Take $B\rho = 2.12998742$ at the start of the tracking, upstream of the resonance (i.e., $|G\gamma| = 4.59646969$, 276.7452 MeV kinetic energy). Calculate what turn $N_{0+\nu_y}$ the resonance is located at.

Consider a particle on $\varepsilon_y = 1.864 \times 10^{-7}\,\pi$m vertical invariant. Assume spin initially vertically aligned. What is the expected asymptotic polarization value, P_f, upon crossing of this resonance?

Run a numerical simulation of this resonance crossing. Note: SCALING in Table 14.12 can be used by simply changing the data under "MULTIPOL QV" so to recover constant tunes $\nu_x = 4.73$, $\nu_y = 4.82$ all the way (as in earlier exercises).

Question 14.1.1.15-2: Change the SCALING input parameters so the setpoint of vertical quadrupoles (labeled QV*) begins to change at turn $N_{0+\nu_y}$-50 and continues to $N_{0+\nu_y}$+50 with a total change of -5%. Set the change to return the nominal vertical quadrupole field value at turn $N_{0+\nu_y}$+1050. These SCALING settings are detailed in Table 14.12.

What is the new crossing speed with this tune-jump setting of the vertical quadrupoles?

Calculate the expected P_f given the resonance strength and the new crossing speed. Does this agree with the value from the simulation?

Table 14.12 Detailed setting of SCALING for tune jump simulation. Compared to earlier exercises, the change essentially concerns the vertical quadrupole scaling data, namely under "MULTIPOL QV*", with SCALING[NT=5], which indicates that a series of 5 different scaling coefficient values follow (the data line following NT) at 5 different timings (shown on the next data line in units of the turn number)

```
'SCALING'                              ! This sets the power supplies for unchenged optics,
1 7                                  ! given a reference rigidity OBJET[BORO=2.12998742e3].
BEND
-1
2.12998742
1
MULTIPOL
-1
2.12998742
1
MULTIPOL  QH*              ! These two families, QH* and QV* (* stands for whatever suffix),
-1                                                                    ! control the tunes.
2.12998742      *   1.0864492
1
MULTIPOL  QV*               ! QV* quadrupole family field changes to cause tune jump in the
5                                                          !  vicinity of the resonance.
2.27000043  2.81833569  2.832133844842106  3.51572336  3.81685555
0 1400 1600 3500 4503
MULTIPOL  SH*                    ! Chromaticies may be controlled, via these two sextupoles
-1                                                                      ! families.
2.12998742
1
MULTIPOL  SV*
-1
2.12998742
1
MULTIPOL DVCA*                              ! Make sure all vertical kickers are zero-ed.
-1
2.12998742
1
```

14.1.1.16 Preserve Polarization Using an AC Dipole

An AC dipole can preserve polarization through intrinsic resonances by driving large amplitude vertical betatron oscillations of the entire bunch. This is done with a horizontal magnetic field that oscillates in phase with the vertical motion of the particles. The amplitude of the driven oscillations, Y_{coh}, follows (Eq. 5.11)

$$Y_{coh} = \frac{B_m L}{4\pi B\rho \delta_m} \beta_y$$

where $B_m L$ is the integrated field of the AC dipole magnet, β_y is the beta function at the AC dipole and $B\rho$ is the bunch rigidity.

For simulation purposes, create a copy of superA.inc Booster superperiod (Table 14.4), which will be called superA2.inc in the following, in which a new half-cell is used, LA32.inc, a copy of LA3.inc (Table 14.6). In LA32.inc, the long drift section now includes a 1 kG, 0.5 m vertical dipole, simulated using MULTIPOL, labeled 'ACD'.

The SCALING command in superA.inc, in addition, uses the option NT=-88 for that 'MULTIPOL ACD' element of the optical sequence, so to define it as an AC dipole. The format for option NT=-88 is:

```
MULTIPOL ACD
-88
0    0.19   0.19   12.2
100  700    1300   700
```

The first line following NT=-88 specifies the AC dipole phase offset, the AC dipole tune Q1 at the start of the sweep, tune Q2 at the end of the sweep, and a scaling factor to be applied to the magnet field. The next line specifies the duration of these steps, namely, N_{in} =hold duration (field held at zero), N_{up} =ramp up, N_{flat} =plateau, N_{down} =ramp down.

Set Q1=Q2=(1-frac(ν_y+0.01))

Use OBJET[KOBJ=2] to create a set of 32 particles with the following coordinates to represent a bunch with RMS size [9]:

$$y = A_n C \cos(j\pi/4) \tag{14.3}$$

and

$$y' = A_n C \sin(j\pi/4) \tag{14.4}$$

for j $\in \{0, 1, 2, \ldots, 7\}$, C $\in \{-0.2671, -0.94, -1.9617, -4.1589\}$ and A_n an amplitude factor.

Question 14.1.1.16-1: Track particles across the $|G\gamma| = 0 + \nu_y$ with AC dipole field scaling factor set to 0.0. Does P_f with the 32 particles equal P_f value obtained with a single particle at the RMS amplitude?

Question 14.1.1.16-2: Set the scale factor to 10 G and track particles again. What is the value of P_f?

Determine what field is needed to get spin-flip from 100% to −99%.

14.1.1.17 Acceleration of a Polarized 6D Bunch

In this question, a simulation of the acceleration of a 100-particle bunch from $G\gamma = -5.5$ to $G\gamma = -13.5$ is set up and run.

The lattice is the same as before, lattice and acceleration parameters are taken from Table 14.2. Bunch parameters are taken from Table 14.3.

Synchrotron motion in the bunch is accounted for in this simulation: use CAVITE [IOPT=2].

Install selected polarization preservation measures based on the previous questions, in order to maximize polarization transmission through the resonances present in that energy range.

In performing the following, comment on the results obtained in regard to expectations, justify results based on theoretical expectations.

From tracking output data (logged turn-by-turn in zgoubi.fai), produce graphs of

- horizontal and vertical beam excursions,
- transverse and longitudinal phase spaces,
- a few individual spins,
- average bunch polarization,

over the acceleration range.

Produce histograms of the 6 beam coordinates at the top energy. Produce the spin component densities at the top energy. Hint: use HISTO; it is possible to plot from zgoubi.HISTO.out—this requires HISTO[PRINT]. Zpop can be used as well by reading the data from zgoubi.fai.

14.1.2 Electron Spin Dynamics, Synchrotron Radiation

The AGS Booster ring is utilized for the exploration of electron polarization. The optical functions of one super cell are displayed in Fig. 14.3, as described in Sect. 14.1.1.1. The electron beam energy is chosen at a relatively high energy of 10 GeV in order to have the beam reach the equilibrium in a short simulation time. The polarization is evaluated after a few damping times. There are three assignments for the electron polarization studies:

- calculation of equilibrium emittances and energy spread,
- study of spin diffusion, and
- exploration of spin matching technique.

In this study, we will be mainly using somewhat modified versions of the input files [10] that were introduced in Sect. 14.1.1.2 and subsequent sections. Note that,

- moving from helions to electrons simulation is essentially a matter of changing the reference rigidity (OBJET[BORO] or MCOBJET[BORO]) and the nature of

Table 14.13 Left: Zgoubi code producing a table of the optical functions zgoubi.TWISS.out. Right: the scaling_10GeVel.inc INCLUDE file, also used in subsequent exercises. The superA.inc INCLUDE file, which defines the Booster ring optical sequence is given in Table 14.4, it describes one of the six booster super-cells

```
Twiss parameters
'OBJET'
33.3564095089e3                  ! 10cGeV E_k+M e- or e+.
5
.01 .001 .01 .001 0. .001
0. 0. 0. 0. 0. 1.

'PARTICUL'   ! e+, not e-, is stated here, as the optics
POSITRON ! was initially set for positive charge (3He2+).

'SPNTRK'
3

'SRLOSS'
0                                !  SR loss on or off (1/0).
BEND                             ! BENDs only are concerned.
1 123456

'INCLUDE'
1
scaling_10GeVel.inc[SCALING_S:SCALING_E]

'INCLUDE'
1
6* superA.inc[superA_S:superA_E]

'TWISS'
2 1. 1.

'SYSTEM'
1
gnuplot <./ gnuplot_TWISS.gnu

'END'
```

```
! scaling_10GeVel.inc INCLUDE  file.
'MARKER'  SCALING_S

'SCALING'
1 6
BEND
-1
33.3564095089
1
MULTIPOL
-1
33.3564095089* 1.
1
MULTIPOL  QH*    ! Quadrupoles set for Qx=4.73, Qy=4.82.
-1
33.3564095089* 1.0864799            !  FIT variable #12.
1
MULTIPOL  QV*
-1
33.3564095089* 1.0657626            !  FIT variable #16.
1
MULTIPOL  SH*
-1
33.3564095089
1
MULTIPOL  SV*
-1
33.3564095089
1

'MARKER'  SCALING_E

'END'
```

the particle (PARTICUL[ELECTRON], from PARTICUL[HELION]). To avoid having to change the polarities of the magnetic fields in the AGS Booster that are designed for the positively charged particles and thus simplify the set-up of the simulation, we use PARTICUL[POSITRON];

- synchrotron radiation from all the dipole magnets is introduced by SRLOSS. With the OPTIONS[WRITE ON] (default option), one can check the expected theoretical synchrotron radiation loss after each BEND in zgoubi.res file. Synchrotron radiation statistics can be logged in zgoubi.res using SRPRNT;
- RF voltage and phase need to be set correctly to compensate the energy loss due to synchrotron radiation.

14.1.2.1 Electron Equilibrium Emittances and Energy Spread

When injected into storage ring, an electron bunch, if unmatched, will eventually reach equilibrium emittances, under the effect of synchrotron radiation (SR). This is the effect addressed in these simulation exercises.

The electron equilibrium emittances and damping rates can be calculated analytically, as discussed in Chap. 6, using the Twiss and dispersion parameters of the linear optics design. These damping parameters in a circular accelerator or in a storage ring can also be obtained from a particle tracking simulation.

Table 14.14 Gnuplot script for plotting the optics and orbit results from zgoubi.TWISS.out

```
set title "Optical functions, from zgoubi.TWISS.out" font "roman,16"

set xlabel "s [m]" font "roman,16"
set ylabel "{/Symbol b}_x, {/Symbol b}_y [m]" font "roman,13"
set y2label "{/Symbol h}_x, {/Symbol h}_y" font "roman,13"

set xtics  font "roman,12" nomirror
set x2tics  font "roman,12" mirror
set ytics  font "roman,12" nomirror
set y2tics  font "roman,12" nomirror

set key t c maxrows 1 width 4
set key font "roman, 14" samplen 1

set xrange  []
set x2range []
set yrange []
set y2range []

plot \
     "zgoubi.TWISS.out" u ($13):($2) axes x1y1 w l lt 1 lc rgb "red" lw 1. tit "{/Symbol b}_x"  ,\
     "zgoubi.TWISS.out" u ($13):($4) axes x1y1 w l lt 1 lc rgb "blue" lw 1. tit "{/Symbol b}_y"  ,\
     "zgoubi.TWISS.out" u ($13):($7) axes x1y2 w l lt 1 lc rgb "black" lw 1. tit "{/Symbol h}_x"  ,\
     "zgoubi.TWISS.out" u ($13):($9) axes x1y2 w l lt 2 lc rgb "green" lw 1. tit "{/Symbol h}_y"

set samples 10000
set terminal postscript eps blacktext color enh size 8.3cm,5cm "Times-Roman" 12
set output "gnuplot_TWISS_btxy.eps"
replot
set terminal X11
unset output

pause 2

set title "Orbit, from zgoubi.TWISS.out" font "roman,16"

set ylabel "x, y [m]" font "roman,13"
set y2label "x, y [m]" font "roman,13"

unset x2tics
set xtics  font "roman,12" mirror
unset y2tics
set ytics  font "roman,12" mirror

plot \
     "zgoubi.TWISS.out" u ($13):($15) axes x1y1 w l lt 1 lc rgb "red" tit "x"  ,\
     "zgoubi.TWISS.out" u ($13):($17) axes x1y1 w l lt 1 lc rgb "blue" tit "y"

set samples 10000
set terminal postscript eps blacktext color enh size 9.3cm,6cm "Times-Roman" 12
set output "gnuplot_TWISS_xy.eps"
replot
set terminal X11
unset output

pause 2

exit
```

Question 14.1.2.1-1: Run the Zgoubi code in Table 14.13 to generate a table of the optical functions of the entire AGS Booster ring, zgoubi.TWISS.out. Generate graphs of the optics and orbit using the Gnuplot script in Table 14.14. Apply the expressions given in Chap. 6 to calculate the damped equilibrium emittances, energy spread and damping times of 10 GeV electrons for the optics tabulated in zgoubi.TWISS.out. Fill out Table 14.15 with your results.
Question 14.1.2.1-2: Run the code in Table 14.16. Obtain the energy loss from zgoubi.res for the electron beam energy at 10 GeV and compare it with the analytical calculation in Table 14.15. Use the energy loss to obtain the RF voltage for the RF in Table 14.15. Compare your result with the CAVITE element setting in Table 14.17.

Table 14.15 Electron beam parameters. Table to be completed as part of the exercises

Parameter	Units	Value
E	[GeV]	10
$a\gamma$		
Energy loss per turn	[MeV]	
RF voltage	[MV]	
RF phase	[rad]	2.618
Harmonic number		100
RF frequency	[MHz]	
Horizontal damping time	[s]	
Vertical damping time	[s]	
Longitudinal damping time	[s]	
Horizontal emittance	[m-rad]	
Energy spread		

Table 14.16 Zgoubi code for calculating the energy loss per turn. Recall: the scaling_10GeVel.inc file is given in Table 14.13

```
Energy loss per turn.
'OBJET'
33.3564095089e3  10GeV E_k+M electron.
1
10000 1 1 1 1 1
0.0   0.0   0.0   0.0   0.00  0.0
0.000   0.000   0.000   0.000   0.00  1.

'PARTICUL'
POSITRON

'SPNTRK'
3

'SRLOSS'
1
BEND
1 123456

'FAISTORE'
zgoubi.fai
1

'INCLUDE'
1
scaling_10GeVel.inc[SCALING_S:SCALING_E]

'INCLUDE'
1
6* superA.inc[superA_S:superA_E]

'FAISCEAU'
'SRPRNT'

'END'
```

Question 14.1.2.1-3: Examine the initial beam setup in Table 14.17. Check whether the initial beam distribution is matched transversely by comparing the beam setup parameters with the periodic Twiss functions in zgoubi.TWISS.out you obtained earlier. Run the code in Table 14.17 with 100 particles up to 1000 turns with synchrotron radiation enabled. Use the Gnuplot script in Table 14.18 (or a code of your own) to obtain the rms vertical beam size σ_y as a function of the turn number from the Zgoubi output zgoubi.fai file. Using the Gnuplot script in Table 14.19,

Table 14.17 Zgoubi code for simulating the beam dynamics with synchrotron radiation

```
Beam dynamics with synchrotron radiation.
'OBJET'
33.3564095089e3  10GeV E_k+M electron.
8
0 100 0
0.0006  -0.00065   0.  0.   0.00  1.00315000
 0.98253425  5.4881122   0
-1.5447545   9.6995264   1e-5
 1.          1.          0.
'PARTICUL'
POSITRON
'SPNTRK'
3

'SRLOSS'
1
BEND
1 123456

'FAISTORE'
zgoubi.fai
10                 ! Log to zgoubi.fai every 10 turn.

'OPTIONS'
1 1                  ! Inhibit writes to zgoubi.res:
WRITE OFF                  ! this saves on CPU time.

'INCLUDE'
1
scaling_10GeVel.inc[SCALING_S:SCALING_E]
'INCLUDE'
1
6* superA.inc[superA_S:superA_E]

'CAVITE'
2
201.780049  100                  !  orbit length, h.
122345.25e3   2.61799387799      ! volts, phi_s rad.

'REBELOTE'
999 0.1 99                  ! 999 additional passes.

'OPTIONS'
0 1
WRITE ON         ! Re-establish writes to zgoubi.res.
'FAISCEAU'          ! Print out particle coordinates.
'SPNPRT'               ! Print out spin coordinates.
'SRPRNT'                        ! Print out SR data.
'END'
```

calculate the vertical rms emittance from the vertical rms beam size and optics parameters, plot evolution of the vertical emittance, and extract the vertical damping time by fitting the data to an exponential. Compare the obtained vertical damping time to the theoretical value in Table 14.15.

14.1.2.2 Spin Diffusion Studies

Synchrotron radiation causes spin-flip through the Sokolov-Ternov effect, and spin diffusion. These effects determine the evolution of polarization, and polarization life time (Sects. 6.3 and 6.5). The evaluation of spin diffusion in general requires numerical simulations, which allow deriving the polarization life-time.

Spin diffusion, i.e. depolarization, of polarized electrons can be suppressed and mitigated through the design of an accelerator and proper correction schemes. Alternatively, spin diffusion can also be enhanced if the design or the correction

Table 14.18 Gnuplot script for calculating the rms beam parameters

```
set fit logfile '/dev/null'

fname="zgoubi.fai"

f(x)=ave

set print "ave_sig.txt"

do for [z=10:1000:10] {

  FIT_STDFIT=0
  fit f(x) fname u 38:(($38==z)?($1==1?$9:1/0):1/0) via ave
  d_ave=ave
  d_sig=FIT_STDFIT

  FIT_STDFIT=0
  fit f(x) fname u 38:(($38==z)?($1==1?$10:1/0):1/0) via ave
  x_ave=ave
  x_sig=FIT_STDFIT

  FIT_STDFIT=0
  fit f(x) fname u 38:(($38==z)?($1==1?$11:1/0):1/0) via ave
  xp_ave=ave
  xp_sig=FIT_STDFIT

  FIT_STDFIT=0
  fit f(x) fname u 38:(($38==z)?($1==1?$12:1/0):1/0) via ave
  y_ave=ave
  y_sig=FIT_STDFIT

  FIT_STDFIT=0
  fit f(x) fname u 38:(($38==z)?($1==1?$13:1/0):1/0) via ave
  yp_ave=ave
  yp_sig=FIT_STDFIT

  print z,d_ave,d_sig,x_ave,x_sig,xp_ave,xp_sig,y_ave,y_sig,yp_ave,yp_sig

}

unset print

exit
```

Table 14.19 Gnuplot script for plotting and fitting the vertical emittance data

```
set term postscript eps enhanced color size 9.3cm,6cm "Times-Roman" 12
set output "damping_time_y.eps"
set grid
set size 1.0,1.0
set xlabel "Turns [x10^{3}]"
set ylabel "{/Symbol e}_{y} [{/Symbol m}m]"
unset key

A = 1
B = 0.175
C = 0

f(x)=A*exp(-x/B)

fit f(x) "./ave_sig.txt" u ($1/1000):($1>0?($9**2*0.01**2/9.6995264*1e6):1/0) via A,B

plot "./ave_sig.txt" u ($1/1000):($1>0?($9**2*0.01**2/9.6995264*1e6):1/0) w l lc rgb 'red' lw 1.5,\
f(x) lc rgb 'blue' lw 1.5

exit
```

schemes are not done properly. In this exercise, we explore how and how fast spin diffusion happens when $\mathbf{n}_0$ changes. We will also demonstrate how spin diffusion can be suppressed by adjustment of the magnet layout and beam optics.

14.1.2.3 Spin Diffusion

Question 14.1.2.2-1: Run the code in Table 14.20 to obtain $\mathbf{n}_0$ at the start point of the ideal lattice. This is done by tracking three electrons with spins aligned along three orthogonal directions with synchrotron radiation disabled. Find the spin transfer matrix and precession axis (i.e. $\mathbf{n}_0$) in zgoubi.res file.
Question 14.1.2.2-2: Set the initial spins of 100 electrons to be aligned with the $\mathbf{n}_0$ axis of the ideal lattice. Enable synchrotron radiation. Track the particles by running the code in Table 14.21. Calculate the average spin, or polarization, of the electrons using the script in Table 14.22. Plot the polarization as a function of the turn number and extract the spin diffusion rate by fitting the data. Refer to Table 14.23.
Question 14.1.2.2-3: Offset the first "QVA1" quadrupole from the start of the lattice by 0.1 cm as shown in Table 14.24 and find the resulting closed orbit using the "FIT2" procedure given in Table 14.25. Make sure that SRLOSS is disabled. The

Table 14.20 Zgoubi code for obtaining $\mathbf{n}_0$ at the start point of the ideal lattice

```
$\vecbold{n}_0$ at the start point of the ideal lattice.
'OBJET'
33.3564095089e3  10GeV E_k+M electron.
1
3  1 1 1 1 1
0.   0.   0.   0.   0.00  0.
0.00   0.00   0.00   0.00   0.00  1.

'PARTICUL'
POSITRON

'SPNTRK'
4
1.    0.    0.
0.    1.    0.
0.    0.    1.

'SRLOSS'
0
BEND
1 123456


'OPTIONS'
1 1
WRITE OFF

'INCLUDE'
1
scaling_10GeVel.inc[SCALING_S:SCALING_E]

'INCLUDE'
1
6* superA.inc[superA_S:superA_E]

 'OPTIONS'
1 1
WRITE ON

'SPNPRT'   MATRIX

'END'
```

Table 14.21 Zgoubi code for tracking electron polarization with synchrotron radiation enabled

```
Electron polarization with synchrotron radiation
'OBJET'
33.3564095089e3  10GeV E_k+M electron.
1
100 1 1 1 1 1
0.   0.   0.   0.   0.00  0.
0.00   0.00   0.00   0.00   0.00  1.

'PARTICUL'
POSITRON

'SPNTRK'
3                      ! All initial spins vertical.

'SRLOSS'
1
BEND
1 123456

'FAISTORE'
zgoubi.fai
10                ! Log to zgoubi.fai every 10 turn.

'OPTIONS'
1 1
WRITE OFF

'INCLUDE'
1
scaling_10GeVel.inc[SCALING_S:SCALING_E]
'INCLUDE'
1
6* superA.inc[superA_S:superA_E]

'OPTIONS'
0 1
WRITE ON

'CAVITE'
2
201.780049  100                  !  orbit length, h.
122345.25e3   2.61799387799       ! volts, phi_s rad.

'REBELOTE'
999 0.1 99

'END'
```

output is saved in the zgoubi.FIT.out.dat. Obtain the $\mathbf{n}_0$ axis by specifying the closed orbit offset at the start of the lattice. Launch 100 electrons along the perturbed closed orbit following the initial beam setup provided in Table 14.26 and track them for 1000 turns with synchrotron radiation enabled. Find the average polarization as a function of the turn number, plot it, and extract the spin diffusion rate as in Question 14.1.2.2-2.

Question 14.1.2.2-4: Repeat the calculation in Question 14.1.2.2-3 and obtain the $\mathbf{n}_0$ vectors and the spin diffusion rates with the quadrupole "QVA1" offset by 0.2 and 0.5 cm. Explain your results.

14.1.2.4 Suppression of Spin Diffusion

We will next illustrate how the spin diffusion can be mitigated by changing the polarities of magnetic fields.

Table 14.22 Gnuplot script for calculating the polarization

```
set fit logfile '/dev/null'

fname="zgoubi.fai"

f(x)=ave

set print "ave_pol_align.txt"

do for [z=1:1:1] {

  FIT_STDFIT=0
  fit f(x) fname u 38:($38==z?($1==1?$20:1/0):1/0) via ave
  px_ave=ave
  px_sig=FIT_STDFIT

  FIT_STDFIT=0
  fit f(x) fname u 38:($38==z?($1==1?$21:1/0):1/0) via ave
  py_ave=ave
  py_sig=FIT_STDFIT

  FIT_STDFIT=0
  fit f(x) fname u 38:($38==z?($1==1?$22:1/0):1/0) via ave
  pz_ave=ave
  pz_sig=FIT_STDFIT

  print z,px_ave,px_sig,py_ave,py_sig,pz_ave,pz_sig

}

do for [z=10:1000:10] {

  FIT_STDFIT=0
  fit f(x) fname u 38:($38==z?($1==1?$20:1/0):1/0) via ave
  px_ave=ave
  px_sig=FIT_STDFIT

  FIT_STDFIT=0
  fit f(x) fname u 38:($38==z?($1==1?$21:1/0):1/0) via ave
  py_ave=ave
  py_sig=FIT_STDFIT

  FIT_STDFIT=0
  fit f(x) fname u 38:($38==z?($1==1?$22:1/0):1/0) via ave
  pz_ave=ave
  pz_sig=FIT_STDFIT

  print z,px_ave,px_sig,py_ave,py_sig,pz_ave,pz_sig

}

unset print

exit
```

Question 14.1.2.2-5: Compare the magnet layouts in Tables 14.27 and 14.28 and describe spin rotations in the two layouts assuming vertical initial spin direction.
Question 14.1.2.2-6: Run the codes in Tables 14.27 and 14.28 and plot the magnetic fields and three spin components along the trajectory using the zgoubi.plt output file (particle and field data logging to zgoubi.plt results from IL=2 in all optical elements; the data format of zgoubi.plt is detailed in [1, Sec. 8.3]). See the plotting examples in Tables 14.29 and 14.30 and use analogous files for the second rotator design. Compare the results with your description in the previous exercise.
Question 14.1.2.2-7: Track the spins of particles with different relative momentum offsets (-0.04, -0.03, -0.02, -0.01, 0, 0.01, 0.02, 0.03, 0.04) in the two spin rotator schematics using the code in Table 14.31 for the first design version and an analogous code for the second one. Explore how the final spin depends on the momentum deviation by plotting the final spin versus the momentum offset in the

Table 14.23 Gnuplot script for plotting the polarization

```
set term postscript eps enhanced \
  color size 9.3cm,6cm "Times-Roman" 12
set output "pol_align.eps"
set grid
set size 1.0,1.0
set xlabel "Turns [x10^{3}]"
set ylabel "P_{z}"
set xtics 0.2
set ytics 0.0005
unset key

A = 1
B = 1000000

f(x)=A*exp(-x/B)

fit f(x) "./ave_pol_align.txt" u ($1/1000):($6) via A,B

plot [][0.999:1.001] "./ave_pol_align.txt" \
u ($1/1000):($6) w l lc rgb 'red' lw 1.5 ,\
f(x) lc rgb 'blue' lw 1.5

exit
```

Table 14.24 Setup of the "QVA1" quadrupole with 1 mm vertical offset

```
'MULTIPOL' QVA1      QUAD
0  .Quad
0.493916E+02 10.0000    0.0000   -0.5472896982 0. 0. 0. 0. 0. 0. 0.
0. 0. 6.00  3.00 1.00 0.00 0.00 0.00 0.00 0. 0. 0. 0.
6  .1122 6.2671 -1.4982 3.5882 -2.1209 1.723
0. 0. 6.00  3.00 1.00 0.00 0.00 0.00 0.00 0. 0. 0. 0.
6  .1122 6.2671 -1.4982 3.5882 -2.1209 1.723
0. 0. 0. 0. 0. 0. 0. 0. 0. 0.
2.00  ! cm  MultQVA1
4 0. 0. 0. 0.1 0                  ! KPOS=4 allows specifying ZS=0.1cm.
```

Table 14.25 Setup of the "FIT2" procedure for finding the closed orbit

```
'FIT2'
4   noSYSout ! final (NOT nofinal) is mandatory: causes store of actual c.o. in zgoubi.SVD.out
1 30 0 [-5.9,5.9]   ! Vary Y0
1 31 0 [-9.9,9.9]   ! Vary T0
1 32 0 [-5.9,5.9]   ! Vary Z0
1 33 0 [-9.9,9.9]   ! Vary P0
4   1e-10
3.1 1 2 #End 0. 1. 0    ! Yfinal = Y0
3.1 1 3 #End 0. 1. 0    ! Tfinal = T0
3.1 1 4 #End 0. 1. 0    ! Zfinal = Z0
3.1 1 5 #End 0. 1. 0    ! Pfinal = P0
```

Table 14.26 Setup of the "OBJET" element for launching 100 electrons along the perturbed closed orbit

```
'OBJET'                                                                                    1
33.3564095089e3  10GeV E_k+M electron.
1
100 1 1 1 1 1
0.E+00   0.E+00   0.E+00   0.E+00   0.00  0.E+00
-5.78398841E-06  -5.02369232E-06  -2.40168827E-01  -5.80016582E-01   0.00  1.
```

Table 14.27 Zgoubi file of a spin rotator lattice where the spin is not longitudinally matched

```
Spin rotator, version 1
'OBJET'
33.3564095089e3  10GeV E_k+M electron.
1
1 1 1 1 1 1
0.E+00   0.E+00   0.E+00   0.E+00   0.00  0.E+00
0.  0.  0. 0. 0.  1.

'PARTICUL'
POSITRON

'SPNTRK'
4.1
0. 0. 1.

'SCALING'
1 1
BEND
-1
1
1

'DRIFT'    DRIF
10.
'SOLENOID'    SOLE
2  .sole
1000.0  2.0  52.3354354
25  25
1.  cm
1 0. 0. 0.
'DRIFT'    DRIF
10.
'BEND'     DHA1T
2  .Bend
100.   0.0E+00   23.08831973         ! 69.2 mrad bend
0.00  0.00   0.00
4 .2401  1.8639  -.5572  .3904 0. 0. 0.
0.00  0.00   0.00
4 .2401  1.8639  -.5572  .3904 0. 0. 0.
1.0000E+00 cm  Bend
3 0. 0. 0.
'DRIFT'    DRIF
10.
'DRIFT'    DRIF
10.
'BEND'     DHA1T
2  .Bend
100.   0.0E+00   23.08831973
0.00  0.00   0.00
4 .2401  1.8639  -.5572  .3904 0. 0. 0.
0.00  0.00   0.00
4 .2401  1.8639  -.5572  .3904 0. 0. 0.
1.0000E+00 cm  Bend
3 0. 0. 0.
'DRIFT'    DRIF
10.
'SOLENOID'    SOLE
2  .sole
1000.0  2.0  52.3354354
25  25
1.  cm
1 0. 0. 0.
'DRIFT'    DRIFEND
10.

'END'
```

Table 14.28 Zgoubi file of a spin rotator lattice where the spin is longitudinally matched

```
Spin rotator, version 2
'OBJET'
33.3564095089e3  10GeV E_k+M electron.
1
1 1 1 1 1 1
0.E+00   0.E+00   0.E+00   0.E+00   0.00  0.E+00
0.  0.  0. 0. 0.  1.

'PARTICUL'
POSITRON

'SPNTRK'
4.1
0. 0. 1.

'SCALING'
1 1
BEND
-1
1
1

'DRIFT'    DRIF
10.
'SOLENOID'    SOLE
2  .sole
1000.0  2.0  52.3354354
25  25
1.  cm
1 0. 0. 0.
'DRIFT'    DRIF
10.
'BEND'     DHA1T
2  .Bend
100.   0.0E+00   23.08831973
0.00  0.00   0.00
4 .2401  1.8639  -.5572  .3904 0. 0. 0.
0.00  0.00   0.00
4 .2401  1.8639  -.5572  .3904 0. 0. 0.
1.0000E+00 cm  Bend
3 0. 0. 0.
'DRIFT'    DRIF
10.
'DRIFT'    DRIF
10.
'BEND'     DHA1T
2  .Bend
100.   0.0E+00   -23.08831973
0.00  0.00   0.00
4 .2401  1.8639  -.5572  .3904 0. 0. 0.
0.00  0.00   0.00
4 .2401  1.8639  -.5572  .3904 0. 0. 0.
1.0000E+00 cm  Bend
3 0. 0. 0.
'DRIFT'    DRIF
10.
'SOLENOID'    SOLE
2  .sole
1000.0  2.0  -52.3354354
25  25
1.  cm
1 0. 0. 0.
'DRIFT'    DRIFEND
10.

'END'
```

Table 14.29 Gnuplot script for plotting the field components

```
set term postscript eps enhanced color size 9.3cm,6cm "Times-Roman" 12
set output "spin_rotator_fields.eps"
set grid
set size 1.0,1.0
set xlabel "s [m]"
set ylabel "B (T)"
set xtics 5
set ytics 2
set key bottom left

plot [-1:][-0.1:] \
"./zgoubi.plt" u ($14/100):($23/10) w l lc rgb 'red' lw 1.5 title "B_{x}",\
"./zgoubi.plt" u ($14/100):($24/10) w l lc rgb 'green' lw 1.5 title "B_{y}",\
"./zgoubi.plt" u ($14/100):($25/10) w l lc rgb 'blue' lw 1.5 title "B_{z}"

exit
```

Table 14.30 Gnuplot script for plotting the spin components

```
set term postscript eps enhanced color size 9.3cm,6cm "Times-Roman" 12
set output "spin_rotator_spin.eps"
set grid
set size 1.0,1.0
set xlabel "s [m]"
set ylabel "S"
set xtics 5
set ytics 0.5
set key bottom left

plot [-1:][-1.1:1.1] \
"./zgoubi.plt" u ($14/100):($33) w l lc rgb 'red' lw 1.5 title "S_{x}",\
"./zgoubi.plt" u ($14/100):($34) w l lc rgb 'green' lw 1.5 title "S_{y}",\
"./zgoubi.plt" u ($14/100):($35) w l lc rgb 'blue' lw 1.5 title "S_{z}"

exit
```

two cases using the script in Table 14.32. Discuss which case you expect to have a lower spin diffusion rate and why. Note that this is the first order spin matching in the longitudinal direction.

14.1.2.5 Spin Matching

This section studies the electron spin dynamics at 5 GeV in the AGS Booster in the presence of a solenoidal snake. We consider the cases of spin-matched and spin-mismatched snake configurations. The spin-matched snake lattice is given by the include file listed in Table 14.33. The snake consists of two solenoids with six quadrupoles between them. The quadrupoles are used to compensate betatron coupling from the solenoids and to satisfy the spin matching conditions.

Question 14.1.2.5-1: Use the snake include file in Table 14.33 to insert the snake at the end of the AGS Booster lattice as shown in Table 14.34. Examine the resulting periodic optics using the Gnuplot script in Table 14.14.
Question 14.1.2.5-2: Obtain the $\mathbf{n}_0$ axis at the start point of the lattice by running the code in Table 14.35 and examining its output "zgoubi.res" file.
Question 14.1.2.5-3: Determine the spin diffusion rate of this lattice. Track 100 electrons for 10^4 turns with synchrotron radiation enabled. Start the electrons

Table 14.31 Zgoubi code for studying the momentum dependence of the spin rotation using the unmatched lattice

```
Momentum dependence of spin rotation - unmatched lattice
'OBJET'
33.3564095089e3  10GeV E_k+M electron.
1
1 1 1 1 1 9
0.E+00   0.E+00   0.E+00   0.E+00   0.00  0.010000E+00
0.  0.  0. 0. 0.  1. 'o'

'PARTICUL'
POSITRON

'SPNTRK'
4.1
0. 0. 1.

'FAISTORE'  ! Hint: use zgoubi_matched.fai for 2nd case.
zgoubi_unmatched.fai DRIFEND
1

'SCALING'
1 1
BEND
-1
1
1

'DRIFT'    DRIF
10.
'SOLENOID'    SOLE
0  .sole
1000.0  2.0  52.3354354
25  25
1.  cm
1 0. 0. 0.
'DRIFT'    DRIF
10.
'BEND'     DHA1T
0  .Bend
100.   0.0E+00   23.08831973
0.00  0.00   0.00
4 .2401  1.8639  -.5572  .3904 0. 0. 0.
0.00  0.00   0.00
4 .2401  1.8639  -.5572  .3904 0. 0. 0.
1.0000E+00 cm  Bend
3 0. 0. 0.
'DRIFT'    DRIF
10.
'DRIFT'    DRIF
10.
'BEND'     DHA1T
0  .Bend
100.   0.0E+00   23.08831973
0.00  0.00   0.00
4 .2401  1.8639  -.5572  .3904 0. 0. 0.
0.00  0.00   0.00
4 .2401  1.8639  -.5572  .3904 0. 0. 0.
1.0000E+00 cm  Bend
3 0. 0. 0.
'DRIFT'    DRIF
10.
'SOLENOID'    SOLE
0  .sole
1000.0  2.0  52.3354354
25  25
1.  cm
1 0. 0. 0.
'DRIFT'    DRIFEND
10.

'FAISCEAU'

'END'
```

Table 14.32 Gnuplot script for plotting the final vertical spin component as a function of the particle's momentum offset for the two rotator schemes

```
set term postscript eps enhanced color size 9.3cm,6cm "Times-Roman" 12
set output "final_spin.eps"
set grid
set size 1.0,1.0
set xlabel "{/Symbol D}p/p"
set ylabel "S_{z}"
set xtics 0.02
set ytics 0.002
set key bottom left

plot [][] \
"< sort -nk2 zgoubi_1.fai" u 2:22 w l lc rgb 'red' lw 1.5 title "Scheme 1",\
"< sort -nk2 zgoubi_2.fai" u 2:22 w l lc rgb 'blue' lw 1.5 title "Scheme 2"

exit
```

on the design trajectory with their initial spins aligned with the $\mathbf{n}_0$ axis. Refer to Table 14.36 for the corresponding Zgoubi code. Calculate the polarization components using a Gnuplot script similar to that in Table 14.22 and plot the total transverse polarization as a function of the turn number following the example of Table 14.23.

Question 14.1.2.5-4: Reverse the polarity of all quadrupoles ("HQ1" through "HQ6") between the snake solenoids in Table 14.33. This change keeps betatron coupling compensated but results in violation of the spin matching conditions. Complete tracking through the AGS Booster with the modified snake lattice and analyze the results as in Question 14.1.2.5-3. Compare the spin diffusion rates obtained in the spin matched and unmatched cases.

14.2 Numerical Simulations: Solutions

This Section details the solutions of the simulation exercises proposed in Sect. 14.1.

Understanding these simulations requires having the code manual at hand, ready to consult, Zgoubi Users' Guide [1] in the present case, or whatever other code the reader my be willing to use otherwise.

In order to reproduce these numerical simulations, the code executable is required. Zgoubi package can be downloaded from its repository in sourceforge:

https://sourceforge.net/p/zgoubi/code/HEAD/tree/trunk/

A README file therein explains how the source code is compiled to generate the executable, zgoubi. Running an optical sequence (say, Booster_Twiss.dat) is then just a matter of executing such command as

[pathTo]/zgoubi -in Booster_Twiss.dat

and the results are listed, *a minima*, in zgoubi.res file, by default.

All necessary optical sequences for the simulation exercises have been provided as part of the assignments in Sect. 14.1, however most of the simulation material

Table 14.33 Contents of the "snake_matched.inc" include file providing the lattice of a spin-matched solenoidal snake

```
'MARKER'   snake_sol_s
'DRIFT'    DRIF      LDH1SN
11.0
'SOLENOID'    SOLE      SN_SOL
0  .sole
40.0  2.0  39.26987500004383
40.  40.
0.1  cm
1  0.0  0.0  0.0
'DRIFT'    DRIF      LSN1
19.5
'MULTIPOL'    HQ1     QUAD
0  .Quad
1.0  10.0  0.0  -9.012691897  0.0  0.0  0.0  0.0  0.0  0.0  0.0  0.0
0.0  0.0  6.00  3.00 1.00 0.00 0.00 0.00 0.00 0. 0.
6  .1122 6.2671 -1.4982 3.5882 -2.1209 1.723
0.0  0.0  6.00  3.00 1.00 0.00 0.00 0.00 0.00 0. 0.
6  .1122 6.2671 -1.4982 3.5882 -2.1209 1.723
0.0  0.0  0.0  0.0  0.0  0.0  0.0  0.0  0.0  0.0
1.  cm
1  0.0  0.0  0.0
'DRIFT'    DRIF      LSN2
19.0
'MULTIPOL'    HQ2     QUAD
0  .Quad
1.0  10.0  0.0  503.4519374  0.0  0.0  0.0  0.0  0.0  0.0  0.0  0.0
0.0  0.0  6.00  3.00 1.00 0.00 0.00 0.00 0.00 0. 0.
6  .1122 6.2671 -1.4982 3.5882 -2.1209 1.723
0.0  0.0  6.00  3.00 1.00 0.00 0.00 0.00 0.00 0. 0.
6  .1122 6.2671 -1.4982 3.5882 -2.1209 1.723
0.0  0.0  0.0  0.0  0.0  0.0  0.0  0.0  0.0  0.0
1.  cm
1  0.0  0.0  0.0
'DRIFT'    DRIF      LSN2
19.0
'MULTIPOL'    HQ3     QUAD
0  .Quad
1.0  10.0  0.0  -535.3938472  0.0  0.0  0.0  0.0  0.0  0.0  0.0  0.0
0.0  0.0  6.00  3.00 1.00 0.00 0.00 0.00 0.00 0. 0.
6  .1122 6.2671 -1.4982 3.5882 -2.1209 1.723
0.0  0.0  6.00  3.00 1.00 0.00 0.00 0.00 0.00 0. 0.
6  .1122 6.2671 -1.4982 3.5882 -2.1209 1.723
0.0  0.0  0.0  0.0  0.0  0.0  0.0  0.0  0.0  0.0
1.  cm
1  0.0  0.0  0.0
'DRIFT'    DRIF      LSN2
19.0
'MULTIPOL'    HQ4     QUAD
0  .Quad
1.0  10.0  0.0  775.4968481  0.0  0.0  0.0  0.0  0.0  0.0  0.0  0.0
0.0  0.0  6.00  3.00 1.00 0.00 0.00 0.00 0.00 0. 0.
6  .1122 6.2671 -1.4982 3.5882 -2.1209 1.723
0.0  0.0  6.00  3.00 1.00 0.00 0.00 0.00 0.00 0. 0.
6  .1122 6.2671 -1.4982 3.5882 -2.1209 1.723
0.0  0.0  0.0  0.0  0.0  0.0  0.0  0.0  0.0  0.0
1.  cm
1  0.0  0.0  0.0
'DRIFT'    DRIF      LSN2
19.0
'MULTIPOL'    HQ5     QUAD
0  .Quad
1.0  10.0  0.0  -437.5504952  0.0  0.0  0.0  0.0  0.0  0.0  0.0  0.0
0.0  0.0  6.00  3.00 1.00 0.00 0.00 0.00 0.00 0. 0.
6  .1122 6.2671 -1.4982 3.5882 -2.1209 1.723
0.0  0.0  6.00  3.00 1.00 0.00 0.00 0.00 0.00 0. 0.
6  .1122 6.2671 -1.4982 3.5882 -2.1209 1.723
0.0  0.0  0.0  0.0  0.0  0.0  0.0  0.0  0.0  0.0
1.  cm
1  0.0  0.0  0.0
'DRIFT'    DRIF      LSN2
19.0
'MULTIPOL'    HQ6     QUAD
0  .Quad
1.0  10.0  0.0  406.0280703  0.0  0.0  0.0  0.0  0.0  0.0  0.0  0.0
0.0  0.0  6.00  3.00 1.00 0.00 0.00 0.00 0.00 0. 0.
6  .1122 6.2671 -1.4982 3.5882 -2.1209 1.723
0.0  0.0  6.00  3.00 1.00 0.00 0.00 0.00 0.00 0. 0.
6  .1122 6.2671 -1.4982 3.5882 -2.1209 1.723
0.0  0.0  0.0  0.0  0.0  0.0  0.0  0.0  0.0  0.0
1.  cm
1  0.0  0.0  0.0
'DRIFT'    DRIF      LSN1
19.5
'SOLENOID'    SOLE      SN_SOL
0  .sole
40.0  2.0  39.26987500004383
40.  40.
0.1  cm
1  0.0  0.0  0.0
'DRIFT'    DRIF      LDH4SN
11.0
'MARKER'   snake_sol_e
```

Table 14.34 Left: Zgoubi file of the AGS Booster lattice with the spin-matched snake for Twiss calculation. Right: the scaling_5GeVel.inc INCLUDE file, also used in subsequent exercises

```
AGS Booster lattice with the spin-matched snake.
'OBJET'
16.67820475445e3    ! reference rigidity -> p = 5 GeV/c
5
.001 .0001 .001 .0001 0. .0001
0. 0. 0. 0. 0. 1.

'PARTICUL'
0.51099892  1.60217653e-19  1.15965218076e-3 0. 0.
'SRLOSS'
0   !  .srloss
BEND
1   123456
'SPNTRK'
3

'INCLUDE'
1
scaling_5GeVel.inc[SCALING_S:SCALING_E]

'INCLUDE'
1
6* superA.inc[superA_S:superA_E]

'INCLUDE'
1
snake_matched.inc[snake_sol_s:snake_sol_e]

'TWISS'
2 1. 1.

'END'
```

```
! scaling_5GeVel.inc INCLUDE  file.
'MARKER'  SCALING_S

'SCALING'
1 7
BEND
-1
16.67820475445
1
MULTIPOL
-1
16.67820475445* 1.
1
SOLENOID
-1
16.67820475445
1
MULTIPOL  QH*    ! Quadrupoles set for Qx=4.73, Qy=4.82.
-1
16.67820475445* 1.0864799            !  FIT variable #12.
1
MULTIPOL  QV*
-1
16.67820475445* 1.0657626            !  FIT variable #16.
1
MULTIPOL  SH*
-1
16.67820475445
1
MULTIPOL  SV*
-1
16.67820475445
1

'MARKER'  SCALING_E

'END'
```

Table 14.35 Zgoubi file of the AGS Booster lattice with the spin-matched snake for $\mathbf{n}_0$ calculation

```
AGS Booster lattice with spin-matched snake for n_0 calculation
'OBJET'
16.67820475445e3    ! reference rigidity -> p = 5 GeV/c
1
3  1 1 1 1 1
0.E+00   0.E+00   0.E+00   0.E+00   0.00  0.E+00
0.00E+00   0.00E+00   0.00E+00   0.00E+00   0.00  1.

'PARTICUL'
0.51099892  1.60217653e-19  1.15965218076e-3 0. 0.

'SRLOSS'
0   !  .srloss
BEND
1   123456

'SPNTRK'
4
1.  0.  0.
0.  1.  0.
0.  0.  1.

'INCLUDE'
1
scaling_5GeVel.inc[SCALING_S:SCALING_E]

'INCLUDE'
1
6* superA.inc[superA_S:superA_E]

'INCLUDE'
1
snake_mismatched.inc[snake_sol_s:snake_sol_e]

'SPNPRT'   MATRIX

'END'
```

Table 14.36 Zgoubi file for tracking 100 electrons for 10^4 turns through the AGS Booster lattice with the spin-matched snake

```
Tracking 100 electrons for 10^4 turns through Booster
'OBJET'
16.67820475445e3    ! reference rigidity -> p = 5 GeV/c
1
100 1 1 1 1 1
0.E+00   0.E+00   0.E+00   0.E+00   0.00  0.E+00
0.00E+00   0.00E+00   0.00E+00   0.00E+00   0.00  1.

'PARTICUL'
0.51099892  1.60217653e-19  1.15965218076e-3 0. 0.

'SRLOSS'
1   !  .srloss
BEND
1   123456

'SPNTRK'
4.1
0.4626 0.8866 0.0

'FAISTORE'
zgoubi.fai
100

'INCLUDE'
1
scaling_5GeVel.inc[SCALING_S:SCALING_E]

'INCLUDE'
1
6* superA.inc[superA_S:superA_E]

'INCLUDE'
1
snake_mismatched.inc[snake_sol_s:snake_sol_e]

'CAVITE'
2
204.2000486  100                  !  orbit length, h
7974784.27279453   2.61799387799   !  volts, phi_s rad, 5 GeV

'REBELOTE'
9999 0.1 99

'END'
```

further discussed and used here (input data files, gnuplot scripts, etc.) is also available in the sourceforge repository, at

https://sourceforge.net/p/zgoubi/code/HEAD/tree/trunk/exemples/uspasSpinClass_2021/

Brief additional introductory guidance to using the code can be found in the Appendix, page 405.

14.2.1 Polarized Helion in AGS Booster

14.2.1.1 AGS Booster Parameters

Table 14.2 has been completed, yielding Table 14.37. Some derivations are detailed hereafter.

Table 14.37 AGS Booster parameters, table completed

Injection β		0.0655
Injection energy, kin.	MeV/u	2.0146
Injection $G\gamma$		-4.19316
Injection $B\rho$	T m	0.30745
Extraction energy, kin.	GeV/u	1.413059
Extraction $G\gamma$		-10.5
Extraction $B\rho$	T m	10.780516
Lattice		
Length	m	201.78
Tunes, ν_x, ν_y		4.73, 4.82
Chromaticities, ξ_x, ξ_y		-4.8, -5.2
Momentum compaction α		0.043998
Transition γ		4.7674
RF system		
Revolution frequency, f_{rev}	MHz	0.09738 to 1.36362
RF harmonic		4
RF frequency	MHz	0.38953 to 5.45449
Peak voltage	kV	400
Synchronous phase	deg	30
Spin		
Crossing speed $dG\gamma/d\theta$		-9.4848×10^{-5}

With $M = 2808.39\,\text{MeV}$, $|G| = 4.18415$, and $dE/dN = q\hat{V}\sin(\phi_s) = 0.4\,\text{MeV/turn}$ (q=2, $\hat{V} = 0.4\,\text{MV}$, $\phi_s = 30\,\text{deg}$), the crossing speed comes out to be

$$\frac{dG\gamma}{d\theta} = \frac{1}{2\pi}\frac{G}{M}\frac{dE}{dN} = -9.4848 \times 10^{-5}.$$

The following excerpt from the "print" file generated by a MAD8 computation of the Booster optical functions is aimed at allowing a comparison with Zgoubi outcomes in the next question:

```
 Linear lattice functions.    TWISS              line: ASUPL6                    range: #S/#E
Delta(p)/p:     0.000000     symm: F            super:   1                                                    page    20

     ELEMENT SEQUENCE       I              H O R I Z O N T A L                I               V E R T I C A L
pos.  element occ.      dist I   betax  alfax   mux    x(co)  px(co) Dx    Dpx  I   betay  alfay   muy    y(co)  py(co) Dy    Dpy
no.   name     no.       [m]  I   [m]    [1]     [2pi]  [mm]   [.001] [m]   [1]  I   [m]    [1]     [2pi]  [mm]   [.001] [m]   [1]
-------------------------------------------------------------------------------------------------------------------------------------
end   LA8        6   201.780    5.485  0.982   4.730  0.0000  0.000  0.739-0.104     9.704 -1.546   4.820  0.0000  0.000  0.000 0.000
end   ASUPL      6   201.780    5.485  0.982   4.730  0.0000  0.000  0.739-0.104     9.704 -1.546   4.820  0.0000  0.000  0.000 0.000
end   ASUPL6     1   201.780    5.485  0.982   4.730  0.0000  0.000  0.739-0.104     9.704 -1.546   4.820  0.0000  0.000  0.000 0.000
-------------------------------------------------------------------------------------------------------------------------------------
total length =       201.780000          Qx          =         4.730145          Qy          =         4.820140
delta(s)     =         0.000000 mm       Qx'         =        -7.313316          Qy'         =        -2.883899
alfa         =         0.439414E-01      betax(max)  =        13.545393          betay(max)  =        13.149980
gamma(tr)    =         4.770492          Dx(max)     =         2.909356          Dy(max)     =         0.000000
                                         Dx(r.m.s.)  =         1.757448          Dy(r.m.s.)  =         0.000000
                                         xco(max)    =         0.000000          yco(max)    =         0.000000
                                         xco(r.m.s.) =         0.000000          yco(r.m.s.) =         0.000000
-------------------------------------------------------------------------------------------------------------------------------------
```

14.2.1.2 Cell and Lattice Optics

Questions 14.1.1.2.1–14.1.1.2.3—Running superA.inc, due to the MATRIX command at the downstream end of the optical sequence, produces the first order transport matrix of the super cell, say T_{cell}, and the corresponding beam matrix, i.e. the periodic optical functions at cell ends (using the relation $T_{\text{cell}} = I \cos\mu + J \sin\mu$).

These two matrices are found at the bottom of the computation listing, zgoubi.res.

Checking against the data in MAD8 'print' output file (Sect. 14.2.1.1) shows a very good agreement.

Question 14.1.1.2.4—Running superA.inc with a TWISS command instead, produces, on the one hand, the following lattice parameter computation outcomes (similar to MATRIX outcomes), found down zgoubi.res listing (an excerpt):

```
************************************************************************************************************************************
  112  Keyword, label(s) :  TWISS                                                                                    IPASS= 4

                     ***********************************************************
                     *************  End  of  TWISS  procedure  **************
    There  has  been          4  pass  through  the  optical  structure

 Reference, before change of frame (particle #  1  - D-1,Y,T,Z,s,time)  :
  0.00000000E+00  -7.65859598E-13   2.62290190E-12   0.00000000E+00   0.00000000E+00   3.36300081E+03   3.68572492E-01
           Frame for MATRIX calculation moved by :
           XC =    0.000 cm , YC =   -0.000 cm ,   A =  0.00000 deg  ( = 0.000000 rad )

 Reference, after change of frame (particle #  1  - D-1,Y,T,Z,s,time)  :
  0.00000000E+00   0.00000000E+00   0.00000000E+00   0.00000000E+00   0.00000000E+00   3.36300081E+03   3.68572492E-01
  Reference particle (#     1), path length :   3363.0008     cm  relative momentum :    1.00000

               TRANSFER  MATRIX  ORDRE  1  (MKSA units)
       -0.716001       -5.32491        0.00000         0.00000         0.00000        0.716859
        0.348220        1.19307        0.00000         0.00000         0.00000       -0.238490
        0.00000         0.00000        1.78816        -9.15235         0.00000        0.00000
        0.00000         0.00000        0.330121       -1.13043         0.00000        0.00000
       -7.886126E-02    0.414707       0.00000         0.00000         1.00000        1.58173
        0.00000         0.00000        0.00000         0.00000         0.00000        1.00000
         DetY-1 =      -0.0000004260,    DetZ-1 =     -0.0000004317
         R12=0 at    4.463     m,        R34=0 at   -8.096     m
     First order symplectic conditions (expected values = 0) :
      -4.2604E-07   -4.3171E-07     0.000         0.000         0.000         0.000

            TWISS  parameters,  periodicity  of   1  is  assumed
                              -  COUPLED  -
      Beam  matrix  (beta/-alpha/-alpha/gamma) and  periodic  dispersion  (MKSA units)
         5.483186     -0.982907      0.000000      0.000000      0.000000      0.742996
        -0.982907      0.358570      0.000000      0.000000      0.000000     -0.104814
         0.000000      0.000000      9.691428      1.545246      0.000000     -0.000000
         0.000000      0.000000      1.545246      0.349565      0.000000      0.000000
         0.000000      0.000000      0.000000      0.000000      0.000000      0.000000
         0.000000      0.000000      0.000000      0.000000      0.000000      0.000000
                           Betatron  tunes  (Q1 Q2 modes)
                  NU_Y =  0.78833338         NU_Z =  0.80333330
                              Momentum compaction :
                         dL/L / dp/p =  4.39982231E-02
                               Transition gamma  =  4.76740921E+00
                               Chromaticities :
                  dNu_y / dp/p = -0.80312438                  dNu_z / dp/p = -0.86404335
************************************************************************************************************************************
```

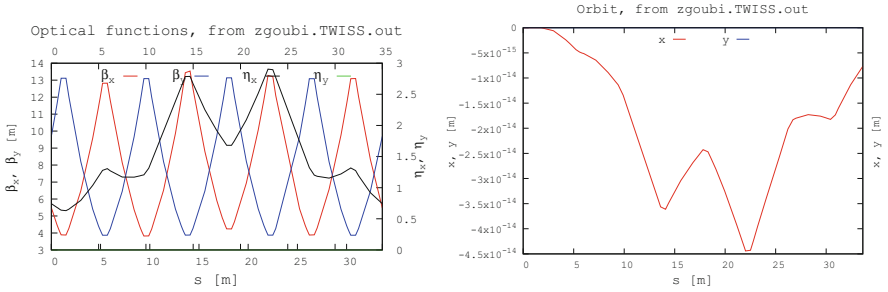

Fig. 14.5 Left: booster super cell optical functions, from a TWISS computation. Right: it is not a bad idea to check what the horizontal and vertical orbits are, zero as expected in the present case

The TWISS command causes in addition the transport of the periodic optical functions throughout the sequence, logged in zgoubi.TWISS.out. These optical functions are displayed in Fig. 14.5.

Note: to produce this set of outputs, the TWISS command performs 4 consecutive passes through the optical sequence, see Users' Guide for details.

14.2.1.3 Spin Optics

The rigidity specified in the provided input data files and used in the previous question (superA.inc, etc.) is 1 T m. However, proper spin motion requires proper $G\gamma$ value! Thus, the rigidity in this exercise has to be changed to the injection value, namely (Table 14.37),

$$B\rho = 0.30745\,\mathrm{T\,m}$$

Question 14.1.1.3.1—The spin motion of a helion is tracked along Booster for the case of an ideal ring (six superA cells, planar, no defects) using the input data file given in Table 14.7. One particle is taken on-momentum, the other two at $\delta p/p = \pm 10^{-4}$ and launched on their respective chromatic closed orbits, given the dispersion and its derivative (Sect. 14.2.1.2)

$$\eta_x = 0.743\,\mathrm{m}, \quad \eta_x' = -0.1048\,\mathrm{rad}$$

Tracking shows that the spin precession direction is vertical around the ring, for both on- and off-momentum particles (Fig. 14.6). This is what's expected as the chromatic closed orbits also lie in the median plane: the field is everywhere vertical along a chromatic closed orbit as well, particles do not experience any horizontal field component, no field may kick spins away from vertical.

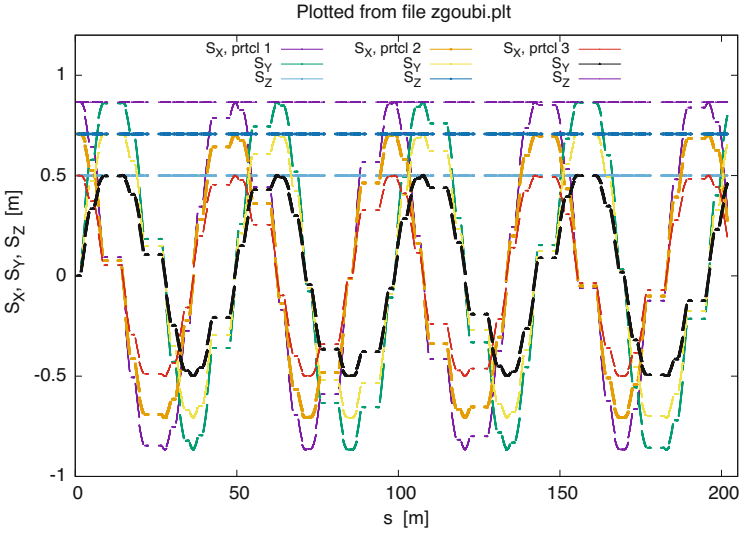

Fig. 14.6 Spins of 3 ions, respectively on- and $\pm 10^{-4}$ off-momentum, along their respective closed orbits around Booster. The vertical component S_Z is constant all along, thus the precession direction is vertical. S_X and S_Y are circling around the Z axis, in the bend plane

Questions 14.1.1.3.2, 14.1.1.3.3—Tracking the spin closed orbit over a turn for particles at $dp/p = 0$ and $dp/p = \pm 10^{-4}$ off-momentum, yields spin motions displayed in Fig. 14.6.

Adding SPNPRT[MATRIX] allows for producing the spin matrices, however that also requires changing OBJET and SPNTRK data in Table 14.7, so to create 3 groups (as many as there are different momenta) of 3 particles each, as follows:

```
'OBJET'
0.3074552E3           ! Reference rigidity/kG.cm, for 3He++, at injection beta value 0.0655.
2          ! An option to define initial particle coordinates, one by one; here, 3 different
9 3      ! momenta, 9 particles; this is ordered to allow spin matrix computation by SPNPRT.
7.43281000E-03 -1.04862116E-02 0. 0. 0. 1.0001 'p'        ! Group 1. Orbit coordinates for a
7.43281000E-03 -1.04862116E-02 0. 0. 0. 1.0001 'p'             ! momentum offset of D=+1e-4.
7.43281000E-03 -1.04862116E-02 0. 0. 0. 1.0001 'p'
0. .0 0. 0. 0. 1.  'o'                                  ! Group 2. On-momentum 3-particle set.
0. .0 0. 0. 0. 1.  'o'
0. .0 0. 0. 0. 1.  'o'
-7.42569731E-03 1.04862063E-02 0. 0. 0.  .9999 'm'                                  ! Group 3.
-7.42569731E-03 1.04862063E-02 0. 0. 0.  .9999 'm'             ! Momentum offset of D=-1e-4.
-7.42569731E-03 1.04862063E-02 0. 0. 0.  .9999 'm'
1 1 1 1 1 1 1 1 1

'PARTICUL'   ! Defining the particle species is necessary, in order for the program to solve
HELION                                                                  ! the T-BMT equation.
'SPNTRK'                          ! The 9 initial spins are organized so to allow spin matrix
4                  ! computation by SPNPRT, for each of the 3 different momenta concerned.
1. 0. 0.                                                                ! S_X, particle 1,
0. 1. 0.                                                                ! S_Y, particle 1,
0. 0. 1.                                                                ! S_Z, particle 1,
1. 0. 0.                                                                ! S_X/ particle 2,
0. 1. 0.                                                                          ! etc.
0. 0. 1.
1. 0. 0.
0. 1. 0.
0. 0. 1.
```

This yields the following, including the spin transport matrix, fractional spin tune and precession axis, for each of the 3 momenta (an excerpt):

```
*****************************************************************************************************************************************************
   641  Keyword, label(s) :  SPNPRT      MATRIX                                                                                    IPASS= 1

                        -- 3  GROUPS  OF  MOMENTA  FOLLOW   --

                        ------------------------------------------------------------
                        Momentum  group  #1 ; average  over 3 particles at this pass :
                     INITIAL                                          FINAL
      <SX>       <SY>       <SZ>       <|S|>            <SX>       <SY>       <SZ>       <|S|>    <G.gma>    <(SI,SF)>  sigma_(SI,SF)
                                                                                                      (deg)       (deg)
  0.333333   0.333333   0.333333   0.577350        -0.195770   0.428831   0.333333   0.577350  -4.193160  46.358429  32.780359

               Spin  components  of  each  of  the      3  particles,  and  rotation  angle :
                     INITIAL                                          FINAL
           SX         SY         SZ         |S|          SX         SY         SZ         |S|       GAMMA   |Si,Sf|   (Z,Sf_yz) (Z,Sf)
                                                                                                              (deg.)    (deg.)    (deg.)
                                                                                                   (Sf_yz : projection of Sf on YZ plane)
p  1  1.000000  0.000000  0.000000  1.000000     0.349592  0.936902  0.000000  1.000000      1.0022   69.538   90.000   90.000    1
p  1  0.000000  1.000000  0.000000  1.000000    -0.936902  0.349592  0.000000  1.000000      1.0022   69.538   90.000   90.000    2
p  1  0.000000  0.000000  1.000000  1.000000     0.000000  0.000000  1.000000  1.000000      1.0022    0.000   45.000    0.000    3

                  Min/Max  components  of  each  of  the      3  particles :
  SX_mi       SX_ma       SY_mi       SY_ma       SZ_mi       SZ_ma       |S|_mi      |S|_ma      p/p_0        GAMMA          I  IEX
 3.4959E-01  3.4959E-01  9.3690E-01  9.3690E-01  0.0000E+00  0.0000E+00  1.0000E+00  1.0000E+00  1.00010E+00  1.00215E+00    1   1
-9.3690E-01 -9.3690E-01  3.4959E-01  3.4959E-01  0.0000E+00  0.0000E+00  1.0000E+00  1.0000E+00  1.00010E+00  1.00215E+00    2   1
 0.0000E+00  0.0000E+00  0.0000E+00  0.0000E+00  1.0000E+00  1.0000E+00  1.0000E+00  1.0000E+00  1.00010E+00  1.00215E+00    3   1

                   Spin transfer matrix, momentum group # 1 :
            0.349592       -0.936902          0.00000
            0.936902        0.349592          0.00000
            0.00000         0.00000           1.00000
       Trace =       1.6991838357,    ;   spin precession acos((trace-1)/2) =      69.5376429739 deg
      Precession axis :  ( 0.0000,  0.0000,  1.0000)  ->  angle to (X,Y) plane,  angle to X axis :    90.0000,    90.0000  degree
      Spin  tune  Qs (fractional) :     1.9316E-01

                        ------------------------------------------------------------
                        Momentum  group  #2 ; average  over 3 particles at this pass :
                     INITIAL                                          FINAL
      <SX>       <SY>       <SZ>       <|S|>            <SX>       <SY>       <SZ>       <|S|>    <G.gma>    <(SI,SF)>  sigma_(SI,SF)
                                                                                                      (deg)       (deg)
  0.333333   0.333333   0.333333   0.577350        -0.195765   0.428834   0.333333   0.577350  -4.193158  46.357996  32.780053

               Spin  components  of  each  of  the      3  particles,  and  rotation  angle :
                     INITIAL                                          FINAL
           SX         SY         SZ         |S|          SX         SY         SZ         |S|       GAMMA   |Si,Sf|   (Z,Sf_yz) (Z,Sf)
                                                                                                              (deg.)    (deg.)    (deg.)
                                                                                                   (Sf_yz : projection of Sf on YZ plane)
o  1  1.000000  0.000000  0.000000  1.000000     0.349603  0.936898  0.000000  1.000000      1.0022   69.537   90.000   90.000    4
o  1  0.000000  1.000000  0.000000  1.000000    -0.936898  0.349603  0.000000  1.000000      1.0022   69.537   90.000   90.000    5
o  1  0.000000  0.000000  1.000000  1.000000     0.000000  0.000000  1.000000  1.000000      1.0022    0.000   45.000    0.000    6

                  Min/Max  components  of  each  of  the      3  particles :
  SX_mi       SX_ma       SY_mi       SY_ma       SZ_mi       SZ_ma       |S|_mi      |S|_ma      p/p_0        GAMMA          I  IEX
 3.4960E-01  3.4960E-01  9.3690E-01  9.3690E-01  0.0000E+00  0.0000E+00  1.0000E+00  1.0000E+00  1.00000E+00  1.00215E+00    4   1
-9.3690E-01 -9.3690E-01  3.4960E-01  3.4960E-01  0.0000E+00  0.0000E+00  1.0000E+00  1.0000E+00  1.00000E+00  1.00215E+00    5   1
 0.0000E+00  0.0000E+00  0.0000E+00  0.0000E+00  1.0000E+00  1.0000E+00  1.0000E+00  1.0000E+00  1.00000E+00  1.00215E+00    6   1

                   Spin transfer matrix, momentum group # 2 :
          0.349603       -0.936898          0.00000
          0.936898        0.349603          0.00000
          0.00000         0.00000           1.00000
       Trace =       1.6992050586,    ;   spin precession acos((trace-1)/2) =      69.5369940370 deg
      Precession axis :  ( 0.0000,  0.0000,  1.0000)  ->  angle to (X,Y) plane,  angle to X axis :    90.0000,    90.0000  degree
      Spin  tune  Qs (fractional) :     1.9316E-01

                        ------------------------------------------------------------
                        Momentum  group  #3 ; average  over 3 particles at this pass :
                     INITIAL                                          FINAL
      <SX>       <SY>       <SZ>       <|S|>            <SX>       <SY>       <SZ>       <|S|>    <G.gma>    <(SI,SF)>  sigma_(SI,SF)
                                                                                                      (deg)       (deg)
  0.333333   0.333333   0.333333   0.577350        -0.195760   0.428836   0.333333   0.577350  -4.193157  46.357564  32.779748

               Spin  components  of  each  of  the      3  particles,  and  rotation  angle :
                     INITIAL                                          FINAL
           SX         SY         SZ         |S|          SX         SY         SZ         |S|       GAMMA   |Si,Sf|   (Z,Sf_yz) (Z,Sf)
                                                                                                              (deg.)    (deg.)    (deg.)
                                                                                                   (Sf_yz : projection of Sf on YZ plane)
m  1  1.000000  0.000000  0.000000  1.000000     0.349613  0.936894  0.000000  1.000000      1.0022   69.536   90.000   90.000    7
m  1  0.000000  1.000000  0.000000  1.000000    -0.936894  0.349613  0.000000  1.000000      1.0022   69.536   90.000   90.000    8
m  1  0.000000  0.000000  1.000000  1.000000     0.000000  0.000000  1.000000  1.000000      1.0022    0.000   45.000    0.000    9

                  Min/Max  components  of  each  of  the      3  particles :
  SX_mi       SX_ma       SY_mi       SY_ma       SZ_mi       SZ_ma       |S|_mi      |S|_ma      p/p_0        GAMMA          I  IEX
 3.4961E-01  3.4961E-01  9.3689E-01  9.3689E-01  0.0000E+00  0.0000E+00  1.0000E+00  1.0000E+00  9.99900E-01  1.00215E+00    7   1
```

```
-9.3689E-01 -9.3689E-01  3.4961E-01  3.4961E-01  0.0000E+00  0.0000E+00  1.0000E+00  1.0000E+00  9.99900E-01  1.00215E+00     8   1
 0.0000E+00  0.0000E+00  0.0000E+00  0.0000E+00  1.0000E+00  1.0000E+00  1.0000E+00  1.0000E+00  9.99900E-01  1.00215E+00     9   1

               Spin transfer matrix, momentum group # 3 :
         0.349613       -0.936894         0.00000
         0.936894        0.349613         0.00000
         0.00000         0.00000          1.00000
     Trace =       1.6992262279,    ;   spin precession acos((trace-1)/2) =      69.5363467325 deg
    Precession axis :  ( 0.0000,  0.0000,  1.0000)  ->  angle to (X,Y) plane,  angle to X axis :    90.0000,    90.0000  degree
    Spin  tune  Qs (fractional) :     1.9316E-01
*************************************************************************************************************************************
```

This simulation confirms the answer to Question 14.1.1.3.1.

The value of the spin precession angle is $\theta_{sp} = G\gamma\alpha$ modulo 360°. The on-momentum value of $G\gamma\alpha$ can be found under PARTICUL in zgoubi.res (an excerpt):

```
*************************************************************************************************************************************
     2  Keyword, label(s) :  PARTICUL                                                                                  IPASS= 1
     Particle  properties :
    HELION
                  Mass          =    2808.39        MeV/c2
                  Charge        =   3.204353E-19    C
                  G  factor     =   -4.18415
                  COM life-time =   1.000000E+99    s
               Reference  data :
                  mag. rigidity (kG.cm)   :   307.45520      =p/q, such that dev.=B*L/rigidity
                  mass (MeV/c2)           :   2808.3916
                  momentum (MeV/c)        :   184.34550
                  energy, total (MeV)     :   2814.4354
                  energy, kinetic (MeV)   :   6.0438039
                  beta = v/c              :  6.5499993689E-02
                  gamma                   :   1.002152052
                  beta*gamma              :  6.5640953062E-02
                  G*gamma                 :  -4.193158315
                  electric rigidity (MeV) :   24.14925821    =T[eV]*(gamma+1)/gamma, such that dev.=E*L/rigidity
*************************************************************************************************************************************
```

which yields a theoretical spin rotation of

$$|G\gamma| \times 360^\circ = 4.193158315 \times 360^\circ = 69.5369934\,[360^\circ]$$

(the on-momentum "group 2" above indicates 69.5369940370 deg) or equivalently a fractional spin tune value of

$$\nu_{sp} = 4.193158315/360 = 0.193158315$$

also in accord with the on-momentum "group 2" above which indicates 1.9316E-01.

From theory (after Eq. 3.11, transposed to 3D space)

$$\mathrm{frac}(\nu_{\mathrm{sp}}) = \frac{1}{2\pi}\mathrm{acos}\frac{\mathrm{Trace(spin\ matrix)} - 1}{2}$$

whereas the spin matrix from tracking says (momentum "group 2" above)

$$\mathrm{Trace}\left[\mathrm{spin\ matrix}\right] = 1.6992050586$$

in accord with the above spin tune value $\nu_{\mathrm{sp}} = 0.193158$.

Off-momentum (groups 1 and 3):

γ needs to be corrected for the $dp/p = \pm 10^{-4}$ particles. The corresponding numerical results can be found under "group 1" and "group 3" above, respectively, and can be checked to agree with the theory.

14.2.1.4 Depolarizing Resonances

Question 14.1.1.4.1—Locations ($G\gamma$ values) of the depolarizing resonances in the range

$$-10.5 \leq \mathrm{G}\gamma \leq -4.19316$$

have been added to Table 14.8, yielding Table 14.38 (integer/imperfection resonances of the form $G\gamma$ = integer), and to Table 14.9, yielding Table 14.39 (systematic intrinsic resonances of the form $G\gamma = 6 \times \text{integer} \pm Q_y$).
Question 14.1.1.4.2—Figure 14.7 illustrates intrinsic resonance crossings with two graphs of $\mathrm{S_y(G}\gamma)$, as follows:

- a few particles are taken evenly distributed in phase with the same vertical invariant ε_y; ε_x value does not matter, it is taken null here, as horizontal motion results in this perfect ring in only vertical perturbing field components—in quadrupoles—and these do not depolarize;
- they are tracked from injection $G\gamma = -4.19316$ (Table 14.37) to $G\gamma = -16$, so crossing in particular the four strong resonances $G\gamma \pm \nu_y = 6n$, $|n| = 0 - 3$. Two different cases of the vertical invariant values are tracked: $\varepsilon_y = 2.5\,\pi\,\mu\mathrm{m}$ and 10 times less.

Table 14.38 Imperfection resonances, location and strengths. Strengths are normalized to the *rms* closed orbit value, $y_{\mathrm{co,\,rms}}$ (the closed orbit is shown in Fig. 14.10). The "theory" column is filled-out using the thin lens model series

$G\gamma$ (Q. 14.1.1.4)	$\lvert\epsilon_n\rvert/y_{\mathrm{co,\,rms}}$		
	Theory	Tracking	
	(Q. 14.1.1.5)	Station.	Crossing
−5	14.8696	13.8520	13.5490
−6	1.1779	1.0839	1.1917
−7	12.5802	11.5867	11.6697
−8	3.0465	2.9006	2.8585
−9	0.2637	0.2196	0.2373
−10	2.5296	2.7105	2.6408

Table 14.39 Systematic intrinsic resonances (M=6 super-periods, $\nu_y = 4.82$), location and strengths. The latter are normalized to $\sqrt{\varepsilon_y/\pi}$, with ε_y/π being the particle invariant value. The "theory" column is filled-out using the thin lens model series. The "station." (stationary) column is filled-out using $|\epsilon_n| \equiv \omega(\delta_n = 0)$, Question 14.1.1.6. Completion of the "crossing" column is addressed in Question 14.1.1.8 and Table 14.43

$kM \pm \nu_y$	$G\gamma$ (Q. 14.1.1.4)	$\lvert\epsilon_n\rvert/\sqrt{\varepsilon_y/\pi}$		
		Theory	Tracking	
		(Q. 14.1.1.6)	Station.	Crossing
$0 - \nu_y$	−4.82	3.3989	3.63	5.2
$-12 + \nu_y$	−7.18	3.1523	3.18	4.0
$-6 - \nu_y$	−10.82	7.9235	8.52	9.13
$-18 + \nu_y$	−13.18	11.072	11.8	12.5

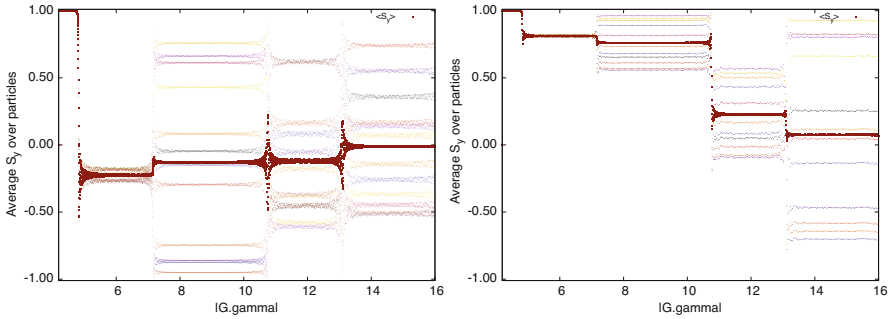

Fig. 14.7 Evolution of the vertical spin component of a few particles launched on the same invariant, with different initial betatron phases. The dark red curve is the average over 23 particles. Left: $\varepsilon_y = 2.5\,\pi\,\mu$m; right: $\varepsilon_y = 0.25\,\pi\,\mu$m

Figure 14.7 is obtained with the following combined awk (left hand side) [11] and gnuplot (right) scripts:

```
! Average over particles of SZ values read in zgoubi.fai
function analyze(x, data){
    n = 0;mean = 0;    val_min = 0;val_max = 0;

    NBturns = 20000;
    Gg1 =4.193158; Gg2 =16; dGg = (Gg2-Gg1)/(NBturns-1);

    for(val in data){
        n += 1;
        delta = val - mean;
        mean += delta/n;
        val_min = (n == 1)?val:((val < val_min)?val:val_min);
        val_max = (n == 1)?val:((val > val_max)?val:val_max);
    }
    if(n > 0){
        print x, mean, val_min, val_max;
    }
}
{
    curr = $38*dGg + Gg1;    yval = $(col_num);

    if(NR==1 || prev != curr){
        analyze(prev, data);
        delete data;
        prev = curr;
    }
    data[yval] = 1;
}
END{
    analyze(curr, data);
}
```

```
set title "SZ(turn) and  <SZ(turn)>_particles"

nbtrj=100; evryNtrj = 5; evryNpass=9

NBturns = 20000
Gg1 =4.193158 ; Gg2 =16 ; dGg = (Gg2-Gg1)/(NBturns-1)


set xlab "turns"; set ylab "Average S_y over particles"
unset colorbox

fName = 'zgoubi.fai'
plotCmd(col_num)=sprintf('< gawk -f analyze.awk -v col_num=%d %s', col_num, fName)

set format y '%0.2f'
set xr [:20e3]; set xr [Gg1:Gg2]; set yr [-1.01:1.01]

plot for [it=1:nbtrj:evryNtrj] "zgoubi.fai" \
u ($26==it && evryNpass*int($38/evryNpass)==$38? $38*dGg + Gg1 :1/0):($22):($26) \
w p pt 7 ps .1 lc palette notit ,\
    plotCmd(22) u 1:2 w p pt 5 ps .4 lc rgb 'dark-red' t '<S_y>'
```

When comparing these two graphs, essentially two things are observed: the spin kick across a resonance and the spin kick spread are smaller, when the invariant is smaller:

(i) a smaller invariant means smaller values of the perturbing $B_x = \mathcal{G}y$ radial field components in quadrupoles, hence smaller spin kicks;

(ii) spread in betatron motion around the ring results from the spread in the initial betatron phase of the particles for a given invariant. Smaller invariant value results in a smaller span of the field values experienced by the different particles in the vertical quadrupoles (Fig. 14.8).

For the record: the resonance strength is $\propto \sqrt{\varepsilon_y/\pi}$ (Eq. 2.35).

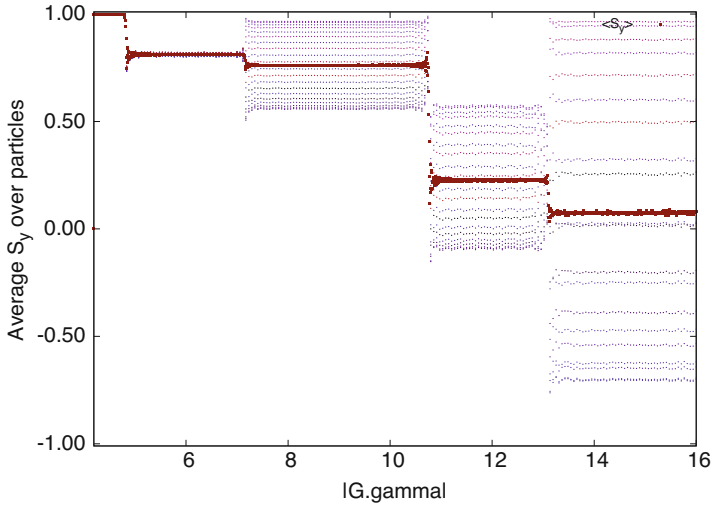

Fig. 14.8 A sensible question at this point is whether these results converge. The present figure is obtained using 200 particles. Comparison with the 23 trajectory case of Fig. 14.7 does not show much difference. The final polarizations is very similar, the problem converges

Fig. 14.9 Fields experienced in vertical quadrupoles during vertical betatron motion: 3 different particles are displayed here, over 3 turns around the ring. They are taken on the same invariant but with different initial betatron phases

Question 14.1.1.4.3—A graph showing the span in magnetic field strengths experienced in the vertical quadrupoles by the 3 orbiting particles with the same invariant value, as an effect of their different initial betatron phases, is given in Fig. 14.9. The

three vastly different torque series experienced by these particles' spins result in largely different spin states upon crossing the resonances (Fig. 14.7).

14.2.1.5 Imperfection Resonance Strengths

An excerpt of the input data file used is given in Table 14.40. It shows in particular

- sample vertical quadrupole misalignments accounted for by means of KPOS=5, which implement Table 14.10 random vertical offset data;
- the use of FIT, preceding TWISS, which allows accounting for the non-zero vertical closed orbit excited by the quadrupole misalignments given in Table 14.10.

The vertical closed orbit so obtained is shown in Fig. 14.10.

The resonance strengths to be computed here, as a function of energy, all assume that very closed orbit (and obviously, the same optical functions).

Resonance strength calculation uses (Eq. 2.29)

$$\left\{ \begin{array}{c} \mathcal{R}e(\epsilon_n^{\text{imp}}) \\ \mathcal{I}m(\epsilon_n^{\text{imp}}) \end{array} \right\} = \frac{1+G\gamma}{2\pi} \sum_{\text{Qpoles}} \left\{ \begin{array}{c} \cos G\gamma\alpha_i \\ \sin G\gamma\alpha_i \end{array} \right\} (KL)_i \; y_{co}(\theta_i)$$

which can be evaluated numerically. In this formula, the following data are read from zgoubi.TWISS.out at the locations of the quadrupoles (i index):

- θ_i: orbital angle, from the origin of the sequence,
- α_i: cumulative orbit deviation, from the origin of the sequence,
- $(KL)_i$: integrated quadrupole strength,
- $y_{\text{co, i}}$: orbit excursion.

These quantities do not depend on $G\gamma$ (magnet fields are ramped to follow the value of the reference rigidity OBJET[BORO]).

Table 14.8 has been updated with the imperfection resonance strengths obtained this way yielding the "theory" column of Table 14.38.

14.2.1.6 Intrinsic Resonance Strengths

The optical functions and periodic vertical orbit are needed here, which means use of the output file zgoubi.TWISS.out. This file is produced using the input data file of the complete ring, equipped with a TWISS command, as in Sect. 14.2.1.2.

Resonance strength is obtained by summing the series (Eq. 2.35)

$$\left\{ \begin{array}{c} \mathcal{R}e(\epsilon_n^{\text{intr}\pm}) \\ \mathcal{I}m(\epsilon_n^{\text{intr}\pm}) \end{array} \right\} = \frac{1+G\gamma}{4\pi} \sum_{\text{Qpoles}} \left\{ \begin{array}{c} \cos(G\gamma\alpha_i \pm \varphi_i) \\ \sin(G\gamma\alpha_i \pm \varphi_i) \end{array} \right\} (KL)_i \sqrt{\beta_{y,i}\frac{\varepsilon_y}{\pi}}$$

Table 14.40 Head, intermediate quadrupoles, and tail of the Booster sequence, including vertical quadrupole misalignments, as well as a FIT-TWISS sequence which computes vertical orbit and optical functions (logged in zgoubi.TWISS.out), accounting for non-zero closed orbit (FIT first finds the orbit, prior to passing on to TWISS). The reference rigidity for this zgoubi.TWISS.out computation is arbitrary as the vertical orbit (and optical functions obviously) are maintained unchanged regardless of $G\gamma$ in these exercises (the fields are ramped to follow the value of the reference rigidity OBJET[BORO]). The final SYSTEM command causes execution of an external file, which plots the closed orbits and optical functions, reading the latter data from zgoubi.TWISS.out

```
Booster ring, complete, with vertical orbit.
'OBJET'
3.0428810404e+03
5
.001 .01 .001 .01 .001 .0001
0. 0. 0.84273180 1.5602297 0. 1. ' '
'PARTICUL'
HELION

'SCALING'
1 3
BEND
-1
3.04288104
1
MULTIPOL QH*   ! QH family is set for Qx=4.73 & Qy=4.82 tunes.
-1
3.30602909
1
MULTIPOL QV*   ! QV family is set for Qx=4.73 & Qy=4.82 tunes.
-1
3.24298881
1

'MARKER'      LA1S
'DRIFT'    DRIF      L057
57.0400
------------------------------------------------
'MULTIPOL' QVA1      QUAD
0  .Quad
0.493916E+02 10.0000 0.  -0.5472896982 0. 0. 0. 0. 0. 0. 0.
0. 0. 6.00  3.00 1.00 0.00 0.00 0.00 0.00 0. 0. 0. 0.
6  .1122 6.2671 -1.4982 3.5882 -2.1209 1.723
0. 0. 6.00  3.00 1.00 0.00 0.00 0.00 0.00 0. 0. 0. 0.
6  .1122 6.2671 -1.4982 3.5882 -2.1209 1.723
0. 0. 0. 0. 0. 0. 0. 0. 0. 0.
2.  ! cm  MultQVA1
5 0.0 0.0 0.67238500 0 0 0
------------------------------------------------
'MULTIPOL' QHA2      QUAD
0  .Quad
0.485016E+02 10.0000 0.   0.5256342158 0. 0. 0. 0. 0. 0. 0.
0. 0. 6.00  3.00 1.00 0.00 0.00 0.00 0.00 0. 0. 0. 0.
6  .1122 6.2671 -1.4982 3.5882 -2.1209 1.723
0. 0. 6.00  3.00 1.00 0.00 0.00 0.00 0.00 0. 0. 0. 0.
6  .1122 6.2671 -1.4982 3.5882 -2.1209 1.723
0. 0. 0. 0. 0. 0. 0. 0. 0. 0.
2.  ! cm  MultQHA2
5 0.0 0.0 0.73457500 0 0 0
------------------------------------------------

'MULTIPOL' QHF8      QUAD
0  .Quad
0.485016E+02 10. 0. 0.5256342158 0. 0. 0. 0. 0. 0. 0.
0. 0. 6.00  3.00 1.00 0.00 0.00 0.00 0.00 0. 0. 0. 0.
6  .1122 6.2671 -1.4982 3.5882 -2.1209 1.723
0. 0. 6.00  3.00 1.00 0.00 0.00 0.00 0.00 0. 0. 0. 0.
6  .1122 6.2671 -1.4982 3.5882 -2.1209 1.723
0. 0. 0. 0. 0. 0. 0. 0. 0. 0.
2.  ! cm  MultQHF8
5 0.0 0.0 0.38532700 0 0 0
'DRIFT'    DRIF      L031
29.9367
'BEND'     DHF8T     SBEN
0  .Bend
1.2096161E+02  0.  7.2121043E-01
0.00  0.00   0.00000000
4 .2401  1.8639  -.5572  .3904 0. 0. 0.
0.00  0.00   0.00000000
4 .2401  1.8639  -.5572  .3904 0. 0. 0.
1.0000E+00 cm  Bend
3 0. 0. 0.
'BEND'     DHF8Z     SBEN
0  .Bend
1.2096161E+02  0.  7.2121043E-01
0.00  0.00   0.00000000
4 .2401  1.8639  -.5572  .3904 0. 0. 0.
0.00  0.00   0.00000000
4 .2401  1.8639  -.5572  .3904 0. 0. 0.
1.0000E+00 cm  Bend
3 0. 0. 0.
'MARKER'      LA2E

'FIT'
2                              ! 2 variables, as follows.
1 32 0 [-1.,1.]           ! Allow +/-1cm variation of Z_0.
1 33 0 [-10.,10.]      ! Allow +/-10mrad variation of P_0.
2  1e-10      ! 2 constraints; requested penalty is 1e-10.
3.1 1 4 #End 0. 1. 0 ! Request final posit. Z=initial Z_0.
3.1 1 5 #End 0. 1. 0  ! Request final angle P=initial P_0.

'TWISS'
2 1. 1.
'FAISCEAU'     ! Allows quick check of initial=final Z, P.
'SYSTEM'       ! Plot closed orbits and optical functions.
1
gnuplot < ./gnuplot_TWISS.gnu
'END'
```

which can be calculated numerically. In this formula, the following data are read from zgoubi.TWISS.out at the locations of the quadrupoles (i index):

- α_i: cumulative orbit deviation, from the origin of the sequence,
- $(KL)_i$: integrated quadrupole strength,
- φ_i: betatron phase advance,
- β_i: betatron function,
- ε_y/π: invariant value.

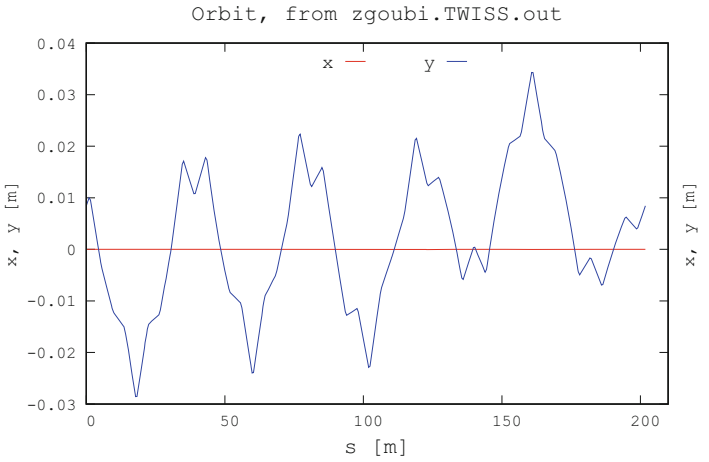

Fig. 14.10 Vertical closed orbit excited by the quadrupole misalignments of Table 14.10

These quantities do not depend on $G\gamma$ (magnet fields are ramped to follow the value of the reference rigidity OBJET[BORO]).

For a reference, the upper and lower parts of zgoubi.TWISS.out data file (as produced by the TWISS command), showing the optical function values along the sequence needed to compute the series above are as follows (excerpts):

```
@ LENGTH            %le     33.63000810
@ ALFA              %le    0.5271462897E-01
@ ORBIT5            %le                  -0
@ GAMMATR           %le     4.355463945
@ Q1                %le    0.7299999804       [fractional]
@ Q2                %le    0.8199999584       [fractional]
@ DQ1               %le   -0.7429052400
@ DQ2               %le   -0.8355856969
@ DXMAX             %le     3.01663095E+00     @ DXMIN             %le     9.49130311E-01
@ DYMAX             %le     0.00000000E+00     @ DYMIN             %le     0.00000000E+00
@ XCOMAX            %le     0.00000000E+00     @ XCOMIN            %le    -5.12842866E-14
@ YCOMAX            %le     0.00000000E+00     @ YCOMIN            %le     0.00000000E+00
@ BETXMAX           %le     1.41491375E+01     @ BETXMIN           %le     4.22123922E+00
@ BETYMAX           %le     1.27947203E+01     @ BETYMIN           %le     3.81920290E+00
@ XCORMS            %le     1.50372304E-14
@ YCORMS            %le    0.    not computed
@ DXRMS             %le     5.94727589E-01
@ DYRMS             %le     0.00000000E+00
@ DELTAP            %le     0.00000000E+00
@ |C|               %le     0.000000000
@ Q1*               %le     0.000000000
@ Q2*               %le     0.000000000
@ TITLE             %12s   "Zgoubi model"
@ ORIGIN            %12s   "twiss.f"
@ DATE              %08s   "  "
@ TIME              %08s   "  "
# From TWISS keyword
# alfx           btx            alfy           bty            alfl           btl            Dx             etc.
# 1              2              3              4              5              6              7
1.0086402E+000  5.8955920E+000 -1.5005233E+000  9.4500882E+000  0.0000000E+000  0.0000000E+000  1.1034842E+000  etc.
1.0086402E+000  5.8955920E+000 -1.5005233E+000  9.4500882E+000  0.0000000E+000  0.0000000E+000  1.1034842E+000
1.0086402E+000  5.8955920E+000 -1.5005233E+000  9.4500882E+000  0.0000000E+000  0.0000000E+000  1.1034842E+000
8.1346059E-001  4.8562657E+000 -1.6967856E+000  1.1273833E+001  0.0000000E+000  0.0000000E+000  1.0186499E+000
8.1346025E-001  4.8562641E+000 -1.6967859E+000  1.1273837E+001  0.0000000E+000  0.0000000E+000  1.0186498E+000
7.8964451E-001  4.7446880E+000 -1.7207337E+000  1.1511696E+001  0.0000000E+000  0.0000000E+000  1.0082983E+000

.............................................
```

```
1.6898235E+000  1.2487484E+001 -6.6866811E-001  4.1920085E+000  0.0000000E+000  0.0000000E+000  1.6554672E+000  etc.
1.3706530E+000  8.7748783E+000 -1.0863704E+000  6.3156052E+000  0.0000000E+000  0.0000000E+000  1.3317807E+000
1.0098358E+000  5.8871527E+000 -1.5040727E+000  9.4500414E+000  0.0000000E+000  0.0000000E+000  1.1034842E+000
1.0098358E+000  5.8871527E+000 -1.5040727E+000  9.4500414E+000  0.0000000E+000  0.0000000E+000  1.1034842E+000
1.0098358E+000  5.8871527E+000 -1.5040727E+000  9.4500414E+000  0.0000000E+000  0.0000000E+000  1.1034842E+000
1.0098358E+000  5.8871527E+000 -1.5040727E+000  9.4500414E+000  0.0000000E+000  0.0000000E+000  1.1034842E+000
```

A detailed description of zgoubi.TWISS.out data column format can be found in the Users' Guide, Section 8.4.

Table 14.9 has been updated with the intrinsic resonance strengths obtained here, yielding the "theory" column of Table 14.39.

14.2.1.7 Spin Motion Through Imperfection Resonances

Input data files similar to those in the answer to Question 14.1.1.5 (Sect. 14.2.1.5 and Table 14.40) are used here. They only differ by

- the reference rigidity (OBJET[BORO]) and, accordingly, field coefficients under SCALING so to maintain unchanged orbit and optics,
- use of CAVITE for acceleration through the resonance, in the second question.

An interface has been developed in python (an evolution, by the present co-authors, of pyZgoubi [4]), which takes care of repeating the tracking at various distances $\Delta G\gamma = G\gamma - G\gamma_n$ from the resonance, in Question 14.1.1.8.1, or at various resonant frequencies $G\gamma_n$ in Question 14.1.1.8.2 thus automating the procedure.

Question 14.1.1.8.1—The following shows the head and tail of the tracking input data file, in the stationary case, on the resonance $G\gamma_n = -6$. Note the INCLUDE of the SCALING segment [SCALING_S:SCALING_E] as defined in Table 14.7, with the field coefficient updated to present BORO/1000 value, namely, 4.8139470584

```
Booster
'OBJET'
4.8139470584e+03                                                    ! Rigidity at G.gamma=-6.
2
1 1
0. 0. 0.84273180 1.5602297 0. 1. ' '         ! Track a single 3He, launched on closed orbit.
1
'PARTICUL'
HELION
'SPNTRK'                                                          ! Start with spin vertical.
3
'FAISTORE'
zgoubi.fai
1

          ! Scaling coefficients in scaling_Gg6.inc are updated to present BORO/1000 value.
'INCLUDE'
1
scaling_Gg6.inc[SCALING_S,*:SCALING_E,*]

'DRIFT'    DRIF      L057
57.0400
..............
'BEND'     DHF8Z     SBEN
0  .Bend
1.2096161E+02   0.0000000E+00   7.2121043E-01
0.00  0.00   0.00000000
4 .2401  1.8639  -.5572  .3904 0. 0. 0.
0.00  0.00   0.00000000
4 .2401  1.8639  -.5572  .3904 0. 0. 0.
1.0000E+00 cm  Bend
```

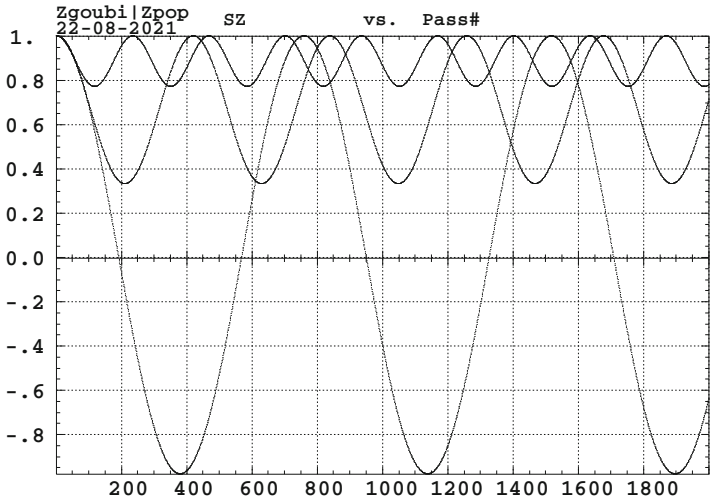

Fig. 14.11 Spin oscillation $S_y(turn)$ for different distances to the resonance $G\gamma_n = -6$. A greater distance δ_n results in a higher oscillation frequency $\omega = \sqrt{|\epsilon_n|^2 + \delta_n^2}$ (Sect. 3.6). On the resonance, the precession axis lies in the median plane, S_y oscillation covers $[-1, 1]$ and $\langle S_y \rangle = 0$

```
3 0. 0. 0.
'MARKER'      LA2E                                          ! Booster lattice ends here.
'REBELOTE'  ! 2000 turns are sufficient to see a complete S_y oscillaiton when on resonance,
1999 0.1 99                    ! from what <S_y> is deduced - greater distance to resonance
                                                           ! results in greater frequency.
'END'
```

Sample tracking results for $S_y(\theta)$ oscillation at various distances to the resonance, are given in Fig. 14.11. The average value $\langle S_y \rangle$ is computed from these tracking data.

The exercise is repeated for the different $-10 \leq G\gamma_n \leq -5$ values, resulting in Fig. 14.12 which shows $\langle S_y \rangle$ dependence on the distance to the resonance so obtained, and fit to Eq. 2.49

$$\langle S_y \rangle = \frac{\delta_n}{\sqrt{\epsilon_n^2 + \delta_n^2}} \tag{14.5}$$

The "stationary" column of Table 14.8 has been completed accordingly (Table 14.38).

Question 14.1.1.8.2—A 400 keV/turn acceleration rate is taken for the crossing ($\hat{V} = 400$ kV, synchronous phase 30°). The following shows the head and tail of the tracking input data file in the case of $G\gamma_n = -6$ crossing:

```
Booster
'OBJET'
3.77645661e+03                          ! Initial rigidity is taken at Ggamma=-5.374744660,
2                                  ! upstream enough not to feel the resonance at G.gamma=-6.
1 1
0. 0. 0.84273180 1.5602297 0. 1. ' '          ! Track a single 3He, launched on closed orbit.
1
'PARTICUL'
```

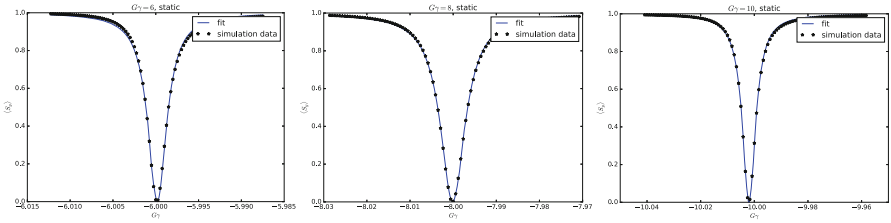

Fig. 14.12 Average value of the vertical spin component S_y, depending on the distance to the resonance for the cases of three different resonances $G\gamma_n = -6$, -8 and -10. The symbols are from tracking, the solid curves are from the theory (Eq. 2.49). $\langle S_y \rangle = 0$ corresponds to S_y oscillating over $[-1, 1]$, thus the precession axis lies in the median plane, $G\gamma$ is on resonance

```
HELION
'SPNTRK'                                                    ! Start with spin vertical.
3
'FAISTORE'
zgoubi.fai
1

         ! Scaling coefficients in scaling_GgXXX.inc are updated to present BORO/1000 value.
'INCLUDE'
1
scaling_Gg5.374.inc[SCALING_S,*:SCALING_E,*]

'MARKER'      LA1S                                        ! Booster lattice starts here.
'DRIFT'    DRIF      L057
57.0400
..............
'BEND'     DHF8Z     SBEN
0  .Bend
1.2096161E+02   0.0000000E+00   7.2121043E-01
0.00  0.00   0.00000000
4 .2401  1.8639  -.5572  .3904 0. 0. 0.
0.00  0.00   0.00000000
4 .2401  1.8639  -.5572  .3904 0. 0. 0.
1.0000E+00 cm  Bend
3 0. 0. 0.
'MARKER'      LA2E                                          ! Booster lattice ends here.
'CAVITE'
2
201.78 1.
4.e+05 0.5235987756                                  ! 400 kV acceleration peak voltage.
'REBELOTE'      ! 2000 turns are sufficient to cross the resonance, leaving from away enough
1999 0.1 99                                            ! ending on the asymtotic region.
'END'
```

The initial $G\gamma$ is taken at -5.374744660, upstream enough not to feel the resonance at $G\gamma_n = -6$.

Sample results for $S_y(\theta)$ during resonance crossing are given in Fig. 14.13, for various $G\gamma_n = n$ values. The resonance strengths are deduced from the respective values of P_f/P_i, using (after Eq. 2.44)

$$|\epsilon_n| = \left(\frac{2\alpha}{\pi} \ln \frac{2}{1 + P_f/P_i} \right)^{1/2} \tag{14.6}$$

with $\alpha = \dfrac{dG\gamma}{d\theta} = 9.484 \times 10^{-5}$ being the resonance crossing speed.

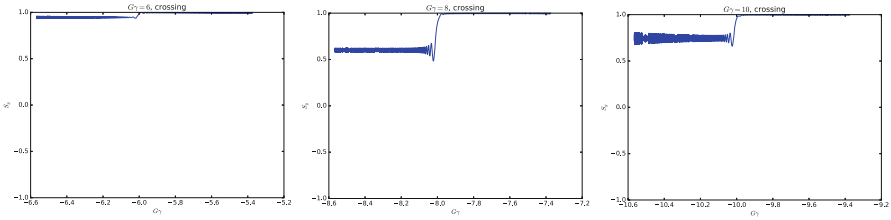

Fig. 14.13 Evolution of the vertical spin component S_y during integer resonance crossing, for the cases of $G\gamma = -6,\ -8$ and -10

The "crossing" column of Table 14.8 has been completed accordingly (Table 14.38).

14.2.1.8 Spin Motion Through Intrinsic Resonances

Questions 14.1.1.8.1, 2—The systematic resonance at $G\gamma_n = 0 - \nu_y = -4.82$ is first considered, $B\rho = 2.67875735816\,\mathrm{T\,m}$.

In the stationary case, the spin precession data are obtained by tracking a single particle with a particular vertical invariant value (use OBJET[KOBJ=8]) for many turns (use REBELOTE[NPASS=2000]) at a fixed energy.

The input data file is given in Table 14.41. It is similar to the input data file of Table 14.7, apart from the few necessary changes: modification the setup under OBJET (KOBJ=8 for a single particle with a certain invariant, on-momentum), SPNTRK, and addition of REBELOTE for multi-turn tracking. Note that the SCALING command and its data list, a segment defined in and included as a part of the input data file in Table 14.7, have been saved in the scaling_GgXXX.inc file, which is subject to an INCLUDE here. This is for the mere purpose of shortness. The values of the scaling coefficients in scaling_GgXXX.inc have to be updated to the present BORO value, for instance, in this case, from BORO/1000=0.3074552 (Table 14.7) to BORO/1000=2.678757358169758 (Table 14.41).

The turn-by-turn spin motion obtained this way is displayed in Fig. 14.14. The slow oscillation in that graph is that of the vertical component S_y (S_Z in Zgoubi notation). The oscillation frequency is $\omega = \sqrt{|\epsilon_n|^2 + \delta_n^2} = |\epsilon_n|$. The amplitude

Table 14.41 Input data file for a 2000-turn tracking of spin motion, at fixed energy in the vicinity of the intrinsic resonance $G\gamma_n = 0 - \nu_y = -4.82$. Note that the SCALING command of Table 14.7 and its data list are subject to an INCLUDE (the scaling_GgXXX.inc file) for shortness

```
 'OBJET'
2.6787573581697584e3
    8
 1 1 1
 0. 0. 0. 0. 0. 1.
 0.982907  5.483186  0.
   -1.54525   9.69143  1.3196407949223E-07
 0. 1. 0.
 'PARTICUL'
  HELION
 'SPNTRK'
 4.1
 0. 0. 1.
 'FAISCEAU'
 'PICKUPS'
 1
 #Start
 'FAISTORE'
 zgoubi.fai
 1
 'MARKER'  #Start

        ! Scaling coefficients in scaling_GgXXX.inc are updated to present BORO/1000 value.
'INCLUDE'
1
scaling_Gg4.82.inc[SCALING_S,*:SCALING_E,*]

'INCLUDE'
1
6* superA.inc[superA_S,*:superA_E,*]

'REBELOTE'
 2000 0.2 99

 'END'
```

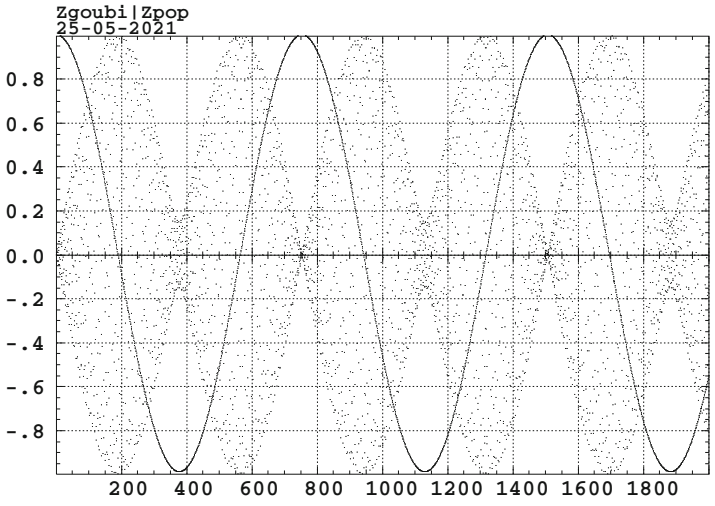

Fig. 14.14 Turn-by-turn motion of the three components of a spin, initially vertical. On-resonance here, $G\gamma = G\gamma_n = -\nu_y$, distance to the resonance $\delta_n = 0$. The slow oscillation (the solid curve with a 754 turn period) is that of the vertical component. The high frequency horizontal components (the high frequency dots, featuring the $\omega = |\epsilon_n|$ modulation) both average to zero, since s_π precesses about $\mathbf{n}$, which itself precesses about the vertical axis

averages to zero ($\langle S_y \rangle = 0$) in this case of being on resonance, since **n** is in the horizontal plane, namely (Eq. 2.48)

$$\delta_n = 0 \qquad \text{thus} \qquad |s_\pi|^2 = \frac{1}{1 + \left(\dfrac{\delta_n}{|\epsilon_n|}\right)^2} = 1 \quad \Rightarrow \langle S_y \rangle = \sqrt{1 - |s_\pi|^2} = 0$$

The horizontal components S_x and S_s (S_Y and S_X in Zgoubi notations) are also displayed (fast oscillatory motion appearing as scattered dots). They oscillate at a much greater frequency $G\gamma_n \gg \omega$. They average to zero, since the eigenvector **n** precesses about the vertical axis with a constant projected n_y component independent of the turn number. Figure 14.15 shows the Fourier spectrum of the motion. On-resonance ($\delta_n = 0$), the oscillation frequency (in units of revolution frequency) is (see Sect. 3.6)

$$\omega \equiv \sqrt{|\epsilon_n|^2 + \delta_n^2} \overset{\delta_n = 0}{=} |\epsilon_n| = 1/754 = 0.00133$$

Given that the period of the slow motion in Fig. 14.15 is about 754 turns, the value of 0.00133 is in a good accord with the distance of the peaks in Fig. 14.15 to frac($G\gamma_n$) = 0.82. Two additional distances to the resonance, $\delta_n = |\epsilon_n|$ and $\delta_n = 2|\epsilon_n|$, are displayed in Fig. 14.16.

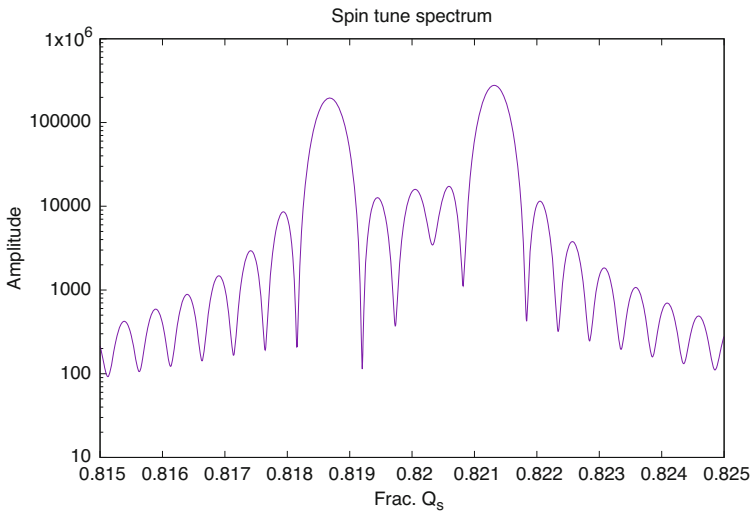

Fig. 14.15 Fourier spectrum of the spin motion (horizontal components). The two peaks at 0.82 ± 0.00135 are the result of combining the $G\gamma_n = 4.82$ frequency of **n** precession about the vertical axis and the $\sqrt{|\epsilon_n|^2 + \delta_n^2} = |\epsilon_n| = 0.00135$ frequency of the spin precession about **n**

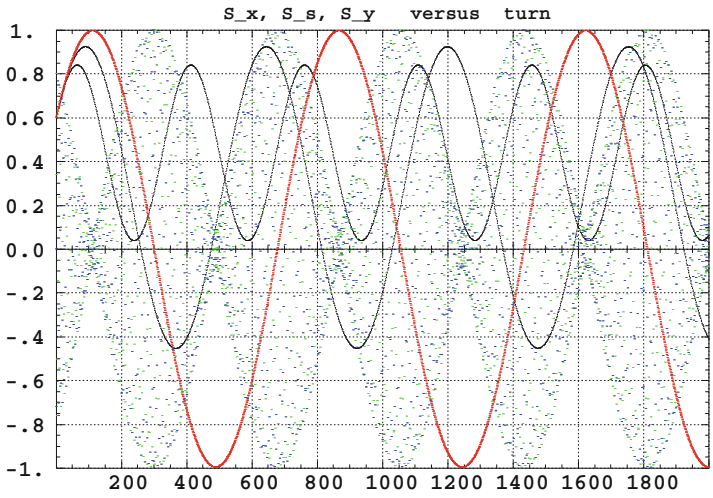

Fig. 14.16 Helion spin precession at $G\gamma = -\nu_y$ in the AGS Booster. S_y oscillates slowly (the solid sine waves), frequency $\omega \ll 1$. Three different distances to the resonance are plotted: $\delta_n = 0$ (the slow wave with a ± 1 amplitude), $\delta_n = |\epsilon_n|$ and $\delta_n = 2|\epsilon_n|$ (the fast wave with the smallest amplitude). S_x and S_s exhibit fast oscillations (dots) at a frequency $G\gamma_n = 4.82 \gg \omega$ modulated by the frequency ω

Stationary tracking can be repeated for the other three systematic intrinsic resonances. The "stationary" column of Table 14.9 has been completed accordingly (Table 14.39).

Questions 14.1.1.8.3, 4—A 100 keV/turn acceleration rate is taken for crossing ($\hat{V} = 100$ kV, synchronous phase 30 deg). However, this is an arbitrary choice. The resonance strength does not depend on the crossing speed, so $\hat{V}$ is a free parameter.

The four systematic resonance cases, namely, $G\gamma_n = \text{integer} \times M \pm \nu_y$ (M=6 cells), are tracked to fill out Table 14.39. The resonance strengths are deduced from the respective values of P_f/P_i, using (after Eq. 2.44)

$$|\epsilon_n| = \left(\frac{2\alpha}{\pi} \ln \frac{2}{1 + P_f/P_i}\right)^{1/2} \tag{14.7}$$

with the resonance crossing speed of $\alpha = \dfrac{dG\gamma}{d\theta} = 2.371 \times 10^{-5}$.

The particle invariant is chosen to ensure $P_f/P_i \approx 0.5$, for convenience. For each $G\gamma_n$ value, three particles are tracked. They are launched with $2\pi/3$ (normalized) betatron phase spacing. It can be observed, however, (Fig. 14.18) that these four different spin motions S_y(turn) essentially superimpose (this would not be the case above a sufficiently large ε_y value causing substantially different betatron excursions along the ring), which implies, in particular, that the asymptotic P_f is independent of the initial ϕ_y for a given invariant ε_y.

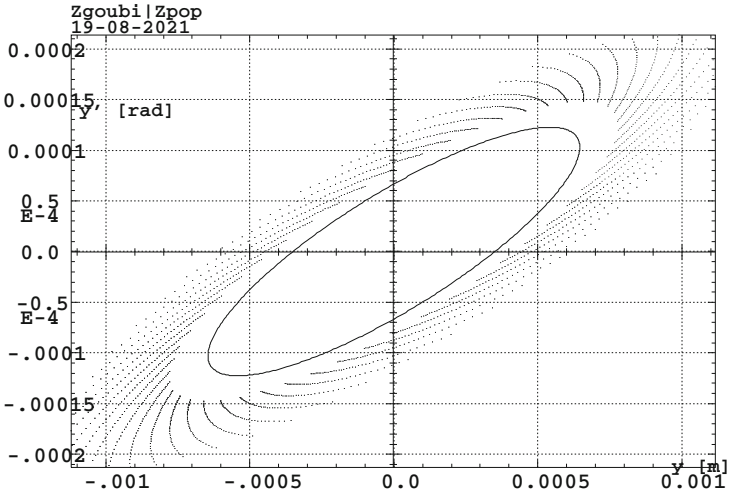

Fig. 14.17 Particle motion in the vertical phase space over the 2000-turn acceleration range (dots) in the case of $|G\gamma_n| = \nu_y$. The particle invariant is damped, from an initial $\varepsilon_{y,i}/\pi$ to a final $\varepsilon_{y,f}/\pi$ value. The solid ellipse is the *rms* ellipse matched to the 2000-turn damped motion

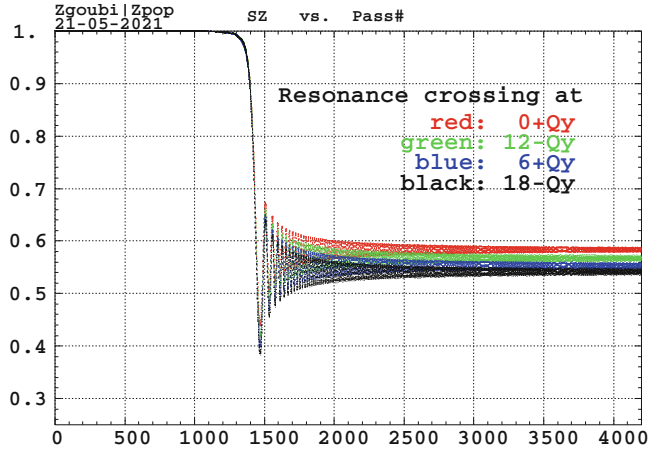

Fig. 14.18 Crossing of each of the four systematic resonances is displayed here. In each case, three particles are tracked. They are launched with $2\pi/3$ (normalized) betatron phase spacing. These three different curves essentially superimpose (they cannot be distinguished on this graph), *i.e.*, P_f is independent of the initial ϕ_y. The starting $G\gamma$ value is $100 \times |\epsilon_n|$ upstream of the resonance. The particle invariant is chosen to ensure $P_f/P_i \approx 0.5$

Particle motion in the vertical phase space is displayed in Fig. 14.17. The motion is damped due to acceleration. The spin motion is displayed in Fig. 14.18. The starting $G\gamma$ value is taken $100 \times |\epsilon_n|$ upstream of the resonance, so that the **n** vector is essentially vertical (for a reference: $7 \times |\epsilon_n|$ corresponds to $\cos\phi = \langle S_y \rangle = 0.99$).

Table 14.42 Input data file for a 4504-turn helion ion acceleration across $G\gamma_n = 0 - \nu_y = -4.82$ at a rate of 100 keV/turn. Note that the value of the scaling coefficient in scaling_GgXXX.inc has to be updated to the present value of BORO/1000=2.12998742

```
4504-turn helion ion acceleration
 'OBJET'                                                                    1
    2.12998742d3
    8
 1 3 1
 0. 0. 0. 0. 0. 1.
 0.982907  5.483186  0.
   -1.54525        9.69143       1.864270E-07
 0. 1. 0.
 'PARTICUL'
  2.808391586E+03  3.204352974E-19  4.184153800E+00  0. 0.
 'SPNTRK'
 3
 'FAISCEAU'
 'PICKUPS'
 1
 #Start
 'FAISTORE'
 b_zgoubi.fai  #End
 1
 'MARKER'  #Start

        ! Scaling coefficients in scaling_GgXXX.inc are updated to present BORO/1000 value.
'INCLUDE'
1
scaling_Gg4.596.inc[SCALING_S,*:SCALING_E,*]

'INCLUDE'
1
6* superA.inc[superA_S,*:superA_E,*]

 'CAVITE'
 3
   201.78004860000      1.00
  1.00000000E+05     5.235987755983E-01
 'MARKER'   #End
 'REBELOTE'
    4503  0.2  99

 'END'
```

Table 14.43 Asymptotic final polarization P_f, starting from $P_i = 1$. The particle invariant is damped over the 2000-turn acceleration range, from $\varepsilon_{y,i}/\pi$ to $\varepsilon_{y,f}/\pi$. $\langle \varepsilon_y/\pi \rangle$ is twice the final *rms* ε_y/π value (i.e., the area enclosed by the *rms* ellipse matched to the damped motion in the phase space)

$\lvert G\gamma_n \rvert$	P_f	$\varepsilon_{y,i}$ [μm]	$\varepsilon_{y,f}$ [μm]	$\frac{\lvert\epsilon_n\rvert}{\sqrt{\langle \varepsilon_y/\pi \rangle}}$
$0 + \nu_y$	0.584	0.162	0.099	5.2
$12 - \nu_y$	0.565	0.25	0.218	4.1
$6 + \nu_y$	0.554	0.0476	0.0442	9.13
$18 - \nu_y$	0.545	0.0261	0.0246	12.5

The input data file for the case $G\gamma_n = 0 + \nu_y$ is given in Table 14.42. The same file is used for the other three resonances. The only changes are the updated values of BORO under OBJET and of the scaling coefficients in the INCLUDEd file scaling_GgXXX.inc (namely, the latter are updated to BORO/1000).

Table 14.43 summarizes the asymptotic P_f values obtained this way for the four systematic intrinsic resonances, and the resulting resonance strengths $|\epsilon_n|$

obtained using Eq. 14.6 with $P_i = 1$. The "crossing" column of Table 14.9 has been completed accordingly (Table 14.39).

14.2.1.9 Spin Motion Through a Weak Resonance

The systematic intrinsic resonance

$$G\gamma_n = -\nu_y = -4.8201$$

is considered, under fast crossing,

$$\hat{V} = 400\,\mathrm{kV}$$

The tune value $\nu_y = -4.8201$ above results from the lattice settings (Sect. 14.2.1.2). Fourier analysis of the multiturn phase space motion displayed in Fig. 14.17 confirms that value.

Compared to the previous simulations, the four times greater acceleration rate here weakens the depolarizing effect. The resonance is made weaker in addition by using a smaller invariant, namely

$$\varepsilon_y/\pi \approx 1.03 \times 10^{-8}$$

at the resonance (the invariant damps during acceleration, the starting value is $\varepsilon_y/\pi \approx 1.3 \times 10^{-8}$ m, Table 14.44). The input data file for this tracking is given in Table 14.44, a copy of Table 14.42, *mutatis mutandis*, namely: with the initial invariant changed to $\varepsilon_y/\pi \approx 1.3 \times 10^{-8}$ under OBJET, the peak voltage changed to $\hat{V} = 400\,\mathrm{kV}$ under CAVITE, and NPASS=2000 under REBELOTE. This results in

$$P_f \approx 0.9906\, P_i$$

as can been seen from Fig. 14.19 showing a graph of the turn-by-turn S_y(turn) motion across the resonance.

Fitting that spin motion S_y(turn) to the Fresnel integral model (Eq. 2.47)

$$\text{For } y > 0 \ \textit{i.e.},\ \theta > 0 \quad \rightarrow \overbrace{\sin^2\varphi = \frac{\pi}{a}\,|\epsilon_n|^2\left[(0.5 + C(y))^2 + (0.5 + S(y))^2\right]}^{\text{downstream of the resonance}}$$

$$\text{For } y < 0 \ \textit{i.e.},\ \theta < 0 \ \textit{pose } y = -x \ \textit{with } x > 0 \quad \rightarrow \underbrace{\sin^2\varphi = \frac{\pi}{a}\,|\epsilon_n|^2\left[(0.5 - C(x))^2 + (0.5 - S(x))^2\right]}_{\text{upstream of the resonance}}$$

Table 14.44 Input data file for 2001-turn helion ion acceleration across $G\gamma_n = -\nu_y = -4.82$ at a rate of 400 keV/turn. Note that the value of the scaling coefficient in scaling_GgXXX.inc has been updated to the present value of BORO/1000=2.12998742

```
Crossing a weak resonance
 'OBJET'
    2.12998742d3
    8
 1 3 1
 0. 0. 0. 0. 0. 1.
 0.982907  5.483186  0.
   -1.54525        9.69143       1.31964E-08
 0. 1. 0.
 'PARTICUL'
  2.808391586E+03  3.204352974E-19  4.184153800E+00  0. 0.
 'SPNTRK'
 3
 'FAISCEAU'
 'PICKUPS'
 1
 #Start
 'FAISTORE'
 zgoubi.fai  #End
 1
 'MARKER'  #Start

        ! Scaling coefficients in scaling_GgXXX.inc are updated to present BORO/1000 value.
'INCLUDE'
1
scaling_Gg4.596.inc[SCALING_S,*:SCALING_E,*]

'INCLUDE'
1
6* superA.inc[superA_S:superA_E]

 'CAVITE'
 3
   201.78004860000      4.00
  4.00000000E+05     5.235987755983E-01

 'MARKER'   #End

 'REBELOTE'
 2000  0.2  99

 'END'
```

yields the respective resonant $G\gamma$ and normalized resonance strength values (with $\varepsilon_y/\pi = 1.03 \times 10^{-8}$ m) of

$$|G\gamma_n| = 4.8202, \quad |\epsilon_n|/\sqrt{\varepsilon_y/\pi} = 5.3$$

The former quantity is in a good agreement with $\nu_y = 4.8201$ from the Fourier analysis of the phase space motion. The latter is in a good accord with the result obtained from the strong resonance simulation crossing, namely (Table 14.39, rightmost column), $|\epsilon_n|/\sqrt{\varepsilon_y/\pi} = 5.2$. The Fresnel integral model and the tracking results in the region of the resonance are superimposed in Fig. 14.19.

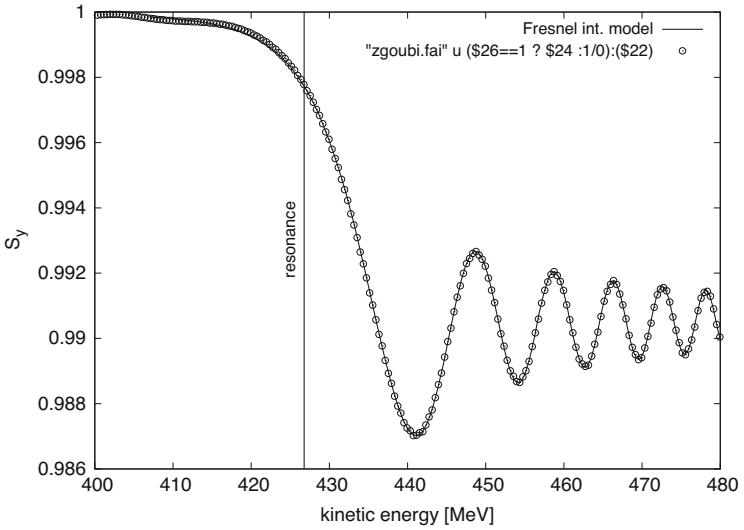

Fig. 14.19 A graph of $S_y(\text{turn} = \theta/2\pi)$. The symbols show the tracking results. The solid curve represents the Fresnel integral model

14.2.1.10 Beam Depolarization Using a Solenoid

A perfect Booster lattice is considered here. The integer resonance $G\gamma = -6$ is used to move initially vertical spins into the horizontal plane. Spin rotation is performed using either

- SOLENOID, in which case the magnetic field has to be provided; in addition, the solenoid is ramped from the initial to final energy in order to maintain a constant strength, which also means a constant spin tilt angle;
- SPINR, in which case the spin tilt angle, constant over the acceleration range, has to be specified; one advantage of SPINR is that it is a pure spin rotation, avoiding any possible orbit or betatron motion side effects.

Question 14.1.1.10-1—The input data file for this simulation is given in Table 14.45. Note that the location of the rotator does not make a difference as the modulus of the depolarizing strength, $|\epsilon_n|$, comes in the Froissart-Stora formula. So, for simplicity, the rotator is placed at the beginning of the optical sequence. The solenoidal field, spin tilt angle and energy range have been determined as follows.

Full depolarization after crossing $G\gamma = -6$ requires a resonance strength (Eq. 14.6 with $P_f = 0$) of

$$|\epsilon_n| = \left(\frac{2\alpha}{\pi}\ln 2\right)^{1/2} = 0.0064694573$$

with the crossing speed $\alpha = 9.484842 \times 10^{-5}$ ($\hat{V} = 400\,\text{kV}$, Table 14.45).

Table 14.45 Input data file for beam depolarization through $G\gamma = -6$ using a longitudinal-axis spin rotation (SOLENOID or SPINR). Note that the value of the SCALING coefficients is updated to the present initial BORO/1000=3.7764566118. SCALING ensures that power supply ramping follows the rigidity boost by CAVITE. The latter accelerates from $B\rho = 3.7764566118\,\mathrm{T\,m}$ ($G\gamma = -5.374744555$), up to $B\rho = 5.92283102938\,\mathrm{T\,m}$ ($G\gamma = -6.7454301$) in the asymptotic spin rotation region. The INCLUDE file here, scaling_SOLENOIDadded_Gg5.374.inc is a copy of scaling_Gg5.374.inc used in earlier exercises, with SOLENOID added

```
Depolarization by G.gamma=-6, using a longitudinal-axis rotation.
'OBJET'
3.7764566118E3 ! reference rigidity (kG.cm) at start of acceleration (G.gamma=-5.374744555).
2                                  ! Option for initial coordinates introduced individually.
1 1                                                          ! Track a single particle.
0.01 0. 0. 0.01 0. 1. 'o'          ! Small motion to check tunes (closed orbit is nul here).
1
'PARTICUL'
HELION
'SPNTRK'
3                                ! Any particle is attributed vertical initial spin vector.
'FAISTORE'
zgoubi.fai                                              ! Log particle data in zgoubi.fai,
1                                                                    ! at every pass.

         ! Scaling coefficients in scaling_GgXXX.inc are updated to present BORO/1000 value,
'INCLUDE'                                  ! SOLENOID has to be added to the list if used.
1
scaling_SOLENOIDadded_Gg5.374.inc[SCALING_S,*:SCALING_E,*]

! Two possibilities to simulate spin rotation (uncomment/comment one or the other:
! SOLENOID (give field value) or SPINR (give rotation angle).

! 'DRIFT'                                                  ! Compensation for added length.
! -100.
! 'SOLENOID'
! 0
! 100. 1. 0.129       ! This field yields Bs=0.0621T at G.gamma=-6, vs. theoretical 0.0615 T
! 10. 10.                                                          ! for beam depolarization.
! 1.
! 1 0. 0. 0.

'SPINR'
1
0 2.36                               ! Theoretical angle for depolarization is 2.3290 deg.
'INCLUDE'
1
6* superA.inc[superA_S:superA_E]
'CAVITE'  accelerating cavity
2
201.780048     4.00 circumf., H
400e3     0.523598775598                  ! Aceleration rate is 400kV*Q*sin(30deg), Q=2.
'REBELOTE'                          ! ~19800 passes from beta=0.0655 (Ek=6.043805MeV) to
2300 0.3 99                                          ! Ggamma=-16 (Ek=7.93076082GeV).
'END'
```

The theoretical solenoid field integral needed to achieve that is obtained from Eq. 2.38 with $|\epsilon_n| = 0.0064694573$ and $B\rho = B\rho_n = 4.8139470584\,\mathrm{T\,m}$ ($G\gamma = -6$), namely

$$B_s L = \frac{2\pi\, B\rho_n\, |\epsilon_n|}{1+G} = 0.061454684\,\mathrm{T\,m}$$

The dependence of the final polarization on the field integral $B_s L$ can be expressed as (the Froissart-Stora formula)

$$P_f = 2\exp\left(-\frac{\pi}{2}\frac{|\frac{1+G}{2\pi B\rho_n}\, B_s L|^2}{\alpha}\right) - 1 \tag{14.8}$$

This dependence is plotted in Fig. 14.20.

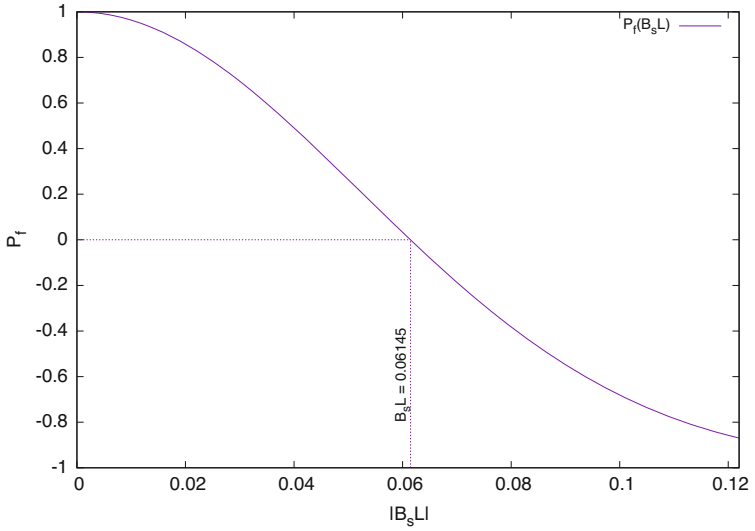

Fig. 14.20 A graph of the dependence of the final polarization on $B_s L = \int B_s(s)\, ds$ field integral (Eq. 14.8), upon crossing of the integer resonance $G\gamma = -6$

The spin rotation angle is maintained constant over the acceleration range, by ramping the SOLENOID field using SCALING (Table 14.45). Its value is

$$\phi_{\rm sp}(1+G)\frac{B_s L}{B\rho_n} = -0.040648\,{\rm rad} \;=\; 2.239^\circ$$

The starting $G\gamma = -5.374744555$ is at a distance of about $100 \times |\epsilon_n|$ from the resonance, which is well away so ensuring absence of depolarizing effects. The spins stay vertical as particles circle around the ring. The final $G\gamma = -6.74543$ is about $100 \times |\epsilon_n|$ downstream of the resonance, in the asymptotic region.

In order for the spins to end up precessing about nearly longitudinal axes with the turn-average $\langle S_y \rangle_{\rm turn} \approx 0$, the respective practical SOLENOID and SPINR settings have to be (these are the settings in the input data file given in Table 14.45),

$$B_s L = 0.0621\,{\rm T\,m},\ {\rm at}\ G\gamma = G\gamma_n, \qquad \phi_{\rm sp} = 2.36^\circ$$

which is reasonably close to the theoretical expectations. The longitudinal field experienced by the particles across the solenoid, when they reached the resonant energy region, is shown in Fig. 14.21.

At this point it is a good idea to ensure that coupling introduced by the solenoid is only a marginal optical perturbation (otherwise, it would have to be compensated). This can be checked with a MATRIX computation, based on the input data file of Table 14.45 (uncomment DRIFT and SOLENOID, comment SPINR, remove or comment CAVITE and REBELOTE, instead add MATRIX[IORD=1,IFOC=11],

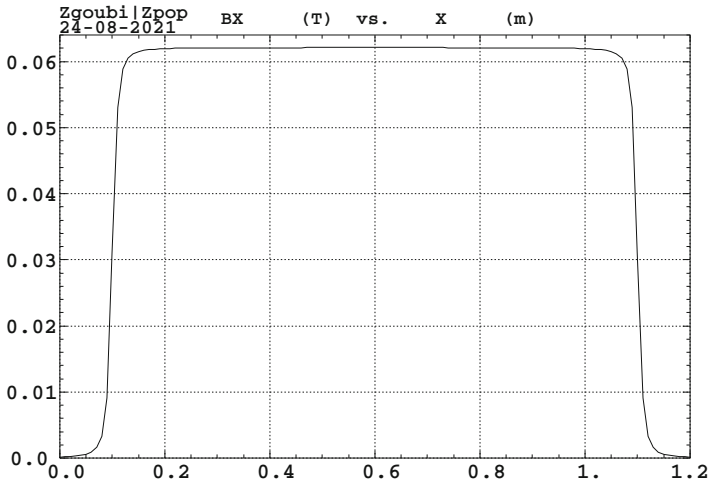

Fig. 14.21 A graph of the SOLENOID longitudinal field $B_s(s)$ ($B_X(X)$ in Zgoubi notations) as experienced by particles in the $G\gamma \approx G\gamma_n = -6$ energy region of the acceleration ramp. The plotted data are read from zgoubi.plt. The plateau is at $\hat{B}_s = 0.0621$ T

use OBJET[KOBJ=5], make sure SOLENOID is added to the SCALING list), yielding the following 1-turn 6×6 matrix:

```
 -1.09944        -5.44039       -6.570868E-03  -3.815489E-02   0.00000        0.985749
  0.355748        0.850847       2.126139E-03   6.053993E-03   0.00000       -0.271888
 -1.090396E-02   5.977518E-02    1.82449        -8.76526       0.00000        0.00000
 -1.889785E-03   6.568228E-03    0.316205      -0.971045       0.00000        0.00000
 -4.427688E-02   0.680976       -2.645957E-04   4.689973E-03   1.00000        8.97276
  0.00000         0.00000         0.00000        0.00000       0.00000        1.00000
```

It can be seen that coupling is weak. No compensation is needed in the current simulations.

The spin tracking results for the cases of both SOLENOID and SPINR are displayed in Fig. 14.22. Note that if a more accurate B_sL value giving precisely $\langle S_y \rangle_{\text{turn}} = 0$ is desired, as indicated in Fig. 14.20, this can be readily achieved by a linear interpolation between a couple of tracking points near $B\rho \approx 0.61 \sim 0.62$.

Question 14.1.1.10-2—The data file for this simulation is the same as for the previous question (Table 14.45) with one change: MCOBJET is used to create a 1000-particle bunch. This requires substitution of OBJET and its data list by the following:

```
'MCOBJET'
3.7764566118E3                                        reference rigidity (kG.cm).
3                                  ! Option to create a 6D bunch with random coordinates.
1000                                                  ! A 1000-particle bunch.
2 2 2 2 2 2
0.0 0. 0. 0.0 0. 1.                                  ! Mean values of the densities.
 0.982907   5.483186 1e-6  2                        ! Horizontal density parameters.
-1.545246   9.691428 1e-6  2                         ! Vertical density parameters.
 0.         1.       1.e-6 2                       ! Longitudinal density parameters.
 123456 234567 345678
```

SPINR is used to be closer to the theoretical assumptions addressed in the previous question (by avoiding possible orbital effects associated with SOLENOID). Two

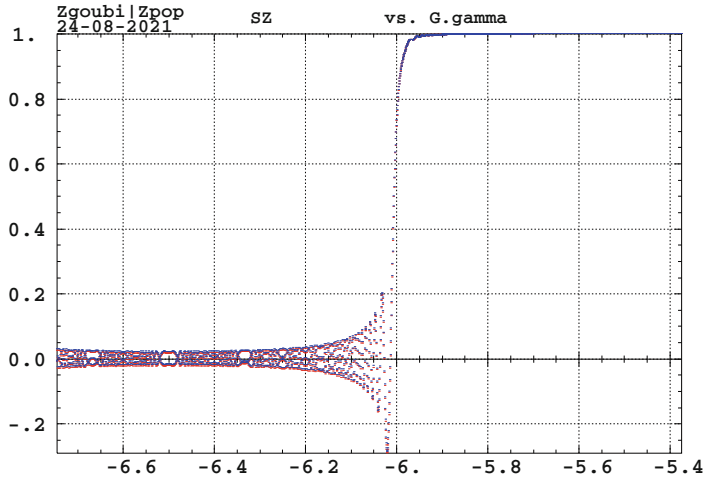

Fig. 14.22 A graph of $S_y(G\gamma)$ ($S_Z(G\gamma)$ in Zgoubi notations) through the integer resonance $G\gamma_n = -6$ excited using a 2.36 deg longitudinal-axis spin rotation. The plotted data are read from zgoubi.fai. The Outcomes of both the SOLENOID and SPINR simulation cases are superimposed here, showing a marginal difference

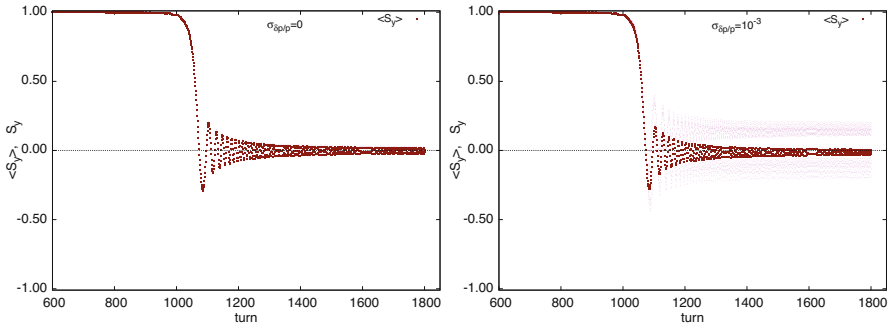

Fig. 14.23 Graphs of $\langle S_y(\text{turn})\rangle$, an average over a 1000-particle set (dark curve), together with a few individual $S_y(\text{turn})$ taken from that random set with various ε_x, ε_y values, for the two cases (as indicated on the respective graph) of $\delta p/p = 0$ (no momentum spread) and non-zero random $\delta p/p$. Spread of the final spin vectors together with a negative offset of $\langle S_y\rangle$ is apparent in the latter case

different 1000-particle sets have been tracked for comparison, one with $\delta p/p = 0$ which ends up with the expected $\langle S_y\rangle \approx 0$, and one with a rms Gaussian momentum spread of $\sigma_{\delta p/p} = 10^{-3}$ which ends up with $\langle S_y\rangle$ being slightly negative. The results are presented in Fig. 14.23.

14.2.1.11 Introduce a Partial Snake

Question 14.1.1.11-1—The input data file to simulate the Booster lattice including vertical misalignment of the lattice quadrupoles (using ERRORS) and a longitudinal axis snake is given in Table 14.46. The snake simulation uses SPINR (a pure spin precession, no orbital effect) with the spin axis set to longitudinal and the spin precession angle ϕ_{snake} to be determined—see next question.

Integer resonances are excited by a non-zero vertical orbit. Their strengths are displayed in Fig. 14.25 over $-12 \leq G\gamma \leq -7$, as obtained using the thin lens model series (Eq. 2.29). Strong resonances are at $G\gamma_n = pM \pm [\nu_y] = 6 + 5 = 11,\ 2 \times 6 \pm 5 = 7,\ 17$, etc. (with $[\nu_y] = 5$ being the nearest integer to the actual $\nu_y = 4.82$). Thus, $G\gamma_n = 7$ is the strongest in the acceleration interval of $G\gamma$: $-6.5 \rightarrow -10.5$ considered in this exercise. Its theoretical strength (using Eq. 2.29) is $|\epsilon_n^{\text{imp}}| = 0.0034$.

Table 14.46 Input data file for a simulation of an acceleration cycle in Booster in the presence of a partial snake. The latter uses SPINR. An orbit distortion is created using ERRORS, which causes a random vertical displacement of quadrupoles with an *rms* value of 0.25 mm and a 3-σ cut-off. Note that the values of the SCALING coefficients are updated to the present initial BORO/1000=5.56832079 ($G\gamma = -6.5$). SCALING ensures that power supply ramps follow the rigidity boost by CAVITE. The latter accelerates from $G\gamma = -6.5$ to $G\gamma = -10.5$ in 6500 turns

```
Partial snake to preserve polarization thru integer resonances.
'OBJET'
5.5683207908096621E3                        Reference rigidity (kG.cm) (G.gamma=-6.5, here).
2                                                                        ! Launch a single
1 1                                                                        ! particle, on
0. 0.   2.81903105E-01   4.05298102E-01   0.00  1. 'o'                    ! closed orbit.
1
'PARTICUL'
HELION

'ERRORS'
1 1 123456 PRINT             ! sig_ZS/cm      ! PRINT logs error inofs to zgoubi.ERRORS.out.
MULTIPOL{Q*,QUAD} 1 ZS A U 0.   .025     3                    ! LensFamiliy{LABEL1, LABEL2}.

'SPNTRK'
4.1                                    ! Particle spin is along stable spin axis, which is,
0. 0. 1.                          ! vertical as starting G.gamma=-6.5, away from resonance.
'FAISTORE'
zgoubi.fai                                                ! Log particle data in zgoubi.fai,
1                                                                        ! at every pass.

         ! Scaling coefficients in scaling_GgXXX.inc are updated to present BORO/1000 value.
'INCLUDE'
1
scaling_Gg6.5.inc[SCALING_S:SCALING_E]              ! SCALING keyword, set for G.gamma=-6.5.

'SPINR'                                        ! Snake, pur spin precession, no orbital effect.
1
0. 1.224    ! Snake axis longitudinal. Change, here, snake angle to 0, 1.224, 2.45 or 12.24.

'INCLUDE'
1
6* superA.inc[superA_S:superA_E]

'CAVITE'  accelerating cavity
2
201.780048     4.00 circumf., H
400e3     0.523598775598                    ! Aceleration rate is 400kV*Q*sin(30deg), Q=2.
'REBELOTE'                              ! ~19800 passes from beta=0.0655 (Ek=6.043805MeV) to
6500 0.3 99                                        ! Ggamma=-16 (Ek=7.93076082GeV).
'END'
```

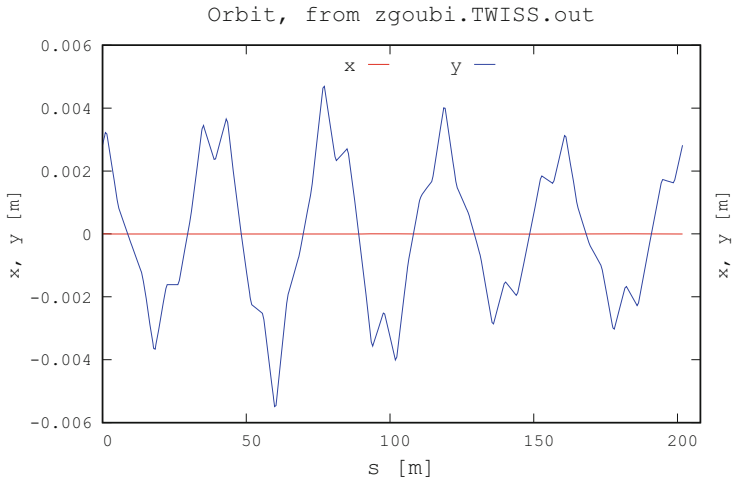

Fig. 14.24 Vertical closed orbit along Booster, with the ERRORS setting as per Table 14.46

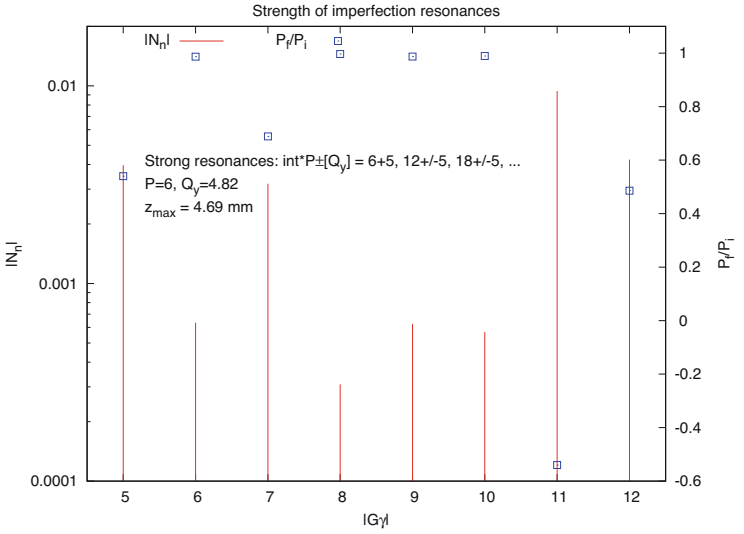

Fig. 14.25 Strengths of integer resonances excited by the orbit distortion displayed in Fig. 14.24

Acceleration through $G\gamma : -6.5 \rightarrow -10.5$ produces S_y(turn) displayed in Fig. 14.29 (the case of $\phi_{\text{snake}} = 0$). The resonances are located at integer $G\gamma$ values distant by $G\Delta\gamma = 1$. Thus, in units of energy (using the particle data from Table 14.1),

$$\Delta E = \frac{M}{|G|} G\Delta\gamma = \frac{M}{|G|} = \frac{2808.3916}{4.18415} = 671.2\text{MeV}$$

Question 14.1.1.11-2—The snake angle is set (under SPINR) to $\phi_{\text{snake}} = 2\pi|\epsilon_n^{\text{imp}}| = 2\pi \times 0.0034\,\text{rad} = 1.224°$, ERRORS is inhibited, the particle data are logged in zgoubi.fai at each optical element along the ring, the reference rigidity is set for $G\gamma = 7$ under OBJET and SCALING. The initial spin coordinates are set (to arbitrary values) under SPNTRK, and FIT is used to change them so to reach $\mathbf{S}_{x,s,y}(s = 0) = \mathbf{S}_{x,s,y}(s = s_{end})$. This yields the input data file of Table 14.47.

Table 14.47 Input data file to find the spin closed orbit at the $G\gamma_n = 7$ resonance (using FIT). It is similar to that of Table 14.46, with the following changes: the reference rigidity is BORO=6.2821070918945 ($G\gamma = 7$); ERRORS[ONF=0] inhibits the error generator; ALL is added under FAISTORE, this logs the particle data at the exits of all optical elements along the sequence in zgoubi.fai for further plotting of $\mathbf{S}_{X,Y,Z}(s)$; scaling_Gg7.inc is INCLUDEd with its scaling coefficients set for $|G\gamma| = 7$; FIT finds the periodic orbit (expected null) and the periodic spin orbit, expected to lie in the median plane due to the snake

```
Partial snake to preserve polarization thru integer resonances.
'OBJET'
6.2821070918945E3                                              reference rigidity (kG.cm).
2                                  ! Option for initial coordinates introduced individually.
1 1                                                            ! Track a single particle.
0.0 0. 0. 0.0  0. 1. 'o'           ! Small motion to check tunes (closed orbit is nul here).
1
'PARTICUL'
HELION
'SPNTRK'
4.1                                      ! Particle spin is along stable spin axis, which is,
0. 1. 0.             ! arbitrarily, along the Y axis, here - FIT will move it to // X-axis.

'ERRORS'                                                       ! Inhibited, due to ONF=0.
0 1 123456 PRINT             ! sig_ZS/cm      ! PRINT logs error inofs to zgoubi.ERRORS.out.
MULTIPOL{Q*,QUAD} 1 ZS A U 0.   .025     3                   ! LensFamiliy{LABEL1, LABEL2}.

'FAISTORE'
zgoubi.fai  ALL                                          ! Log particle data in zgoubi.fai,
1                                                                        ! at every pass.

         ! Scaling coefficients in scaling_GgXXX.inc are updated to present BORO/1000 value.
'INCLUDE'
1
scaling_Gg7.inc[SCALING_S:SCALING_E]                  ! SCALING keyword, set for G.gamma=-7.

'SPINR'                                        ! Snake, pur spin precession, no orbital effect.
1
0. 1.224    ! Snake axis longitudinal. Change, here, snake angle to 0, 1.224, 2.45 or 12.24.

'INCLUDE'
1
6* superA.inc[superA_S:superA_E]

'FIT2'
7
1 30 0 [-5,5]        ! First 4 lines: vary initial particle coordinates, Y, T, Z, P, iOBJET.
1 31 0 [-5,5]
1 32 0 [-5,5]
1 33 0 [-5,5]
3 10 0 [-1.01,1.01]              ! These 3 lines: vary initial spin coordinates, SX, SY, SZ.
3 11 0 [-1.01,1.01]
3 12 0 [-1.01,1.01]
8  1e-10
3.1 1 2 #End 0. 1. 0    ! First 4 lines: request equal particle coordinates at sart and end.
3.1 1 3 #End 0. 1. 0
3.1 1 4 #End 0. 1. 0
3.1 1 5 #End 0. 1. 0
10.1 1 1 #End 0. 1. 0       ! These 3 lines: request equal spin coordinates at sart and end.
10.1 1 2 #End 0. 1. 0
10.1 1 3 #End 0. 1. 0
10   1 4 #End 1. .0001 0     ! Request spin vector modulus =1, with a great weight (0.0001).
'END'
```

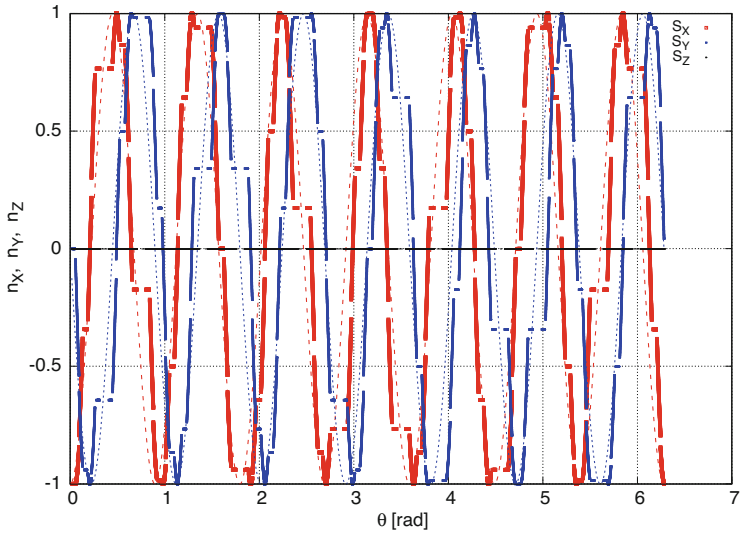

Fig. 14.26 Spin closed orbit along Booster in terms of its azimuthal angle at the $G\gamma = 7$ integer resonance. The snake is located at $\theta = 0$. The $\mathbf{n}_0$ vector lies in the median plane, and undergoes rotation about the Z-axis at a frequency of $\nu_{\rm sp} = G\gamma$: SX (the thick red curve) and SY (blue) oscillate while SZ=0. The theoretical $\mathbf{n}_0$ vector components (Eq. 14.9) are superimposed (the dashed curves). At the azimuthal angle of $\theta = \pi$ rad, which is the location opposite to the snake, the stable spin direction vector is parallel to the longitudinal axis ($\mathrm{n_s} \equiv \mathrm{SX} = 1$ and $\mathrm{n_x} \equiv \mathrm{SY} = 0$)

The presence of the snake produces the spin closed orbit displayed in Fig. 14.26. Plotted data are read from zgoubi.fai, generated using FAISTORE[LABEL=ALL], which logs the particle data at the exits of ALL optical elements around the ring (FAISTORE[LABEL=DRIF] would probably be sufficient). The spinor methods (Chap. 3) allow for deriving the eigenvectors

$$\mathbf{n} = \begin{pmatrix} n_x \\ n_s \\ n_y \end{pmatrix} = \frac{(\pm)}{\sin \pi \nu_{\rm sp}} \begin{pmatrix} -\sin(G\gamma(\pi - \theta)) \sin \dfrac{\phi_{\rm snake}}{2} \\ \cos(G\gamma(\pi - \theta)) \sin \dfrac{\phi_{\rm snake}}{2} \\ \sin(G\gamma\pi) \cos \dfrac{\phi_{\rm snake}}{2} \end{pmatrix} \tag{14.9}$$

and the spin tune

$$\cos \pi \nu_{\rm sp} = \cos(\pi G\gamma) \cos(\pi \epsilon_n) = \cos(\pi G\gamma) \cos \frac{\phi_{\rm snake}}{2} \tag{14.10}$$

On the $G\gamma = 7$ resonance, $n_y = 0$, the spin closed orbit lies in the median plane. Figure 14.26 shows its theoretical $n_s(\theta)$ and $n_x(\theta)$ components (Eq. 14.9) superimposed on the numerical tracking results (this graph uses the gnuplot script

Table 14.48 A gnuplot script to produce the graph of the numerical and theoretical spin closed orbit vectors around the ring in Fig. 14.26. This script specifies the positions (the column numbers) of the data read from zgoubi.plt

```
set xlabel "{/Symbol q}  [rad]" ;  set ylabel "n_X,  n_Y,  n_Z"
set key t r maxrow 5   width -3

pi = 4.*atan(1.) ; deg = 180./pi ; cm = 1e2 ; am = 2808.391585; G = 4.1841538; q = 2.
R = 201.78/ (2.*pi) *cm ; qsi= 1.224/deg ; Gg = 7.

# n_0 components, theory:
SY(x) = -1./sin(acos(cos(pi*Gg)*cos(qsi/2.))) * sin( Gg* (pi -x)) * sin(qsi/2.)   # x/e1
SX(x) =  1./sin(acos(cos(pi*Gg)*cos(qsi/2.))) * cos( Gg* (pi -x)) * sin(qsi/2.)   # s/e2
SZ(x) =  1./sin(acos(cos(pi*Gg)*cos(qsi/2.))) * sin( Gg* pi) * cos(qsi/2.)        # z/e3
set sample 1000

print " Qs = ",acos(cos(pi*Gg)*cos(qsi/2.))/pi,";  1-Qs = ",1-acos(cos(pi*Gg)*cos(qsi/2.))/pi

plot [] [-1:1] \
"zgoubi.plt" u ($14/R):($33) w p pt 4 ps .4 lc rgb "red"   tit "S_X" , SX(x) lw 2. dt 2 lc rgb "red" notit ,\
"zgoubi.plt" u ($14/R):($34) w p pt 4 ps .2 lc rgb "blue"  tit "S_Y" , SY(x) lw 2. dt 3 lc rgb "blue" notit ,\
"zgoubi.plt" u ($14/R):($35) w p pt 4 ps .1 lc rgb "black" tit "S_Z" , SZ(x) lw 2. dt 4 lc rgb "black" notit
```

given in Table 14.48). The oscillation frequency (Eq. 14.10 with $\phi_{\text{snake}} = 1.224°$) is

$$\text{frac}(\nu_{\text{sp}}) = \frac{\phi_{\text{snake}}}{2} = 0.0034$$

Question 14.1.1.11-3—An input data file to compute the spin closed orbit for $G\gamma = 7$, using FIT, is given in Table 14.49. A script (as in Table 14.50) changes the reference rigidity (OBJET[BORO]) and the corresponding SCALING factors in the ancillary file scaling.inc, and the repeats the computation for the sampled $-G\gamma$ values over $[-6.5, -7.5]$ (Figs. 14.27 and 14.28).

Question 14.1.1.11-4—Quadrupole misalignments are enabled (ERRORS[ONF=1]), the snake angle is set to $\phi_{\text{snake}} = 1.224°$.

Acceleration through $G\gamma : -6.5 \rightarrow -10.5$ produces S_y(turn) displayed in Fig. 14.29 (the case of $\phi_{\text{snake}} = 1.224°$). The spin appears to be tilted after crossing the integer resonances. However, the snake rotation is too weak to overcome the effect of the vertical orbit distortion.

Question 14.1.1.11-5—In order to determine the minimum angle of the snake spin rotation, it is necessary to know the strengths of the resonances to be crossed.

A partial snake generates a spin resonance strength

$$|\epsilon^{\text{snake}}| = \frac{\phi_{\text{snake}}}{2\pi}$$

Upon crossing of the resonance, the ratio of the final and initial polarizations satisfies (the Froissart and Stora formula, Eq. 2.44)

$$\frac{P_f}{P_i} = 2e^{-\frac{\pi}{2\alpha}|\epsilon^{\text{snake}} + \epsilon_n^{\text{imp}}|^2} - 1$$

Table 14.49 Input data file to find the spin closed orbit at a $G\gamma_n$ resonance ($G\gamma_n = 7$, here) using FIT. FIT finds the spin closed orbit for particle 4, which is $G\gamma$ dependent (Eq. 14.9). A trick is used here: the first three particles are left out of the fit, they are used to compute the spin matrix (SPNPRT[MATRIX], logged in zgoubi.SPNPRT.Out by SPNPRT[PRINT]) for comparison with the spin closed orbit of particle 4 found by FIT. Additional particles 5 and 6 are dummies and unused. They are only needed for proper operation of SPNPRT[MATRIX], which requires 3-particle subsets

```
spinN0_FIT_template.dat tmeplate input data file
'OBJET'
6.2821070918945E3                          ! Reference rigidity (kG.cm) - G.gamma=7, here.
2                                  ! Option for initial coordinates introduced individually.
6 2    ! Spin MATRIX computation requires 3 times the same particle, with spin SX, SY or SZ.
0. 0. 0. 0.  0. 1. 'o'                     ! First 3 particles used to compute spin matrix.
0. 0. 0. 0.  0. 1. 'o'
0. 0. 0. 0.  0. 1. 'o'
0. 0. 0. 0.  0. 1. 'o'              ! 4th particle used to get spin closed orbit, using FIT.
0. 0. 0. 0.  0. 1. 'o'  ! 2 additional particles unused, only needed for proper operation of
0. 0. 0. 0.  0. 1. 'o'                   ! SPNPRT[MATRIX] as it requires 3-particle subsets.
1 1 1 1 1 1 1
'PARTICUL'
HELION
'FAISCEAU'
'SPNTRK'
4
1. 0. 0.                    ! Initial spins of first 3 particles are left untouched, used to
0. 1. 0.                                                          ! compute spin matrix.
0. 0. 1.
1. 0. 0.                              ! Spin of prtcl 4 varied by FIT, to find spin orbit.
1. 0. 0.                                                                    ! unused.
1. 0. 0.                                                                    ! unused.

'INCLUDE'
1      ! scaling.inc is a cpy of scaling_Gg7.inc, scaling factors therein suited to present
scaling.inc[SCALING_S:SCALING_E]       ! OBJET[BORO] (they are changed by the repeat scrit).

'SPINR'                                    ! Snake, pur spin precession, no orbital effect.
1
0. 1.224    ! Snake axis longitudinal. Change, here, snake angle to 0, 1.224, 2.45 or 12.24.
'INCLUDE'
1
6* superA.inc[superA_S:superA_E]

'FIT2'
3
4 40 0 [-2.0,2.0]      ! These 3 lines: vary initial spin coordinates SX, SY, SZ of prtcl 4.
4 41 0 [-2.0,2.0]
4 42 0 [-2.0,2.0]
4  1e-20
10.1 4 1 #End 0. 1. 0       ! These 3 lines: request equal spin coordinates at sart and end.
10.1 4 2 #End 0. 1. 0
10.1 4 3 #End 0. 1. 0
10   4 4 #End 1. .0001 0     ! Request spin vector modulus =1, with a great weight (0.0001).

'FAISCEAU'  ! Allows to check final particle coordinates (perfect ring: should all be zero).

!     In the following: spin closed orbit from spin MATRIX (computed using particles 1-3) is
!   stored in zgoubi.SPNPRT.Out. It is expected to confirm spin closed orbit for particle 4,
!                                                                      computed using FIT.
'SPNPRT' MATRIX PRINT
'END'
```

Note: the overall strength $\epsilon^{\text{snake}} + \epsilon_n^{\text{imp}}$ results from a combination of the longitudinal and radial perturbative terms $\lambda_s \dfrac{B_s}{B_{y0}}$ and $\lambda_x \dfrac{B_x}{B_{y0}}$ in Eq. 2.26, with the B_s contribution coming from the snake and B_x arising from the vertical orbit in the quadrupoles.

Thus, for the snake to dominate the spin resonance dynamics, one needs

$$|\epsilon^{\text{snake}}| \gg |\epsilon_n^{\text{imp}}|$$

Table 14.50 A Fortran script to repeat the orbit finding of Table 14.49, for sampled values $G\gamma$: $-6.5 \rightarrow -7.5$. When the scan is completed, gnuplot_SPNPRT_N0-Qs-fromFIT.gnu (Table 14.51) is executed

```
character(300) cmnd; character(12) txt12
parameter (c = 2.99792458e8)
G = 4.1841538; am = 2808.391585; q = 2.

Gg0=6.5; N = 60

dGg = 1./float(N-1); Gg0=Gg0 -dGg
do i = 1, N
  Gg = Gg0 + dGg*float(i);  gma = Gg/G
  p = sqrt((gma*am)**2 - am**2); brho = p/c/q *1e6
  cmnd='cp -f spinN0_FIT_template.dat spinN0_FIT.dat'
  call system(cmnd)
  cmnd='cp -f spinN0_FIT_template.dat spinN0_FIT.dat'//
>  " ; sed -i 's@6.2821070918945@"//txt12//"@g' spinN0_FIT.dat"
  call system(cmnd)
  cmnd='cp -f scaling_Gg7.inc scaling.inc'//
>  "; sed -i 's@6.2821070918945@"//txt12//"@g' scaling.inc"
  call system(cmnd)
  cmnd = '/home/meot/zgoubi/SVN/current/zgoubi/zgoubi'
>  //' -in spinN0_FIT.dat ; '
>  //'/home/meot/zgoubi/current/toolbox/rzgRevision ; '
>  //'cat zgoubi.SPNPRT.Out >> zgoubi.SPNPRT.Out_cat'
  call system(cmnd)
enddo

call system('gnuplot <./gnuplot_SPNPRT_N0-Qs-fromFIT.gnu')

stop
end
```

Table 14.51 Typical gnuplot commands to obtain graphs of spin tune and spin closed orbit components from particle 4 data logged in zgoubi.SPNPRT.Out during tracking

```
# Spin tune vs. G.gamma:
am = 938.27203; G = 1.79284735

plot "zgoubi.SPNPRT.Out_cat"  u ($21==1 ? abs($18)/G*am/1e3 : 1/0):($51)  axes x2y1 w lp ps 0.6 lw 0.
pause 3

# Spin closed orbit components vs. G.gamma:
Nprtcl = 4
plot \
"zgoubi.SPNPRT.Out_cat" every 1 u ($21==Nprtcl? abs($18): 1/0):(    $13) w p pt 4 ps .6 lc rgb "red"   tit "n_Y"  ,\
"zgoubi.SPNPRT.Out_cat" every 1 u ($21==Nprtcl? abs($18): 1/0):(-10*$14) w p pt 5 ps .6 lc rgb "blue"  tit "10 n_Y"  ,\
"zgoubi.SPNPRT.Out_cat" every 1 u ($21==Nprtcl? abs($18): 1/0):(    $15) w p pt 6 ps .6 lc rgb "black" tit "n_Z"
pause 3
```

This is qualitatively verified in Fig. 14.29, which displays motion of the spin of a particle traveling along the vertical closed orbit, while it is accelerated over $G\gamma$: $-6.5 \rightarrow -10.5$: a snake precession of $10 \times 2\pi|\epsilon_n^{\text{imp}}| = 12.2°$ allows overcoming the resonances by causing a full flip at each integer $G\gamma$ value. The lower values of $\phi_{\text{snake}} = 2\pi|\epsilon_n^{\text{imp}}| = 1.22°$ and $\phi_{\text{snake}} = 2 \times 2\pi|\epsilon_n^{\text{imp}}| = 2.45°$ are too weak for spin flipping.

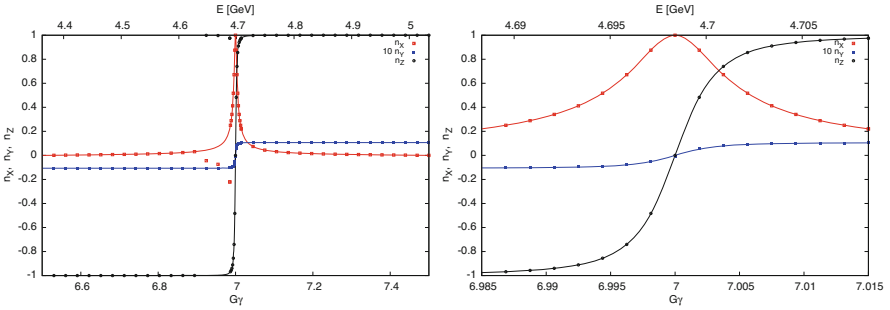

Fig. 14.27 $G\gamma$ dependence of the spin closed orbit, over $6.5 < |G\gamma| < 7.5$ (left), and a zoomed-in view of the central region (right). The symbols are from spin tracking, the solid lines are from the theory (Eq. 14.9 wherein $n_{s,x,y}$ corresponds to the present Zgoubi notation $n_{X,Y,Z}$). Note the value of the n_Y component at half-integer $G\gamma$ of $n_x \equiv n_Y = 0.01068$ enhanced by a factor 10 for accuracy (with the theoretical n_x given by Eq. 14.9)

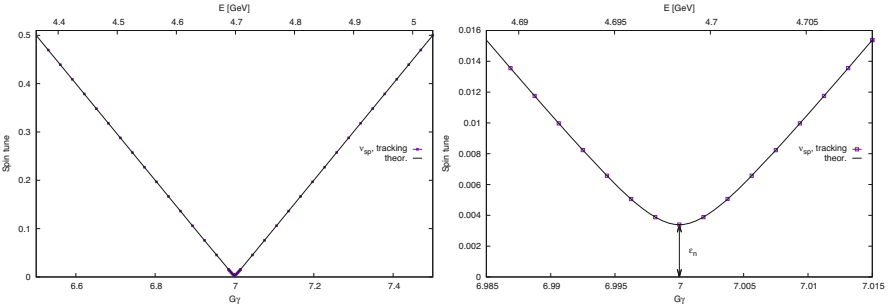

Fig. 14.28 $G\gamma$ dependence of the spin tune, over $6.5 < |G\gamma| < 7.5$, and a zoom-in of the central region. The symbols are from spin tracking, the solid lines are from the theory (Eq. 14.10). The width of the forbidden spin tune region, or "spin tune gap", is the resonance strength, or resonance width, $\epsilon_n = \phi_{\text{snake}}/2\pi = 0.0034$

14.2.1.12 Introduce Full Snakes

A non-zero vertical invariant is accounted for. It causes betatron motion through the lattice fields exciting systematic intrinsic spin resonances, which, given $\nu_y = 4.82$, are located at $G\gamma = -12 + \nu_y = -7.18, -6 - \nu_y = -10.82, -18 + \nu_y = -13.18$.

The same vertical closed orbit distortion as in exercise 14.2.1.11 is introduced, using ERRORS with the same data.

Question 14.1.1.12-1—The methods here are very similar to what is done in 14.2.1.11. The spin closed orbit is found using the same input data file (Table 14.47). The FIT procedure in that file simultaneously finds the particle closed obit (x_0, x'_0, y_0, y'_0) ((Y_0, T_0, Z_0, p_0) in Zgoubi notation), and the spin closed orbit (which by definition is that of the particle on closed orbit). Thus, that FIT procedure holds for chromatic closed orbits. All that needs be changed is the particle D value

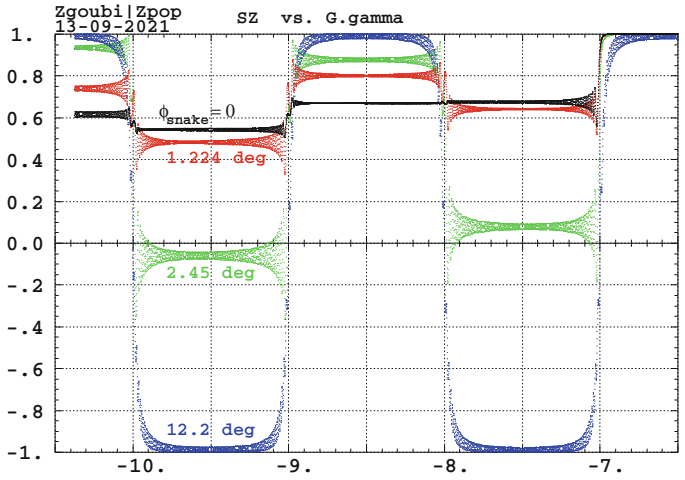

Fig. 14.29 Spin motion over $G\gamma : -6.5 \rightarrow -10.5$, for the cases of 4 different snake precession angles: null, $\phi_{\text{snake}} = 2\pi|\epsilon_n^{\text{imp}}| = 1.22°$, $2 \times 2\pi|\epsilon_n^{\text{imp}}| = 2.45°$, and $10 \times 2\pi|\epsilon_n^{\text{imp}}| = 12.2°$, with $|\epsilon_n^{\text{imp}}| = 0.0034$ being the strength of the imperfection resonance excited by vertical quadrupole misalignments. The initial spin is along the vertical stable spin direction at $G\gamma = -6.5$

(relative momentum) under OBJET. The closed orbits of interest here are detailed below.

The one-turn spin matrix, and thus the spin tune, the local spin precession axis at the start of the sequence, etc., can be computed using SPNPRT[MATRIX]. Computation of the spin matrix at different momenta requires defining groups of momenta, using OBJET[KOBJ=2,IDMAX=3]. The input data file used is given in Table 14.52. It defines 3 respective groups of $D - 1 = dp/p_0 = 0,\ 10^{-4},\ 10^{-3}$. SPNPRT[MATRIX] manages that information and produces the corresponding 3 one-turn spin matrices. Excerpts from zgoubi.res given in Table 14.53 detail the momentum dependence of the numerical parameter values. At $G\gamma = -6.5$, the spin closed orbit at the snake is along the transverse horizontal axis, and is longitudinal at the azimuthal angle opposite to the snake, as seen in the following excerpts from zgoubi.res:

– at the snake (s=0.57 m, the end of the first drift, element number 12 in the optical sequence):

```
      12  Keyword, label(s) :  DRIFT       DRIF                 L057
                               Drift,  length =    57.04000   cm
TRAJ #1 IEX,D,Y,T,Z,P,S,time :  1  0.  0.  0.  3.050213E-01  4.052981E-01  5.7040005E+01  2.48626E-03
TRAJ #1 SX, SY, SZ, |S| :  1    1.962212E-05  -9.999958E-01   2.897616E-03   1.000000E+00
 Cumulative length of optical axis =   0.5704 m   ;  Time (for reference rigidity & particle) =  2.486264E-09 s
```

Table 14.52 Input data file to compute the one-turn spin matrices for 3 different momenta, $D = p/p_0 = 1,\ 1.0001,\ 1.001$. In order to produce the respective matrices, SPNPRT[MATRIX] requires defining 3 groups of momenta in the proper order. This can be achieved using OBJET[KOBJ=2,IDMAX=3]. The same particle coordinates are repeated three times in each group. Then SPNTRK sets the three initial spin vectors to (1,0,0), (0,1,0), and (0,0,1), respectively

```
Full snake to preserve polarization thru integer resonances.
'OBJET'
5.5683207908096621E3                        Reference rigidity (kG.cm) (G.gamma=-6.5, here).
2
9 3                                                    ! 9 particles, 3 different momenta.
0. 0.  2.81903105E-01  4.05298102E-01   0.  1. 'o'       ! On-momentum closed orbit, dp/p=0.
0. 0.  2.81903105E-01  4.05298102E-01   0.  1. 'o'
0. 0.  2.81903105E-01  4.05298102E-01   0.  1. 'o'
7.4360716E-03 -1.0564233E-02 0.2809611 0.4040692   0.  1.0001 'd'  ! closed orbit, dp/p=1e4.
7.4360716E-03 -1.0564233E-02 0.2809611 0.4040692   0.  1.0001 'd'
7.4360716E-03 -1.0564233E-02 0.2809611 0.4040692   0.  1.0001 'd'
7.4744578E-02 -0.1053352 0.2727098 0.3932872  0.  1.001 'd'        ! closed orbit, dp/p=1e3.
7.4744578E-02 -0.1053352 0.2727098 0.3932872  0.  1.001 'd'
7.4744578E-02 -0.1053352 0.2727098 0.3932872  0.  1.001 'd'
1 1 1 1 1 1 1 1 1
'PARTICUL'
HELION
'ERRORS'
1 1 123456 PRINT             ! sig_ZS/cm         ! Vertical alignment random error, uniform.
MULTIPOL{Q*,QUAD} 1 ZS A U 0.    .025     3                  ! LensFamiliy{LABEL1, LABEL2}.
'SPNTRK'
4                                          ! SX, SY, SZ spin values of the 3*3 particles.
1. 0. 0.
0. 1. 0.
0. 0. 1.
1. 0. 0.
0. 1. 0.
0. 0. 1.
1. 0. 0.
0. 1. 0.
0. 0. 1.

'FAISTORE'
zgoubi.fai                                             ! Log particle data in zgoubi.fai,
1                                                                  ! at every pass.

        ! Scaling coefficients in scaling_GgXXX.inc are updated to present BORO/1000 value.
'INCLUDE'
1
scaling_Gg6.5.inc[SCALING_S:SCALING_E]             ! SCALING keyword, set for G.gamma=-6.5.

'SPINR'
1
0. 180.                                              ! Snake axis longitudinal. Full snake.

'INCLUDE'                                                        ! Include Booster ring.
1
6* superA.inc[superA_S:superA_E]

'FAISCEAU'
'SPNPRT' MATRIX

'END'
```

– at the azimuthal location opposite to the snake (s=100.9 m away, element number 330 in the optical sequence):

```
    330  Keyword, label(s) :  DRIFT       DRIF                 L057
                              Drift,  length =    57.04000  cm
 TRAJ #1 IEX,D,Y,T,Z,P,S,time :  1  0.  2.708E-05 -5.847E-05 -3.839713E-01 -3.940313E-01  1.0146044E+04  4.42247E-01
 TRAJ #1 SX, SY, SZ, |S| :  1    9.999388E-01  -1.416886E-05   1.106666E-02   1.000000E+00
  Cumulative length of optical axis =    101.460424 m ;  Time (for reference rigidity & particle) =  4.422465E-07 s
```

Question 14.1.1.12-2—Acceleration over $G\gamma : -6.5 \rightarrow -13.5$ uses the input data file given in Table 14.54. It is similar to that of Table 14.46 but with

Table 14.53 SPNPRT[MATRIX] listing in zgoubi.res (excerpts): one-turn spin matrices and other information, at relative momenta $D-1=dp/p_0=0,\ 10^{-4},\ 10^{-3},\ 10^{-2}$

```
                  ------------------------------------------------------------------------
                  Momentum  group  #1 (D=   1.000000E+00) ; average  over 3 particles at this pass :

                Spin transfer matrix, momentum group # 1 :
        -0.999945        8.562650E-06   -1.050193E-02
         6.942346E-05    0.999983       -5.794851E-03
         1.050171E-02   -5.795260E-03   -0.999928

Trace =      -0.9998897078,     ;   spin precession acos((trace-1)/2) =     179.3982765528 deg
Precession axis :  (-0.0000, -1.0000,  0.0029)  ->  angle to (X,Y) plane,  angle to X axis :  0.1660,  90.3855  degree
Spin  tune  Qs (fractional) :     0.49833


                  ------------------------------------------------------------------------
                  Momentum  group  #2 (D=   1.000100E+00) ; average  over 3 particles at this pass :

                Spin transfer matrix, momentum group # 2 :
        -0.999943       -2.383130E-03   -1.045329E-02
        -2.322598E-03    0.999980       -5.799063E-03
         1.046690E-02   -5.774451E-03   -0.999929

Trace =      -0.9998905823,     ;   spin precession acos((trace-1)/2) =     179.4006668061 deg
Precession axis :  ( 0.0012, -1.0000,  0.0029)  ->  angle to (X,Y) plane,  angle to X axis :  0.1658,  67.8736  degree
Spin  tune  Qs (fractional) :     0.49834


                  ------------------------------------------------------------------------
                  Momentum  group  #3 (D=   1.001000E+00) ; average  over 3 particles at this pass :

                Spin transfer matrix, momentum group # 3 :
        -0.999664       -2.391167E-02   -1.002755E-02
        -2.385398E-02    0.999698       -5.834018E-03
         1.016403E-02   -5.592859E-03   -0.999933

Trace =      -0.9998980571,     ;   spin precession acos((trace-1)/2) =     179.4215005685 deg
Precession axis :  ( 0.0119, -0.9999,  0.0029)  ->  angle to (X,Y) plane,  angle to X axis :  0.1637,  13.4539  degree
Spin  tune  Qs (fractional) :     0.49839


                  ------------------------------------------------------------------------
                  Momentum  group  #4 (D=   1.010000E+00) ; average  over 3 particles at this pass :

                Spin transfer matrix, momentum group # 4 :
        -0.971396       -0.237373       -6.677918E-03
        -0.237335        0.971409       -5.970173E-03
         7.904151E-03   -4.214493E-03   -0.999960

Trace =      -0.9999460691,     ;   spin precession acos((trace-1)/2) =     179.5792323606 deg
Precession axis :  ( 0.1195, -0.9928,  0.0026)  ->  angle to (X,Y) plane,  angle to X axis :  0.1469,   1.2291  degree
Spin  tune  Qs (fractional) :     0.49883
```

OBJET[KOBJ=8] to generate a few particles on a matched ellipse with a given invariant (to study the dependence of the spin motion on the betatron motion), and with the number of turns increased to 11750 under REBELOTE so to reach $G\gamma=-13.5$.

The results are displayed in Fig. 14.30. The initial spins are along the transverse horizontal axis (Y, in Zgoubi notation), which is the orientation of the local spin closed orbit. No polarization loss is observed the stable spin direction exhibits rotation about the vertical axis.

Table 14.54 Input data file for a simulation of an acceleration cycle in Booster in the presence of a single full snake. The latter implemented using SPINR. An orbit distortion is created using ERRORS, which causes random vertical displacements of the quadrupoles with an *rms* value 0.25 mm and a 3-σ cut-off. Note that the values of the SCALING coefficients are updated to the present initial BORO/1000=5.56832079 ($G\gamma = -6.5$). SCALING ensures that power supply ramps follow the rigidity boost by CAVITE. The latter accelerates from $G\gamma = -6.5$ to $G\gamma = -13.5$ in 11700 turns. The initial coordinates are taken on a matched ellipse with a normalized $\varepsilon_y = 2.5\,\pi\,\mu$m

```
Full snake to preserve polarization thru integer resonances.
'OBJET'
5.5683207908096621E3                        Reference rigidity (kG.cm) (G.gamma=-6.5, here).
8
1 3 1
0. 0.   2.81903105E-03   4.05298102E-04   0.00  1. 'o'                        ! closed orbit.
 0.982907  5.483186  0.
-1.545246  9.691428  3.e-6            ! Vertical invariant value is 2.5 pi.mu_m, normalized.
 0. 1. 0.
'PARTICUL'
HELION
'ERRORS'
1 1 123456 PRINT             ! sig_ZS/cm         ! Vertical alignment random error, uniform.
MULTIPOL{Q*,QUAD} 1 ZS A U 0.   .025     3                    ! LensFamiliy{LABEL1, LABEL2}.
'SPNTRK'
4.1
0. 1. 0.                                                        ! Initial particle spins.

'FAISTORE'
zgoubi.fai                                                ! Log particle data in zgoubi.fai,
1                                                                      ! at every pass.

         ! Scaling coefficients in scaling_GgXXX.inc are updated to present BORO/1000 value.
'INCLUDE'
1
scaling_Gg6.5.inc[SCALING_S:SCALING_E]              ! SCALING keyword, set for G.gamma=-6.5.
'SPINR'
1
0. 180.                                               ! Snake axis longitudinal. Full snake.

'INCLUDE'                                                              ! Booster lattice.
1
6* superA.inc[superA_S:superA_E]

'CAVITE'  accelerating cavity
2
201.780048     4.00 circumf., H
400e3     0.523598775598                    ! Aceleration rate is 400kV*Q*sin(30deg), Q=2.
'REBELOTE'                              ! ~19800 passes from beta=0.0655 (Ek=6.043805MeV) to
11750 0.3 99                                        ! Ggamma=-16 (Ek=7.93076082GeV).

'FAISCEAU'                                        ! Log local particle data to zgoubi.res.
'SPNPRT'                                             ! Log local spin data to zgoubi.res.
'END'
```

Question 14.1.1.12-3—Horizontal motion is added: 9 particles are launched with normalized $\varepsilon_x = \varepsilon_y = 2.5\,\pi\,\mu$m and 9 combinations of the initial betatron phases, by *ad hoc* modification of OBJET[KOBJ=8]:

```
 'OBJET'
5.5683207908096621E3                        Reference rigidity (kG.cm) (G.gamma=-6.5, here).
8
3 3 1
0. 0.   2.81903105E-03   4.05298102E-04   0.00  1. 'o'                        ! closed orbit.
 0.982907  5.483186  3.e-6
-1.545246  9.691428  3.e-6            ! Vertical invariant value is 2.5 pi.mu_m, normalized.
 0. 1. 0.
```

The results are essentially unchanged. Motion of the spins is similar to that in Fig. 14.30 found earlier.

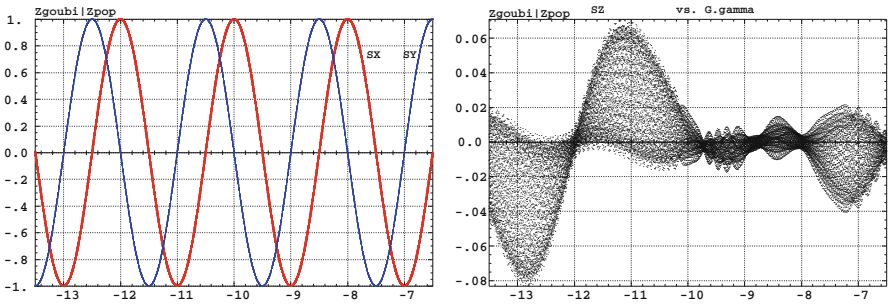

Fig. 14.30 Evolution of the stable spin direction adiabatically followed by the spins, as observed at the snake (the mid-plane components S_X and S_Y versus $G\gamma$) (left), and the (marginal) vertical component (S_Z versus $G\gamma$) (right), during acceleration over $G\gamma : -6.5 \rightarrow -13.5$, in the presence of a single full snake. Three particles are tracked, with different initial betatron phases on the same matched phase-space ellipse with a normalized invariant $\varepsilon_Y = 2.5\,\pi\,\mu$m. Their spin trajectories overlap. The initial spins are along the Y axis corresponding to the local spin closed orbit at $G\gamma = -6.5$

14.2.1.13 Preserve Polarization Using Tune Jump

Question 14.1.1.15-1—For a 100 kV RF voltage the crossing speed is

$$\frac{dG\gamma}{d\theta} = 2.37121051717 \times 10^{-5}$$

Given the tune $\nu_Z = 0.82$, the acceleration rate and the energy at the start of the tracking, the resonance $|G\gamma| = 0 + \nu_Z$ occurs at a turn number

$$N_{0+\nu_y} \approx 1530$$

The resonance strength ϵ_n is in question. It can be determined from the particle invariant using Table 14.39. Given ϵ_n and the crossing speed $\alpha = \frac{dG\gamma}{d\theta}$, the Froissart-Stora formula (Eq. 2.44) yields the expected asymptotic polarization after crossing of

$$P_f \approx 0.53$$

A numerical simulation of this resonance crossing yields the result displayed in Fig. 14.31 and confirms the expected $P_f \approx 0.53$.

Question 14.1.1.15-2—The new crossing speed, including the effect of the tune jump, is (Eq. 14.2)

$$\alpha = 2.60504500631 \times 10^{-4}$$

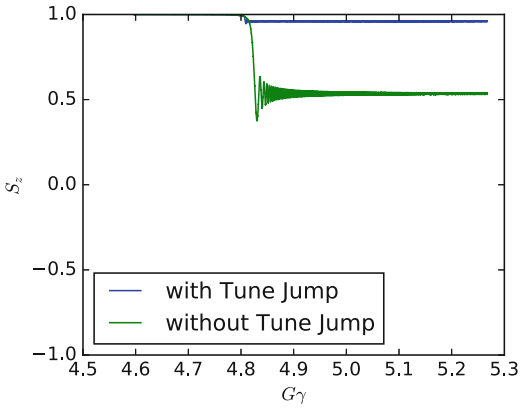

Fig. 14.31 Evolution of the polarization component $S_z(G\gamma)$ of helions when crossing the $|G\gamma| = 0 + \nu_Z$ resonance, with and without use of the tune jump quadrupoles. The plotted turn-by-turn data are read from zgoubi.fai

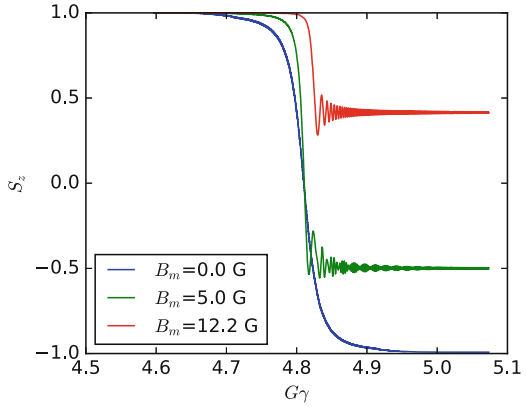

Fig. 14.32 Helions crossing the $|G\gamma| = 0 + \nu_Z$ resonance, with an AC dipole operating at $B_m = 5$ and 12.2 G. Crossing without the AC dipole (the $B_m = 0$ case) is shown for comparison. The plotted turn-by-turn data are read from zgoubi.fai

With this increased crossing speed, the Froissart-Stora formula yields an expected final polarization of

$$P_f = 0.9234742$$

This theoretical value agrees with the value obtained from a crossing simulation within 0.03%. The result of the latter is displayed in Fig. 14.31.

14.2.1.14 Preserve Polarization Using an AC Dipole

With the scale_factor set to 0.0, tracking a 32 particle set yields an average $P_f = 41.5\%$, compared to the expectation of $P_f = 40.0\%$.
With the scale factor set to 5 G, tracking the 32 particle set yields $P_f = -50\%$.
An AC dipole field of $B_m = 12.2$ G allows a full spin-flip.

The tracking results are displayed in Fig. 14.32.

14.2.2 Electron Spin Dynamics, Synchrotron Radiation

14.2.2.1 Electron Equilibrium Emittances and Energy Spread

Question 14.1.2.1-1—Figure 14.33 shows the optical functions and the orbit of a perfectly aligned AGS Booster ring. It was generated by a Gnuplot script (Table 14.14) using the Zgoubi Twiss output following the question's instructions in Sect. 14.1.2.1. The Twiss output file contains a table of the Twiss functions specified at the end of each element in the lattice. An easy way to find the damped equilibrium emittances, energy spread and damping times of 10 GeV electrons in this lattice is to open the output text file in a spreadsheet and then evaluate the integrals in the expressions for the equilibrium parameters given in Chap. 6. We can calculate approximate integral values by summing the integrand expressions over all elements. This is an accurate approximation in our case, since the Twiss functions do not change significantly over a single element. The resulting equilibrium parameters are summarized in Table 14.55.

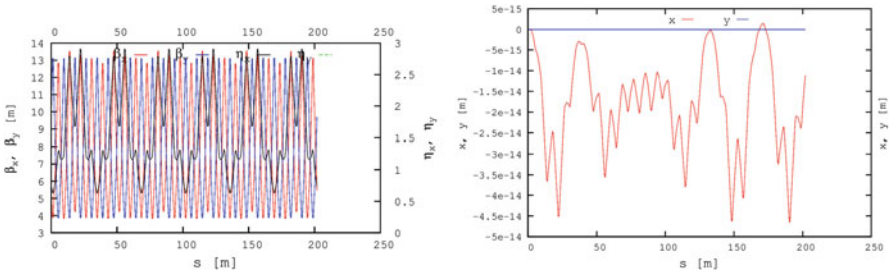

Fig. 14.33 Left: twiss optical functions of the entire AGS Booster ring. Right: orbit in the AGS Booster ring with perfect element alignment

Table 14.55 Electron beam parameters

Parameter	Units	Value
E, total	[GeV]	10
$a\gamma$		22.6938
Energy loss per turn	[MeV]	63.8
RF voltage	[MV]	127.6
RF phase	[rad]	2.618
Harmonic number		100
RF frequency	[MHz]	1.487
Horizontal damping time	[ms]	0.235
Vertical damping time	[ms]	0.211
Longitudinal damping time	[ms]	0.100
Horizontal emittance	[μrad]	4.53
Energy spread	$\times 10^{-3}$	2.24

Question 14.1.2.1-2—The SRPRNT keyword at the end of the code in Table 14.16 activates printout of the SR loss statistics in zgoubi.res output file. An excerpt of zgoubi.res file showing the SR information is:

```
 * Monte Carlo S.R. statistics, from beginning of structure,
       10000 particles,  a total of        87840762 integration steps :
   Average energy loss per particle per pass :        63968.01     keV.       Relative to initial energy :  6.3968014E-03
   Critical energy of photons (average) :             158.9614     keV
   Average energy of radiated photon :                49.30345     keV
   rms energy of radiated photons :                   92.27650     keV
   Smallest, BIGEST photon :                        0.0000E+00      9.9915E+03     keV
   Number of photons radiated - Total :                          1.2974348E+07
                              - per particle per pass :           1297.435
                              - per particle, per step :         0.1477030
```

As one can see, the average particle energy loss per turn obtained in the Monte-Carlo simulation is in a good agreement with the theoretical prediction in Table 14.55. One must restore this energy loss at a synchronous phase necessary for longitudinal stability. Therefore, the cavity voltage amplitude is $|\hat{V}| = \Delta E/q/\sin\phi_s = 127.6$ MV. This number is consistent with the rf cavity setting under CAVITE in Table 14.17, namely $\hat{V} = 122.345$ MV. The cavity setting is slightly lower than the theoretical prediction because it accounts for the change in the particle energy as it moves around the ring.

Question 14.1.2.1-3—The initial beam distribution in Table 14.17 is generated on a matched vertical phase-space ellipse, using OBJET[KOBJ=8]. The ellipse parameters are specified by the appropriate option of the OBJET element using the Twiss functions at the start point and the beam emittances. The matched Twiss function values were taken from the Twiss table that was generated as a result of Question 14.1.2.1-1. For simplicity, the horizontal emittance was set to zero while the vertical emittance was set to a relatively large value of 10 μrad for synchrotron damping demonstration. After running the simulation and analyzing, plotting and fitting the resulting data as described in the question's statement in Sect. 14.1.2.1, we obtain evolution of the vertical beam emittance as a function of the turn number shown in Fig. 14.34. The vertical emittance ε_y is obtained from the rms beam size σ_y as $\varepsilon_y = \sigma_y^2/\beta_y$.

An exponential fit to the simulation data in Fig. 14.34 gives a vertical emittance damping time of 155.3 turns. Note that the equations of Chap. 6 and the values listed in Table 14.55 are for the amplitude damping times rather than the emittance ones. Since the emittance is proportional to the second power of the betatron amplitude, the vertical betatron amplitude damping time is a factor of two longer than the vertical emittance one and equals 310.6 turns. Given the electron circulation frequency in the AGS Booster listed in Table 14.55, this number corresponds to 0.209 ms, which is in a good agreement with the theoretical prediction of 0.211 ms in Table 14.55.

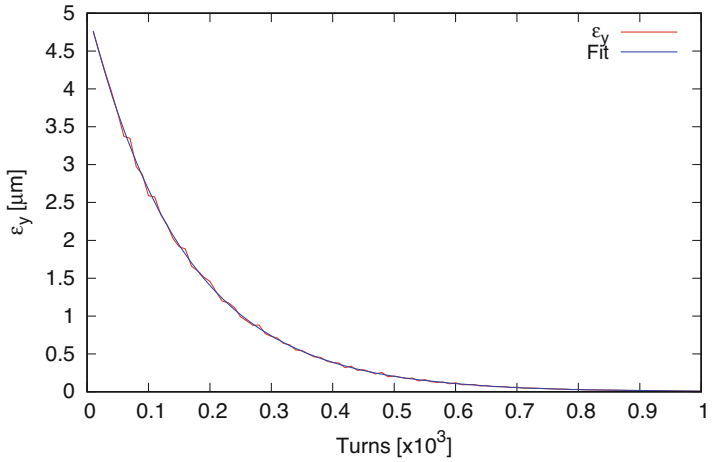

Fig. 14.34 Damping of the vertical emittance of a 10 GeV electron beam in the AGS Booster lattice. Note a good agreement of the exponential fit with the Monte-Carlo data for only 100 electrons

14.2.2.2 Spin Diffusion Studies

14.2.2.3 Spin Diffusion

Question 14.1.2.2-1—Here is an excerpt of zgoubi.res file showing the spin transfer matrix, $\mathbf{n}_0$ and spin tune:

```
                Spin transfer matrix, momentum group # 1 :

          -0.345661       -0.938359         0.00000
           0.938359       -0.345661         0.00000
            0.00000         0.00000         1.00000

Trace =       0.3086770996,     ;   spin precession acos((trace-1)/2) =     110.2221783671 deg
Precession axis :  ( 0.0000,  0.0000,  1.0000)  ->  angle to (X,Y) plane,  angle to X axis :  90.000,  90.000 degree
Spin  tune  Qs (fractional) :     3.0617E-01
```

As one can see, in a perfectly aligned lattice, $\mathbf{n}_0$ is exactly vertical.

Question 14.1.2.2-2—The electron polarization is plotted against the turn number in Fig. 14.35. It was obtained by tracking 100 electrons through a perfectly aligned AGS Booster lattice with synchrotron radiation enabled. At the start, the electron spins were set along the $\mathbf{n}_0$ axis. Figure 14.35 illustrates that in a perfectly aligned ring, there is no detectable polarization degradation on this time scale even when synchrotron radiation is present, i.e. the spin diffusion rate is zero within our numerical precision. This case presents interest primarily as a sanity check of the spin tracking code. It confirms that at this level, the code does not introduce unphysical spin effects.

Question 14.1.2.2-3—The 4D transverse closed orbit offset ($Y\ T\ Z\ P$) caused by a 1 mm vertical misalignment of the "QVA1" quadrupole is

```
-5.78398841E-06  -5.02369232E-06  -2.40168827E-01  -5.80016582E-01
```

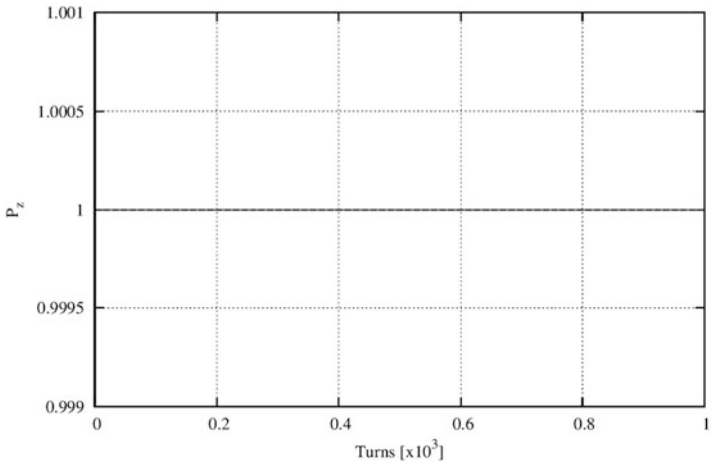

Fig. 14.35 Polarization of 100 electrons as a function of the turn number in a perfectly aligned AGS Booster ring with synchrotron radiation enabled. The electron spins are initially aligned with the $\mathbf{n}_0$ axis

The $\mathbf{n}_0$ axis at the beginning of this perturbed lattice is

```
(0.0137, -0.0568,  0.9983)
```

Time evolution of the polarization in this case is compared to that of the perfectly aligned case of Question 14.1.2.2-2 in Fig. 14.36. An exponential fit to the data gives a spin diffusion time of $17.9 \cdot 10^3$ turns corresponding to 12 ms. Note the rapid spin diffusion caused by misalignment of even a single element.

Question 14.1.2.2-4—Similarly to the solution of Question 14.1.2.2-3, we find that vertical misalignments of "QVA1" by 2 and 5 mm result in transverse closed orbit shifts of

```
-2.41767056E-05   3.83288439E-05  -4.80358495E-01  -1.16006824E+00
```

and

```
-1.49937996E-04   1.83685654E-04  -1.20099981E+00  -2.90035565E+00 ,
```

respectively. The corresponding $\mathbf{n}_0$ axes are

```
(0.0273, -0.1132,  0.9932)
```

and

```
(0.0660, -0.2769,  0.9586) .
```

Note that the closed orbit offset and the x and y components of $\mathbf{n}_0$ scale linearly with the size of the misalignment as expected. The polarization behavior in these two cases is plotted as a function of the turn number in Fig. 14.36. Exponential fits to these data give spin diffusion times of $6.4 \cdot 10^3$ and 800 turns, or 4.3 and 0.54 ms, for the 2 and 5 mm misalignment scenarios, respectively.

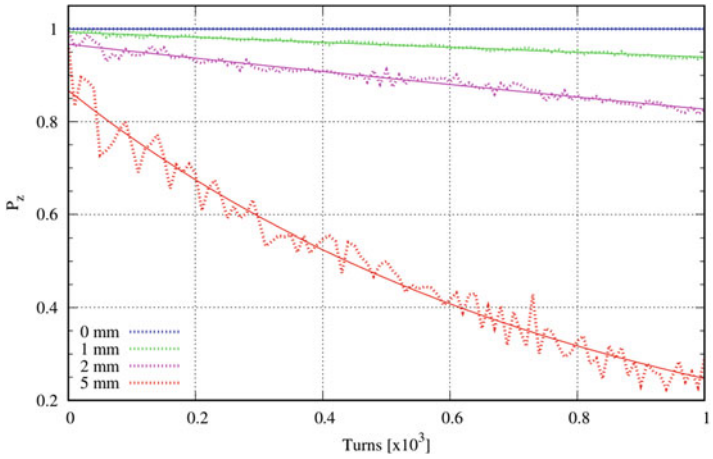

Fig. 14.36 Polarization of 100 electrons as a function of the turn number in the AGS Booster lattice for 0, 1, 2, and 5 mm vertical offsets of the first "QVA1" quadrupole. Synchrotron radiation is enabled. The electron spins in each case are initially aligned with the corresponding $\mathbf{n}_0$ axis

In a perfectly aligned lattice without transverse coupling, particles with different momentum offsets δ experience only vertical bending and focusing magnetic fields. Therefore, the precession axes of all particles $\mathbf{n}(\delta)$ are aligned with the same vertical $\mathbf{n}_0$ axis. Change in momentum of a particle due to emission of a synchrotron radiation photon does not change the direction of its $\mathbf{n}(\delta)$ and causes no polarization loss as illustrated by Question 14.1.2.2-2. In case when the closed orbit experiences vertical excursion, the radial fields of the focusing quadrupoles tilt $\mathbf{n}_0$ from the vertical. The amount of this tilt is momentum dependent thus resulting in a spread of the $\mathbf{n}(\delta)$ directions for different δ. Emission of a synchrotron radiation photon changes the direction of $\mathbf{n}(\delta)$ and only the component of the original spin direction along the new $\mathbf{n}(\delta)$ is preserved. The greater the change in $\mathbf{n}(\delta)$, the smaller the fraction of the spin that is preserved and thus the higher the spin diffusion rate. Greater misalignments lead to greater closed orbit distortion and subsequently greater deviation of $\mathbf{n}_0$ from the vertical, greater $\mathbf{n}(\delta)$ spread and finally greater spin diffusion rate as demonstrated in Question 14.1.2.2-4.

14.2.2.4 Suppression of Spin Diffusion

Question 14.1.2.2-5—Both lattices considered in this exercise consist of a solenoid followed by two dipoles and then another solenoid. Both schemes are simplified versions of an electron spin rotator, a device rotating the electron polarization from vertical to longitudinal and then back. Such an insertion is needed to provide longitudinal polarization in the experimental section without causing fast spin diffusion in the arcs. The first solenoid rotates the polarization about the longitudinal

axis from positive vertical to positive radial. The subsequent dipole rotates the polarization about the vertical axis from positive radial to positive longitudinal. The difference between the two schemes is in how the polarization is returned back to positive vertical. In the first scenario, the second dipole bends the beam in the same direction as the first one and continues polarization rotation in the same direction from positive longitudinal to negative radial. The second solenoid has the same field polarity as the first one. It rotates the polarization from negative radial to positive vertical. This dynamics can be graphically summarized as

$$\uparrow \text{ Solenoid } \odot \text{ Dipole } \rightarrow \text{ Dipole } \otimes \text{ Solenoid } \uparrow . \tag{14.11}$$

In the second scenario, the polarities of the second dipole and solenoid are reversed resulting in the following rotation sequence

$$\uparrow \text{ Solenoid } \odot \text{ Dipole } \rightarrow \text{ Anti} - \text{Dipole } \odot \text{ Anti} - \text{Solenoid } \uparrow . \tag{14.12}$$

In both cases, the polarization is positive vertical at the entrance and exit. From geometrical point of view, the first arrangement causes 138.4 mrad net orbital bend while the second configuration has zero net bend.

Question 14.1.2.2-6—The field and spin components along the reference trajectories of the two spin rotator configurations are shown in Figs. 14.37 and 14.38, respectively. These graphs demonstrate implementation of the design philosophy described in the solution to Question 14.1.2.2-5.

Question 14.1.2.2-7—Figure 14.39 shows the electron vertical spin component at the end of the spin rotator as a function of the particle's relative momentum offset. The momentum dependencies are compared for the two spin rotator configurations. In this study, different-momentum electrons with initially vertical spins were launched on the design orbit at the beginning of the spin rotator and tracked to its end. As we can see, the spin effects of the two rotator designs are equivalent for the on-momentum particles resulting in a perfect restoration of the vertical spin at the end. However, there are significant differences for the off-momentum particles. The

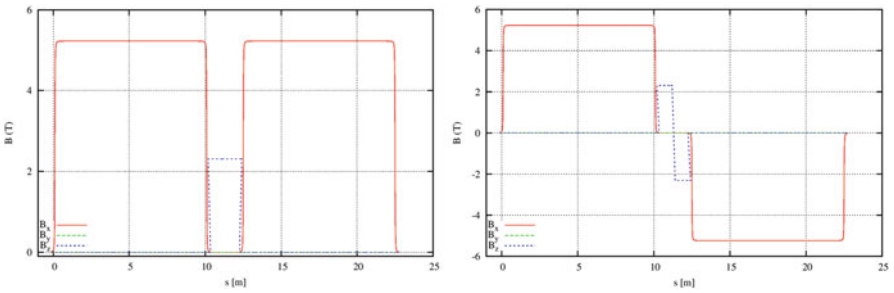

Fig. 14.37 Left: field components along the reference trajectory in the same-field-polarity design. Right: field components along the reference trajectory in the reversed-field-polarity design

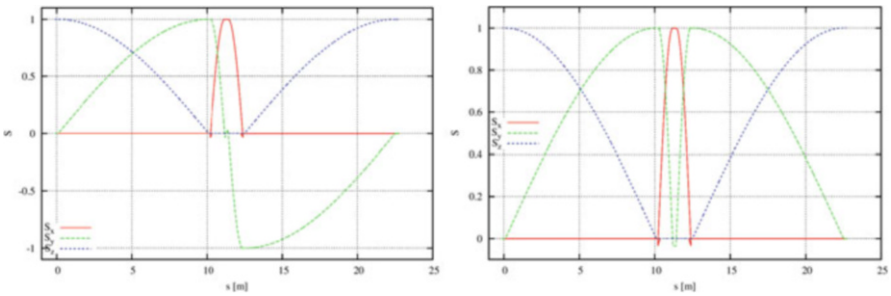

Fig. 14.38 Left: spin components along the reference trajectory in the same-field-polarity design. Right: spin components along the reference trajectory in the reversed-field-polarity design

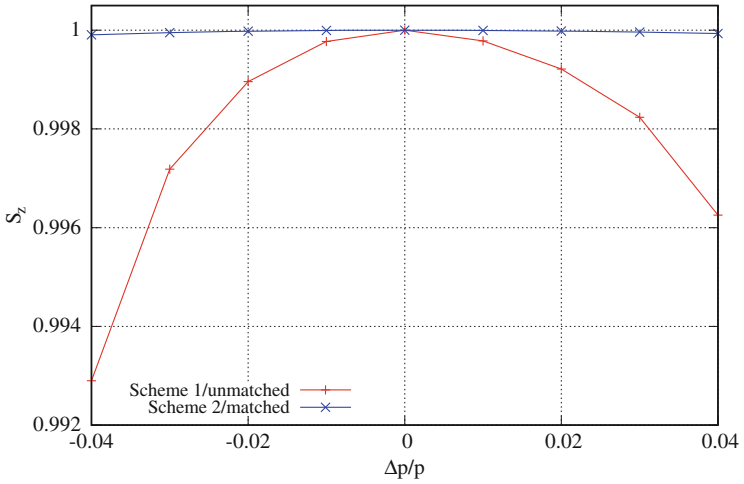

Fig. 14.39 Final vertical spin component as a function of the particle's relative momentum offset for the same-field- (Scheme 1) and reversed-field-polarity (Scheme 2) spin rotator configurations

reversed-field-polarity design demonstrates a much weaker momentum dependence of the final spin. The remaining dependence is due to dispersion that has not been accounted for in this simplified scheme.

The spin precession in each of the spin rotator elements is of course momentum dependent. The spin rotation of an off-momentum electron deviates from that of the reference particle. In the same-field-polarity configuration, this deviation accumulates from magnet to magnet resulting in a relatively large tilt of the spin at the end. In the opposite-field-polarity configuration, the spin deviation accumulated in the first half of the spin rotator is precisely compensated by the matching opposite-field magnets in the second half causing equal-size opposite-direction spin rotations. As we demonstrated in the solution to Question 14.1.2.2-4, greater deviation of the spin from vertical in the arcs results in a higher spin diffusion rate. Therefore, the same-field-polarity configuration is expected to generate a much

higher spin diffusion rate than the opposite-field-polarity one. The opposite-field-polarity design is an illustration of the concept of first-order longitudinal spin matching.

14.2.2.5 Spin Matching

Question 14.1.2.5-1—The snake lattice in Table 14.33 is close to an identity transformation in the horizontal plane and a $-I$ transformation in the vertical plane. Therefore, its insertion into the AGS Booster lattice results in a reasonable periodic solution not requiring any rematch. For simplicity, we ignore the fact that the ring is no longer geometrically closed, since this does not alter the below general conclusions about the spin dynamics. The optics of the entire ring and an expanded view of the snake section are shown in Fig. 14.40 (left) and (right), respectively.
Question 14.1.2.5-2: The $\mathbf{n}_0$ axis at the start of the AGS Booster lattice with the solenoidal snake (Table 14.35) can be found in the following excerpt of zgoubi.res:

```
                Spin transfer matrix, momentum group # 1 :

     -0.571992        0.820259        8.558277E-14
      0.820258        0.571991       -1.676874E-03
     -1.375471E-03   -9.591582E-04   -0.999999

Trace =      -0.9999993982,    ;   spin precession acos((trace-1)/2) =     179.9555530060 deg
Precession axis :   ( 0.4626,   0.8866, -0.0007)  ->  angle to (X,Y) plane,  angle to X axis :    -0.0426,    -0.0921  degree
Spin  tune  Qs (fractional) :     4.9988E-01
```

As expected for a ring with one snake, $\mathbf{n}_0$ lies in the horizontal plane and the spin tune is 0.5.

Question 14.1.2.5-3 and 4: Figure 14.41 compares the polarization behavior in the AGS Booster lattice with a solenoidal snake for the spin-matched and spin-mismatched snake configurations. From the beam dynamics point of view, the two configurations are similar. They only differ by rotation of the snake section by 90° about the longitudinal axis. However, in the spin-mismatched case, the spin diffusion rate is several times greater than in the spin-matched situation. This result illustrates the effect of proper optics design on the spin dynamics and the importance of spin matching. Note that spin diffusion is present in the matched case as well. It cannot be avoided in this ring configuration due to $\mathbf{n}_0$ being horizontal in the arcs at a

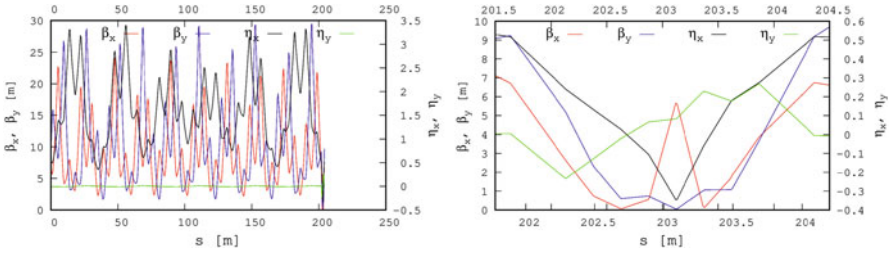

Fig. 14.40 Left: optics of the AGS Booster ring with the spin-matched snake insertion. Right: expanded view of the optics of the spin-matched snake insertion

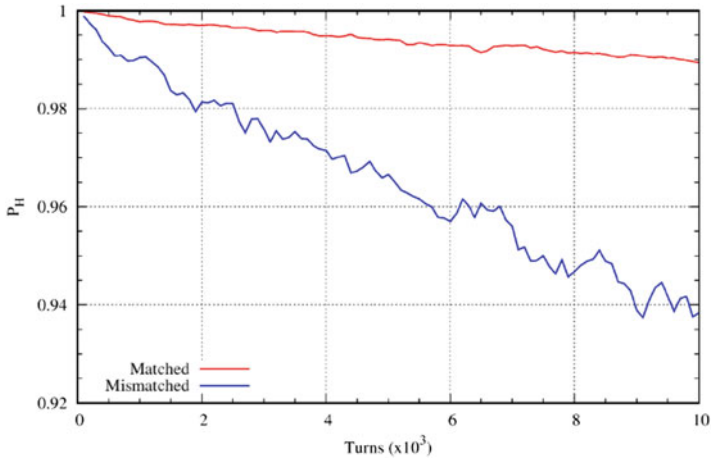

Fig. 14.41 Polarization of 100 electrons as a function of the turn number in the AGS Booster lattice with a solenoidal snake for the spin-matched (red) and spin-mismatched (blue) snake configurations

sufficiently high synchrotron radiation rate. This scenario is used for demonstration purposes only. It shows that spin diffusion due to improper spin matching can dominate over other depolarizing effects.

Appendix

A run of Zgoubi code, in addition to zgoubi.res execution listing, and depending on user's requests, may produce various output files. An example is zgoubi.plt which stores particle coordinates, spin coordinates, electric and magnetic field vectors, etc., step-by-step across optical elements. Another instance is zgoubi.fai which can be used for turn-by-turn particle data storage during multiturn tracking in a circular accelerator. In the present problems, data treatment and graphs can be obtained by reading these files, using gnuplot for instance, or Zgoubi graphic/data treatment interface program Zpop [3]. A brief introduction to these aspects of code and output data handling is given below, and all details can be found in Zgoubi Users' Guide regarding the many storage files at disposal; besides, guidance is provided in due place in the problem assignments (Sect. 14.1) and their solutions (Sect. 14.2).

- Data analysis and plotting:
  - in the matter of graphics it is foreseeable to achieve about any type of graphic, from Zgoubi output files, using gnuplot; if data analysis and other averaging are needed it can be managed via gnuplot scripts (using for instance awk commands, external programs, etc.);

– an additional possibility is to use Zpop, which is part of Zgoubi package. Zpop provides most of the data treatment and graphics means needed to analyze and display the contents of Zgoubi output files.

Besides the run listing zgoubi.res, the main two Zgoubi output files, generally used for data analysis or graphics, are zgoubi.fai (created when introducing the keyword FAISTORE (or FAISCNL, similar), it stores local particle data next to an optical element), and zgoubi.plt recorded if the flag IL=2 is present in optical elements: it logs step-by-step particle and field data, during numerical integration through the element.

Many additional files can be produced (usually by means of a PRINT argument in a keyword, see the Users' Guide), for instance to log data produced by various optical elements and commands, during ray-tracing, in view of data treatment, plotting, debugging, etc. Instances are SPNPRT[PRINT] (spin data logged in zgoubi.SPNPRT.Out), SRLOSS[PRINT] (synchrotron radiation Monte Carlo data logged in zgoubi.SRLOSS.Out).

- Keywords in Zgoubi: by "keyword" it is meant, the name of the optical elements (such as BEND, MULTIPOL, WIENFILT), or input/output procedures (such as FAISCEAU, FAISTORE, SPNPRT, SRPRNT), or commands (such as REBELOTE, TWISS, FIT, GOTO, SYSTEM), as they appear in a simulation input data file. Keywords are most of the time referred to without any additional explanation in the exercises: details and explanations regarding the use and functioning of keywords are to be found in the Users' Guide [1].
- It is recommended, when setting up the input data files to work out the simulations, to have Zgoubi Users' Guide at hand. PART B of the guide in particular, details the formatting of the input data which follow most keywords, and their units (a few keywords only, for instance FAISCEAU, MARKER, do not require additional data). PART A is the "physics content" and details what keywords are doing and how. The Users' Guide INDEX is a convenient tool to navigate keywords. A complete list may also be found in the "Glossary of Keywords" Sections, at the beginning of both PART A and PART B, and an overview of what they can be used at is given in "Optical elements versus keywords" Sections.

  – A concise notation KEYWORDS[ARGUMENT1, ARGUMENT2, ...] may be used in the assignments: it follows the nomenclature of the Users' Guide, Part B. A couple of examples:

    OBJET[KOBJ=1] stands for keyword OBJET, and the value of KOBJ=1 retained here;
    OPTIONS[CONSTY=ON] stands for keyword OPTIONS, and the option retained here, CONSTY, switched ON.

  – The keyword INCLUDE is used at times. The goal is mostly to modularize input data sequences, with usually the benefit of reduced file lengths and improved clarity. In a very similar way to the Latex or Fortran "include" command, a segment of an optical sequence subject to an INCLUDE by a

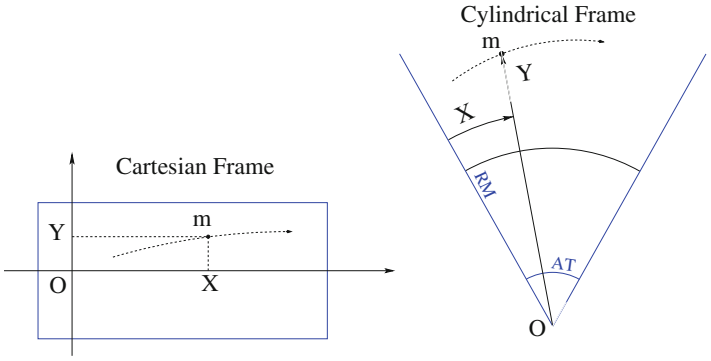

Fig. 14.42 Cartesian and cylindrical reference frames in optical elements. Let a particle location M(X,Y,Z) project to m(X,Y) (the dashed curve shows the projected trajectory). In the case of an optical element defined in Cartesian coordinates (shown here as a rectangular box; for instance, the cases of *BEND*, *MULTIPOL*), X and Y in zgoubi.plt denote the coordinates taken along the reference frame axes. In the case of an optical element (depicted here as an angular sector AT with some reference radius RM) (for instance, the case of *DIPOLE[S]*), X is the polar angle, counted positive clockwise, Y is the radius

parent input data file, may always be replaced by that very sequence segment, in the parent file.

- (O;X,Y,Z) coordinates in an optical element: this is the coordinate system in which the field $\mathbf{E}(X, Y, Z)$ and/or $\mathbf{B}(X, Y, Z)$ is defined (the origin for X depends on the optical element). Depending on the optical element concerned, this (O;X,Y,Z) reference frame may be
  - either Cartesian, in which case X, Y, and Z denote the particle position in that frame, T and P the horizontal and vertical trajectory angles (Figs. 1, 2 in the Users' Guide, and Fig. 14.42 here),
  - or cylindrical, in which case, given m the projection of particle position M in the Z=0 plane (Fig. 14.42), Y denotes the radial coordinate: $Y = |\mathbf{Om}|$, whereas X denotes the polar angle **OX**-**Om** (as a matter of fact, the nature of the variables named X and Y in the source code does change, and in zgoubi.plt as well) T is the horizontal trajectory angle with respect to the normal to **Om**, P is the vertical trajectory angle.

References

1. F. Méot, The ray-tracing code Zgoubi. NIM A **767**, 112–125 (2014). Zgoubi Users' Guide: https://sourceforge.net/p/zgoubi/code/HEAD/tree/trunk/guide/Zgoubi.pdf. Zgoubi download package at sourceforge: https://sourceforge.net/p/zgoubi/code/HEAD/tree/trunk/
2. gnuplot portable command-line driven graphing utility: http://www.gnuplot.info/

3. Zpop graphic/data treatment interface to zgoubi output files. See Zgoubi Users' Guide [1], PART D, Sec. 1. Zpoo code package is part of Zgoubi download package at sourceforge https://sourceforge.net/p/zgoubi/code/HEAD/tree/trunk/
4. S. Tygier, D. Kelliher, PyZgoubi. https://zenodo.org/record/3597426
5. zgoubidoo python interface to zgoubi. https://ulb-metronu.github.io/zgoubidoo/
6. Zgoubi on Sirepo by Radiasoft. https://www.sirepo.com/en/apps/particle-accelerators/
7. H. Grote, F.C. Iselin, The MAD Program, User's Reference Manual. CERN/SL/90-13 (AP) Rev. 5 (1996)
8. USPAS Summer 2021 Spin Class, mini-workshop, helion files repository. https://sourceforge.net/p/zgoubi/code/HEAD/tree/trunk/exemples/uspasSpinClass_2021/mini-workshop/AGSBooster_helion/
9. M. Bai, Overcoming the Intrinsic Spin Resonance in AGS by Using an RF Dipole. PhD thesis, Indiana University (1999). https://www.rhichome.bnl.gov/RHIC/Spin/papers/baithesis.pdf
10. USPAS Summer 2021 Spin Class, mini-workshop, electron files repository. https://sourceforge.net/p/zgoubi/code/HEAD/tree/trunk/exemples/uspasSpinClass_2021/mini-workshop/AGSBooster_electronPolarization/
11. B.P. Welford, Note on a method for calculating corrected sums of squares and products. Technometrics **4**(3), 419–420 (1962). https://doi.org/10.2307/1266577.JSTOR1266577. https://en.wikipedia.org/wiki/Algorithms_for_calculating_variance#Online_algorithm; https://stackoverflow.com/questions/42677017/plot-average-of-nth-rows-in-gnuplot